AD-A286 646

94-1065

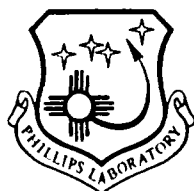# DEVELOPMENT OF AN ANNULAR ELECTRON BEAM HPM AMPLIFIER

Kyle J. Hendricks et al.

September 1994

Final Report

APPROVED FOR PUBLIC RELEASE; DISTRIBUTION IS UNLIMITED.

94-35242

PHILLIPS LABORATORY
Advanced Weapons and Survivability Directorate
AIR FORCE MATERIEL COMMAND
KIRTLAND AIR FORCE BASE, NM 87117-5776

PL-TR--94-1065

This final report was prepared by the Phillips Laboratory, Kirtland Air Force Base, New Mexico, under Job Order 5797AK04. The Laboratory Project Officer-in-Charge was Dr. Kyle J. Hendricks (WSR).

This report has been reviewed and is approved for publication.

KYLE J. HENDRICKS, GS-13
Senior Physicist
Project Officer

FORREST J. AGEE, GM-15
Chief, Electromagnetic Sources
 Division

FOR THE COMMANDER

WILLIAM L. BAKER, GM-15
Acting Director, Advanced Weapons
 and Survivability Directorate

REPORT DOCUMENTATION PAGE

Public reporting burden for this collection of information is estimated to average 1 hour per response, including the time for reviewing instructions, searching existing data sources, gathering and maintaining the data needed, and completing and reviewing the collection of information. Send comments regarding this burden estimate or any other aspect of this collection of information, including suggestions for reducing this burden, to Washington Headquarters Services, Directorate for information Operations and Reports, 1215 Jefferson Davis Highway, Suite 1204, Arlington, VA 22202-4302, and to the Office of Management and Budget, Paperwork Reduction Project (0704-0188), Washington, DC 20503

1. AGENCY USE ONLY (Leave blank)	2. REPORT DATE September 1994	3. REPORT TYPE AND DATES COVERED Final, Aug 91 - Jan 94

4. TITLE AND SUBTITLE	5. FUNDING NUMBERS
DEVELOPMENT OF AN ANNULAR ELECTRON BEAM HPM AMPLIFIER	PE: 62601F PR: 5797
6. AUTHOR(S) Kyle J. Hendricks, Walter R. Fayne, Thomas A. Spencer, Lester A. Bowers, M.J. Arman, Charles E. Davis, Phillips Lab/WSR; Michael D. Haworth, Robert C. Platt, James Wells, SAIC;*	TA: AK WU: 04

7. PERFORMING ORGANIZATION NAME(S) AND ADDRESS(ES)	8. PERFORMING ORGANIZATION REPORT NUMBER
Phillips Laboratory 3550 Aberdeen Avenue SE Kirtland AFB, NM 87117-5776	PL-TR--94-1065

9. SPONSORING/MONITORING AGENCY NAME(S) AND ADDRESS(ES)	10. SPONSORING/MONITORING AGENCY REPORT NUMBER

11. SUPPLEMENTARY NOTES
*Miguel D. Sena, Dale E. Ralph, Maxwell Labs, Inc; Raymond W. Lemke, M. Collins Clark, Sandia National Laboratory, Albuquerque, NM.

12a. DISTRIBUTION AVAILABILITY STATEMENT	12b. DISTRIBUTION CODE
Approved for public release; distribution is unlimited.	

13. ABSTRACT (Maximum 200 words)

Experiments and computer simulations of annular electron beam powered microwave devices have been conducted. This work included the generation of an annular electron beam using the IMP pulser (500 kV, 5 Ω, 300 ns), the modulation of this beam via a two-cavity klystron-like amplifier, and the extraction or radiation of the microwave power. Results of computer simulations from several codes used to design the experiments and results of experiments on propagating the electron beam, injecting a magnetron signal into the two-cavity klystron-like amplifier via a vacuum coaxial line, and initial work on modulating the electron beam are presented.

14. SUBJECT TERMS			15. NUMBER OF PAGES 72
high power microwaves, amplifier, relativistic klystron amplifier, electron beam, vacuum diode, microwave cavity			**16. PRICE CODE**

17. SECURITY CLASSIFICATION OF REPORT	18. SECURITY CLASSIFICATION OF THIS PAGE	19. SECURITY CLASSIFICATION OF ABSTRACT	20. LIMITATION OF ABSTRACT
Unclassified	Unclassified	Unclassified	SAR

CONTENTS

iii

FIGURES (Continued)

1.0 INTRODUCTION

High Power Microwave (HPM) research of the past 10 to 15 years has focused on developing high peak power (> 1 GW), high energy (> 1 kJ) sources which have moderate frequency tunability (Refs. 1 to 20). Repetitive pulse power operation Ref. 13) is also a desired parameter, however this report will not address the rep-rate issue. The standard research approach is to develop a concept, model the instability on a computer, and then build and rebuild the device until the desired performance is obtained. This procedure typically requires rebuilding the experimental device several times, which is typically expensive. The research has focused on how this process may be improved. Specifically, by working with the various calculational tools (MAGIC, SOS, , EGUN, etc.) what important aspects need to be incorporated into these tools to enable the researcher to produce better designs prior to "cutting metal".

The technique has been to take an existing, demonstrated HPM device and compare calculation and experiment to find what physics may not have been included in the simulation, but may be essential for agreement between theory and experiment. Obviously, these codes have been benchmarked and their validity established, however the rigor of the solution has been limited to establishing trends but not numerical design accuracy. Numerical design accuracy is clearly required to make these codes true source design tools.

Based on the published results of the Relativistic Klystron Amplifier (RKA) (Ref. 4) and the future ability to phase lock amplifiers for HPM arrays we chose the RKA as a prototype HPM system to begin a study of HPM amplifiers. This report will document the experimental progress of the Annular Beam Amplifier (ABA) during the past 18 months, and the success simulating the amplifier (Fig. 1). The discussion will include the concept for building a HPM amplifier, design of the foilless diode, demonstration of the electron beam modulation, and the insertion of assorted diagnostics to compare with the computer codes. The report will conclude with a discussion of the upcoming experiments. For future reference sample input files for the various computer codes are included as appendices.

1
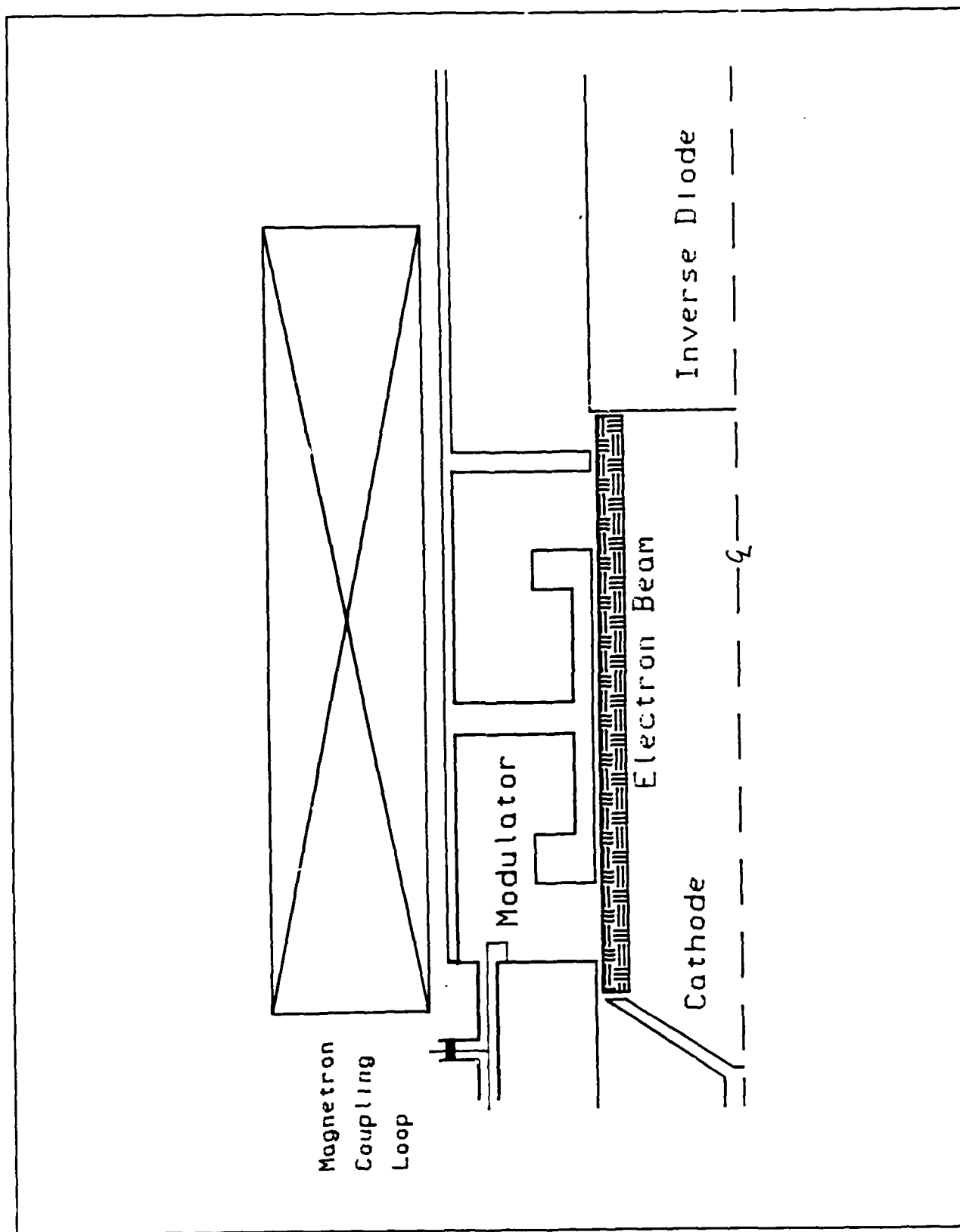
Figure 1 Drawing of the amplifier concept.

2.0 EXPERIMENTAL APPARATUS

The choice of the RKA allowed one to break the problem into pieces which could be individually studied, e.g. the vacuum diode to provide the electron beam power to be converted into the microwave signal. We follow the procedure of Reference 2 to validate coupling the signal into the modulation cavity. One then observes the growth of the radiofrequency (rf) current as the modulated beam propagates from the modulation cavity. At the peak of the rf current on the electron beam one places the first idler cavity. Then again the peak of the rf current is determined and another idler cavity to provide further modulation, or an extractor is placed to separate the rf wave from the beam. A number of diagnostics are required for comparison with the codes, e.g. cavity electric field probes to monitor the gap voltages, current diagnostics to observe the beam optics and beam losses, and beam collector to observe the cross-sectional area of the electron beam.

2.1 DESIGN OF AMPLIFIER

To build flexibility into the amplifier, the microwave circuit was designed to be modular and to be insertable within a vacuum vessel. This allows for future investigations with other microwave circuits without needing to rebuild the vacuum vessel. Tolerances were quite restrictive (0.001") in machining the various stainless steel parts. Copper finger stock was used to make good rf electrical contact. This was done to maximize the quality factor (Q). As stated above, the majority of the parts were machined from stainless steel to allow diffusion of a pulsed magnetic field (20 ms rise time) through the vacuum vessel/microwave circuit. The design of the magnetic field coils will be discussed below.

The guiding philosophy of this effort has been to make all components as flexible as possible. This was done for two reasons. First, a typical set of parameters for research devices do not match requirements of other users. Secondly, the computer simulations might show a radical design change to be necessary. This was found to be true early in the research program when the original three-quarter wavelength ($\frac{3}{4}\lambda$) mode modulating cavity supported self-oscillation in the quarter wavelength ($\frac{1}{4}\lambda$) mode. The solution was to complete the simulation with $\frac{1}{4}\lambda$ cavities, with the plan to suppress the fundamental mode in the experiment if required. This lower frequency operation has been observed by Friedman (Ref. 2).

The cathode placement should allow generation of a large electron beam current pulse, constrained to be less than the Child-Langmuir, space-charge limiting current in the beam line. This removes the potential of forming a virtual cathode (Ref. 19). The requirement for high beam power requires the beam to travel close to the beam drift pipe wall. The beam trajectory limits the maximum tolerable variation of the axial and radial magnetic field. Also, minimal electron beam loss through the microwave circuit is required to maximize the rf power and to reduce plasma formation within the microwave circuit. All the above requirements translate to the highest power/energy electron beam for conversion to a HPM pulse.

The initial solution was a aluminum "cookie cutter" cathode of outer radius 7.0-cm in a 7.65-cm beam line immersed in a uniform DC axial magnetic field. The second cathode (Fig. 2) was a stainless steel right circular truncated cone immersed in a pulsed uniform magnetic field, with electron emission from the edge of the base of radius 7.0 cm. Both cathodes suffered from equal emitted currents parallel and anti-parallel to the symmetry axis. This resulted in only half of the electron beam power going into the microwave amplifier circuit.

3
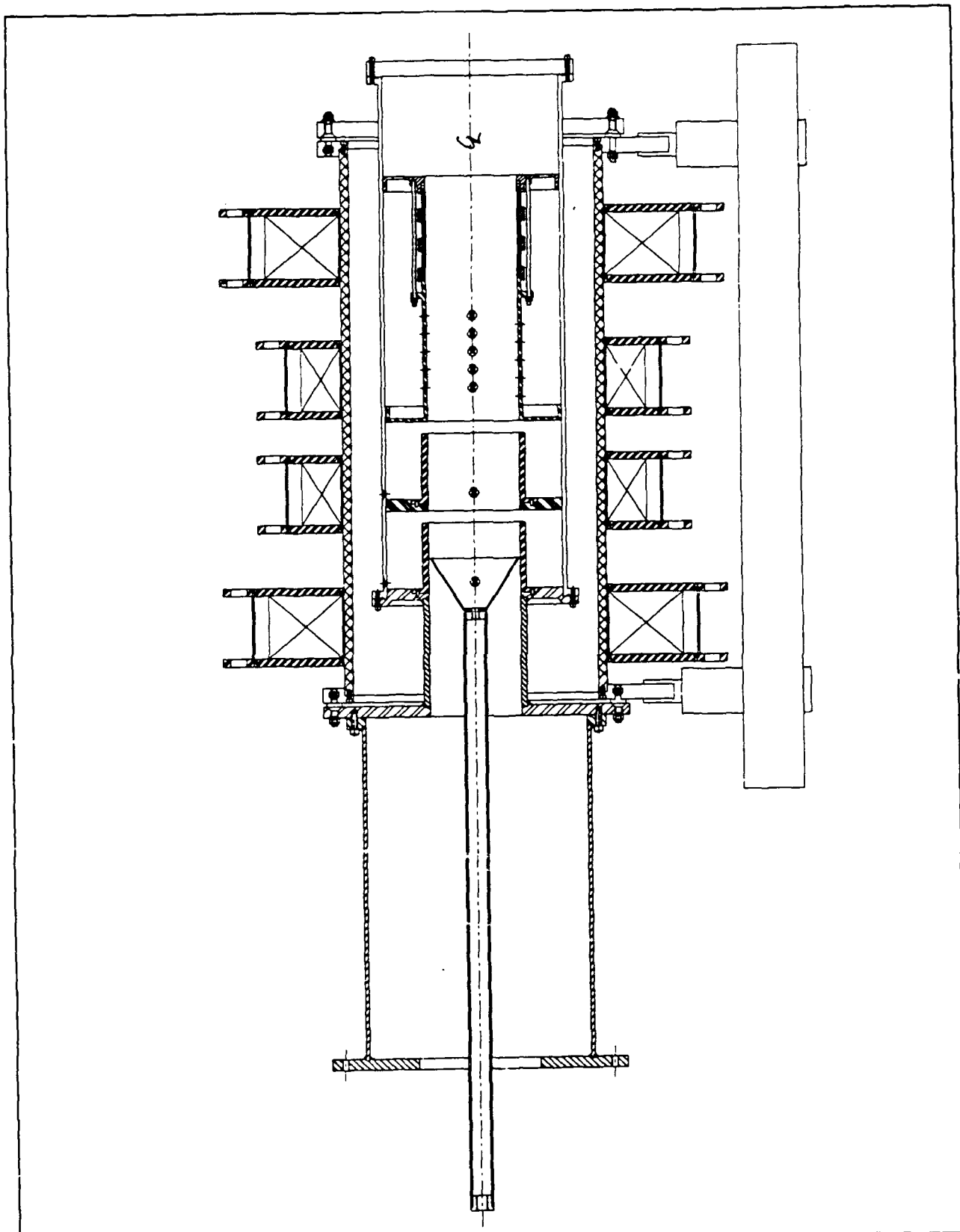
Figure 2 Drawing of the amplifier using the inverted truncated cone cathode.

The present cathode is being tested (Fig. 3). The focusing magnetic field causes the electron beam to be focused to a smaller radius than the emission radius. The larger diameter of the cathode provides a collector for electrons that are emitted away from the amplifier cavities. Since the electrons are collected at the cathode potential there are no resultant particles created which may cause problems of secondary electrons and plasma formation, as one would expect when the electrons are collected at ground potential. The cathode has been successfully simulated using EGUN and MAGIC when the proper B_z and B_t fields are used.

The microwave circuit and drift spaces were designed to allow positional flexibility during the project. All internal sections are machined to 0.001 inch and finger stock is used to provide good electrical contact (quality factors of 700 to 800 were easily obtained). All sections slide within the vacuum vessel. This allows easy adjustments in cavity dimensions, gap spaces, and drift spaces. These parameters must be optimized to allow the highest efficiency of beam power to rf power conversion.

Not shown in Figure 3 is the double stub tuner built to provide impedance matching between the external oscillator and the B-dot loop used to excite the modulation cavity. The selection of a B-dot loop with a vacuum co-axial transmission line was necessitated by the space available to inject power into the amplifier. Previous experiments have used waveguide feeds with various iris couplers (Refs. 4,10,13). The iris provides the same impedance matching as obtained with the double stub tuner. A double stub tuner was required since proper placement of a single stub tuner relative to the B-dot coupling loop was not possible. Calibration data will be presented in Section 4.

Fazio (Ref. 13) reported that overcoupling of the rf oscillator to the modulator cavity was required due to electron beam loading of the cavity. This phenomena has been observed in simulation and experiment and will be discussed later. Data are presented in Section 4 which show how this overcoupling is achieved with the double stub tuner.

The drift space containing an axial and azimuthal array of B-dot probes, shown in Figure 3 following the idler cavity, is used to measure the modulation generated by both cavities. An array of 20 zero area B-dot loops and a Rogowskii loop are used to monitor beam propagation and beam modulation. The array is composed of 4 axial lines of 5 B-dots each. As shown in Fig.3 the lines are separated in angle by 90°, and two lines are axially matched while the other two lines are positioned to be centered between the first two lines. This provides determination of the azimuthal symmetry and 1-cm resolution on the beam modulation. With the idler cavity removed we simply slide the "diagnostic package" toward the cathode, causing the left wall of the "diagnostic package" to form the final wall of the modulating cavity. By using the same probes greatly eases the calibration requirements and data reduction.

An rf extractor design for this experiment has not been finalized. Fazio (Ref. 13) has been working on an extractor, however the Q of the extractor at a value < 10 allows one to develop sufficient voltage to reflect the electron beam back to the idler cavity, or to overvolt the extractor gap causing an rf arc. At this point the amplifier suffers from breakdown and the rf pulse terminates. The primary problem with the extractor is the plasma and secondary particles created by collecting the energy of the unmodulated portion of the electron beam. This problem is not restricted to HPM amplifiers; any HPM device which requires a long electron beam pulse, long being defined as > 500 ns.
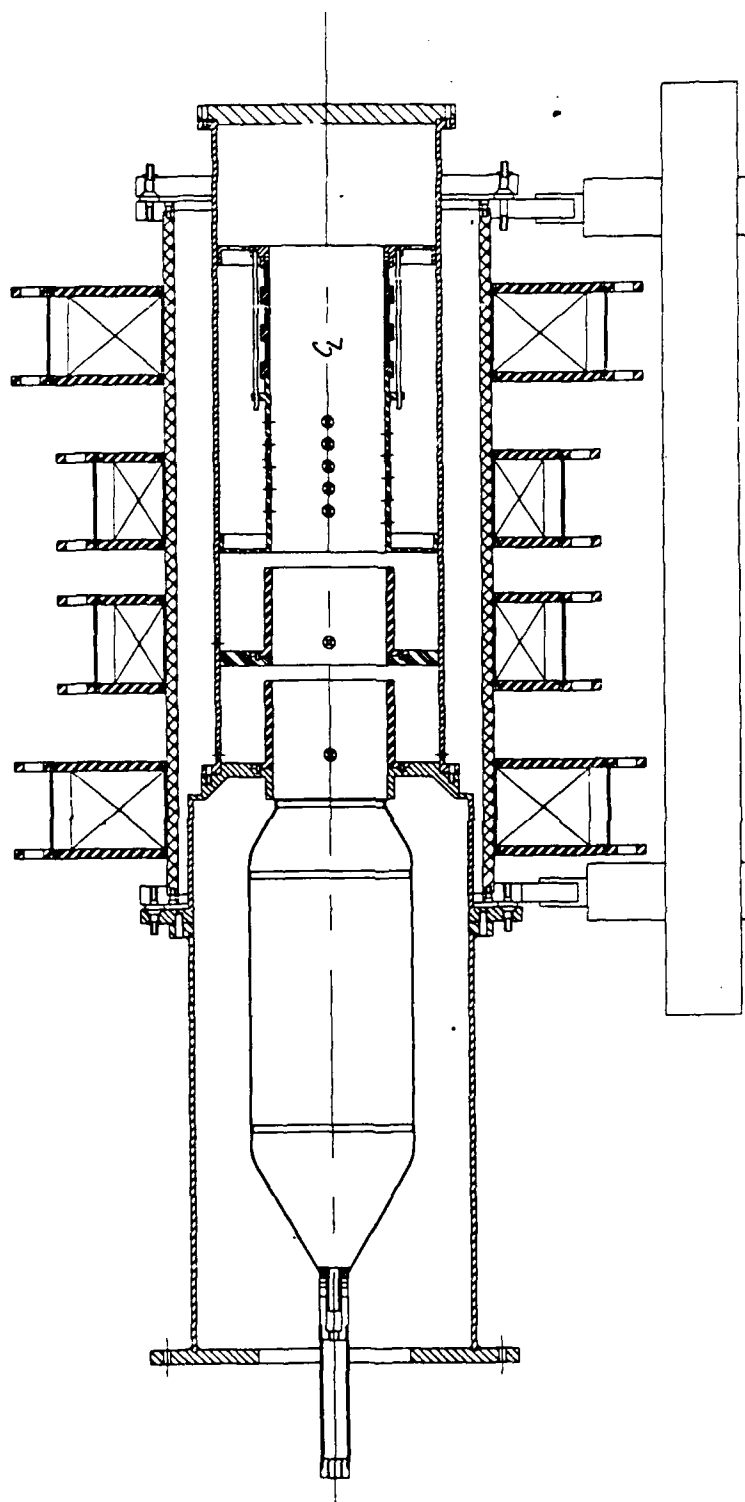
Figure 3 Drawing of the amplifier using the magnetically focused cathode.

2.2 DIAGNOSTICS AND CALIBRATIONS

In completing this experiment, we have tried to use sufficient diagnostics to validate critical data and to allow comparison with simulation. This has resulted in using E-dot probes in the rf cavities to monitor the electric field in the cavities and modulating gaps, B-dot probes in the drift spaces to monitor the beam current modulation as a measure of the amplifier beam power to rf power efficiency, and a Rogowskii current monitor for the current exiting the drift space.

The E-dot probes (Ref. 21) are cut flush to the wall, and made from SMA bulkhead feedthroughs. These probes are calibrated with a ruler, and also cross calibrated with the oscillator input and reflected power monitors to validate that all the oscillator power is injected in the cavity during the electron beam pulse. This coupling coefficient is the S_{21} parameter found on a vector network analyzer. These E-dot probes are also used to determine the axial electric field/potential applied to the modulator gap during the presence of the electron beam. The ratio of the radial electric field at the probe to the axial gap electric field at the radius of the beam may be estimated by SHY (Ref. 22) and MAGIC (Ref. 23). The accuracy of this estimate will have to be determined in future measurements of the beam modulation or extracted power.

The B-dot probes are zero area probes based on the design of Voss[*]. The B-dot probes are calibrated on the Transmission Line Calibration Fixture ("Tin Man") a 50 Ω air coaxial transmission line. Tin Man allows determination of the effective area of the B-dot probe (see Appendix A), which is ideally found to be independent of the frequency of the oscillator up to some maximum determined by the geometry of the probe. This area may also be determined by pulsing currents on a rod on the geometric axis of the "diagnostic package" or by generating an electron beam and propagating the beam past the B-dot probes and the exit Rogowskii. Without an external oscillator signal injected into the modulation cavity these diagnostics should agree, modulo the geometric centering of the electron beam.

The anticipated results are that the 3 different calibration techniques should provide the same effective area for each B-dot probe. The results from "Tin Man" were a factor of $1/\sqrt{2}$ lower than found from beam shots or short shots. This was due to an implicit assumption that "Tin Man" uses CW, or RMS power rather than the pulse value used in beam or short shots. Graphs of the data with and without the factor of $1/\sqrt{2}$ show this comparison (Fig. 4).

A primary consideration of the experimental design was that enough diagnostics be available to monitor the important physics of the amplifier. This includes the requirement that the diagnostics allow for comparison with simulation. Also, the diagnostic techniques must be self-consistent. That is, if we observe a certain potential in the gap with the modulation cavity E-dot probe, then the induced beam modulation found with the "diagnostic package" B-dot array should be consistent with simulation results.

---

[*] D.E. Voss, private communication
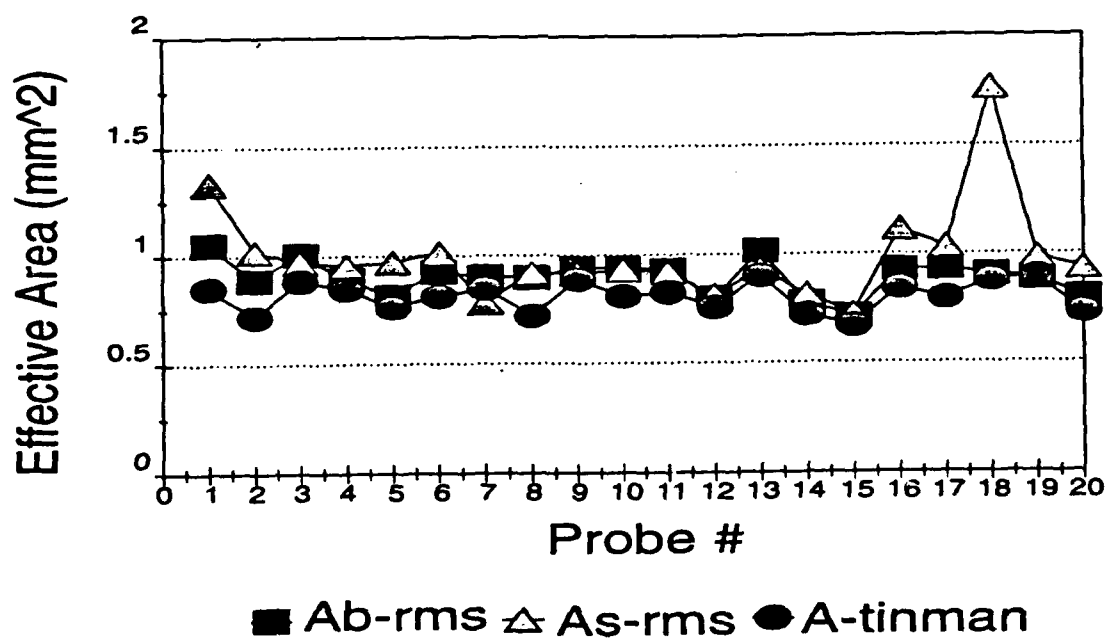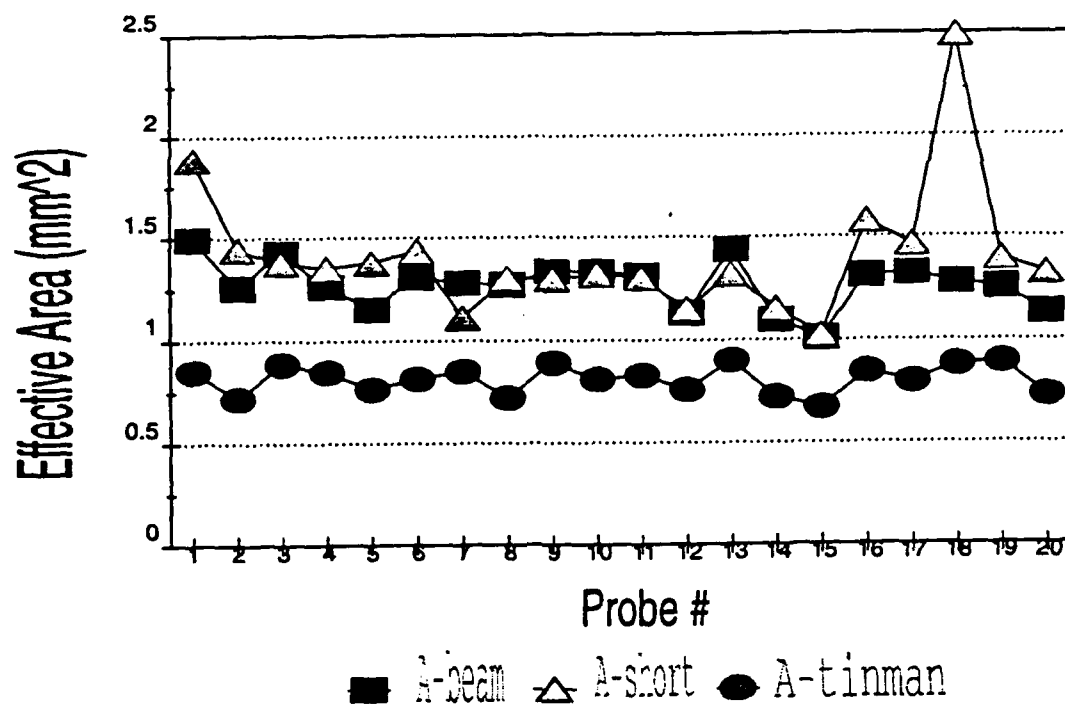
Figure 4 Comparison of B-dot probe effective areas.

8

3.0 SIMULATIONS

An assortment of simulations or calculations have been completed in preparing for the design of this experiment. Sample results of these simulations are presented in this section. Complete input data files and additional input are listed in the appendices.

3.1 SUPERFISH

The POISSON/ (Ref. 22) group of codes were used to simulate the "cold" steady-state response of the amplifier modulation and idler cavities. The calculation provides information on the resonant modes of the microwave cavities and measurements of electric field amplitudes throughout the cavity. The code group is very well documented in the users manuals, and the reader is referred to them.

To use the group of codes, one begins with a geometry of the device. This input is first processed by the code AUTOMESH. Two output files are created. One file is the output on how a triangular mesh is fit to the problem and the second is an input file for the code LATTICE. During execution of LATTICE, the AUTOMESH output file is read and the user is prompted for input for the "CON" array, which may be used to change various defaults such as the problem boundary conditions, problem symmetry, etc. LATTICE also produces two output files, the first being an ASCII file summarizing the execution of the program LATTICE, and the second is an input file for the codes PSFPLOT and . PSFPLOT may be used to verify the geometry, mesh relaxation, and to plot the electric field profile of the cavity. is executed to determine the resonant frequency of the cavity mode. An initial guess for the resonant frequency is used to select which mode the code iterates toward. The accuracy of the guess determines how hard the code must work to find a solution. One may also have search a range of frequencies to look for the number of modes supported by the cavity within that frequency range. A postprocessor code SHY may be used to determine ratios of electric field components throughout the geometry. This was used in conjunction with electric field probes to determine the modulation voltage established by the modulation cavity. Sample input is listed in Appendix B. Results for the lowest two modes of the ABA are shown in Figure 5.

3.2 MAGNET

The magnetic field coils were initially designed using the MAGNET[*] code developed by John Freeman of Sandia National Laboratory. This code requires a definition of the geometry of the magnetic field coils, specifically the left and right boundaries of each coil, the number of turns per layer and number of layers for each coil, and the current flowing in each layer (see sample input deck in Appendix C.). By setting the current to 1 Ampere the code results were in units of Gauss per Ampere. The code calculates the spatial variation of the steady state axial and radial magnetic fields along various radial contours as a function of the axial coordinate. This requires one to verify that magnetic diffusion is not an issue when using pulsed coils.

The large number of turns (550) used in the magnetic field coil design required a better way to define the coil geometry to MAGNET. A short Fortran program was written to generate the input deck for MAGNET. This allowed faster changes to the input deck, and sped the design process. For this application minimal axial non-uniformity at the beam radius was required to achieve beam transport. A check on the axial uniformity was accomplished by calculating the radial magnetic field component at the beam radius and

---

[*] M.D. Haworth, private communication

RKA, 12/3/91 (NEW version)   FREQ= 394.901

RKA, 12/3/91 (NEW version)   FREQ= 1287.051
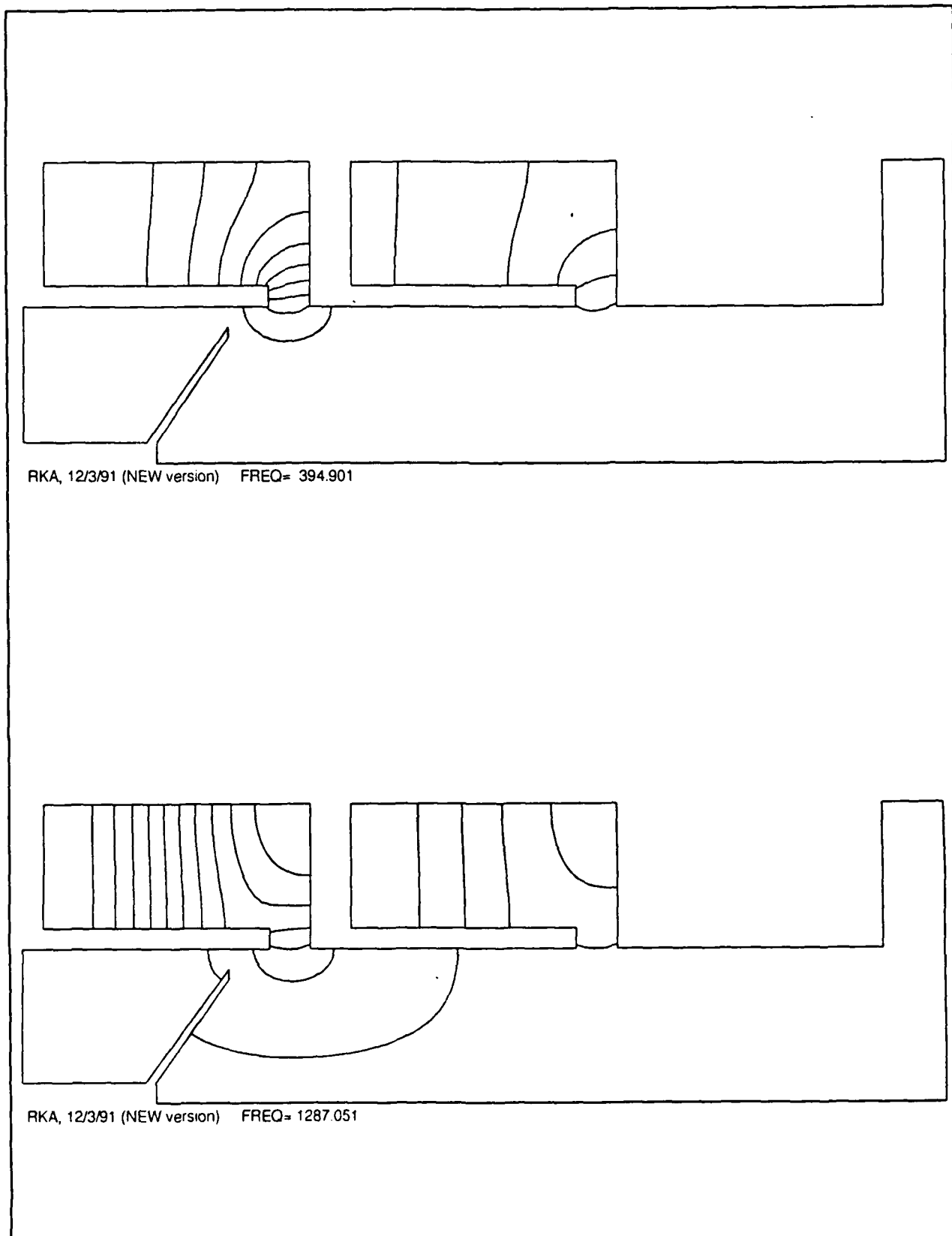
Figure 5 Sample results of the mode patterns/resonant frequencies from SUPERFISH.

plotting this component against the axial position. Additionally, the quality of the magnetic field system is indicated by comparing the axial variation of B_z on axis and at the beam radius(Figure 6). The radial and axial fields computed by MAGNET were reformatted into arrays and used as input for the applied magnetic field used in the MAGIC PIC simulations of the RKA (Figure 7).

A comparison of the magnetic flux of the designed magnet was done with the code POISSON (Ref. 22). POISSON calculates the magnetic flux distribution as functions of r and z. POISSON belongs to the same group of codes as . One defines the geometry similarly to SUPERFISH, however, where SUPERFISH uses cylindrical z-r on an x-y grid to determine cylindrical electromagnetic modes, POISSON uses cylindrical r-z on an x-y grid for cylindrical magnetic flux plots. The magnetic flux plots were also used to aid in the placement of the new cathode (Fig. 8).

An additional consideration in the design of the magnetic field coils is whether or not a pulsed current source is to be used to generate the magnetic field. The eddy currents generated by a pulsed magnetic field passing through the material used to assemble the vacuum vessel cause a time lag of the magnetic field amplitude within the electron beam line. The code MAGDIF* was used to simulate the magnetic flux penetration through the stainless steel vacuum vessel. The results showed that the conductivity of stainless steel was not sufficient to reduce the magnetic flux by the presence of eddy currents. A sequence of time snapshots of the magnetic flux generated by MAGDIF are shown in Figure 9 and the steady state results in Figure 10 which agree well with Figure 8.

3.3 EGUN

The trajectory code EGUN (Ref. 24) is used to design the vacuum diode. EGUN determines the steady-state current emitted by the cathode, and the final trajectories of the emitted electrons subject to the applied potentials and magnetic fields. A sample of the result of the diode used in a uniform magnetic field is shown in Figure 11. The input file is listed in the Appendix D. The converging magnetic field was included later to verify the diode design.

EGUN is described fairly completely in the user's manual. However, this computational tool is only easily used by an experienced user, and the input deck is somewhat counter-intuitive in the method of defining conductors. The version we had access to did not include all the present interfaces to commercial CAD software and this probably eases use by novice users. The definition of the magnetic field is also nonintuitive from the point of defining magnetic fields for annular electron beams. The magnetic field is defined at each mesh point on axis and then computed for the beam radius. This feature led to confusion in understanding the magnetic field components computed for the beam radius. It required some time to understand why the magnetic field did not resemble any magnetic field profiles calculated by other codes. The beam emission results were only understood following comparison with MAGIC.

---

* G. Marklin, private communication
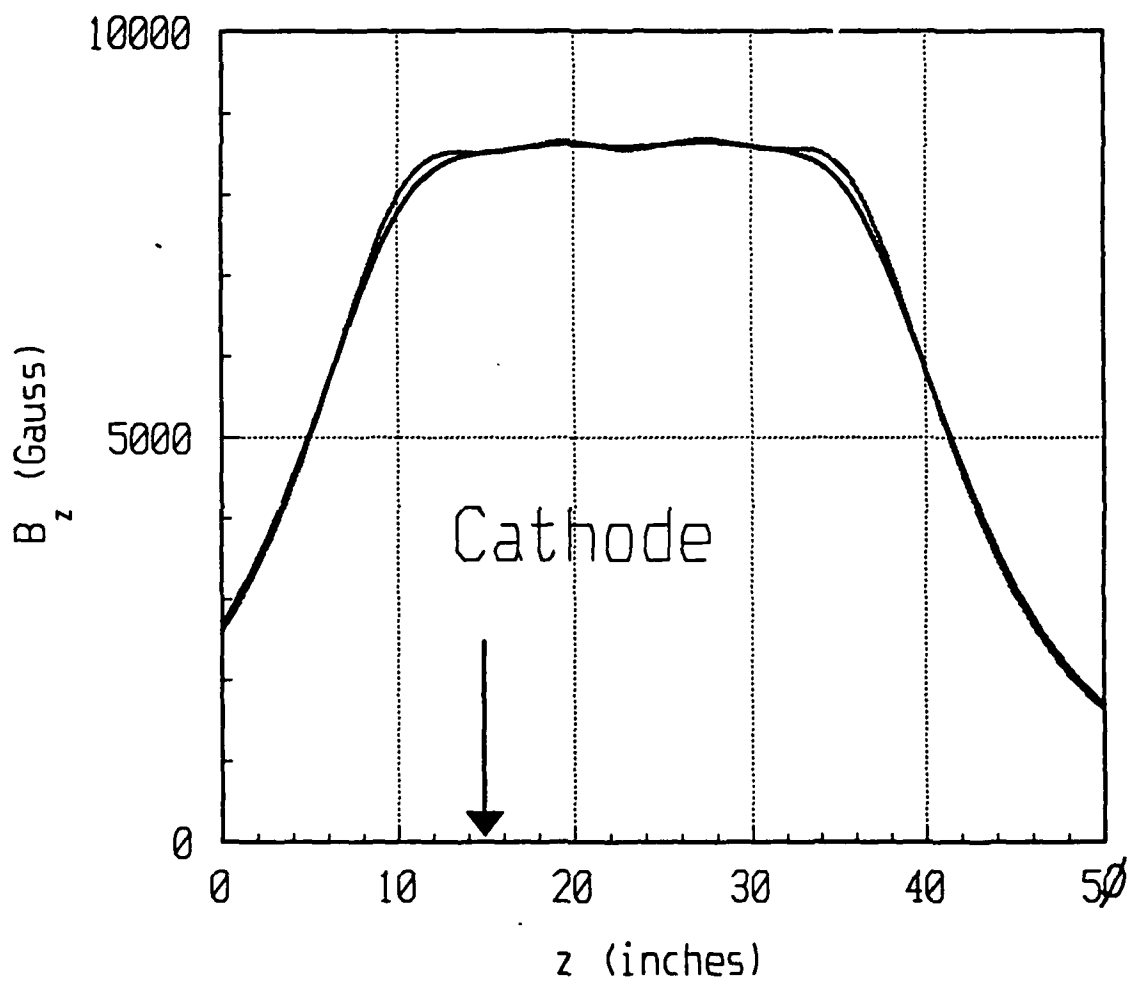
Figure 6 Comparison of axial magnetic field on axis and at the beam radius.

12

Axial Magnetic Field

B
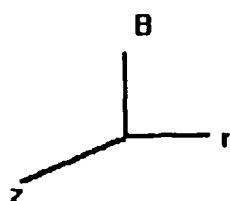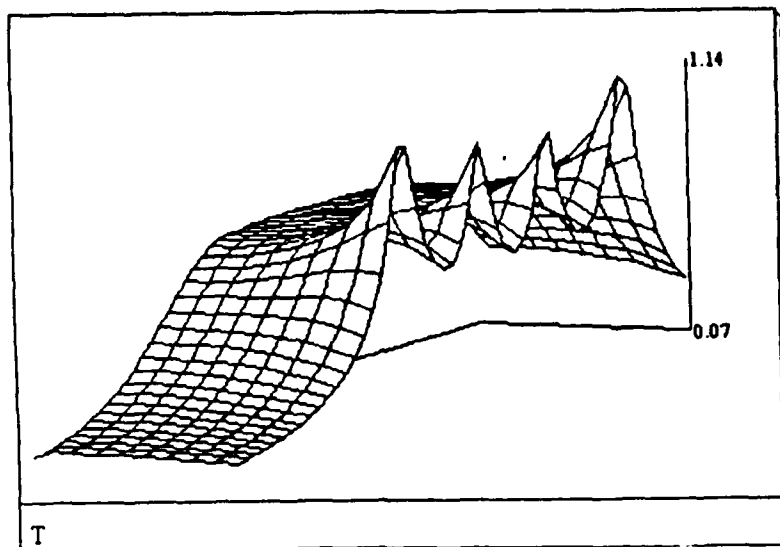
Radial Magnetic Field
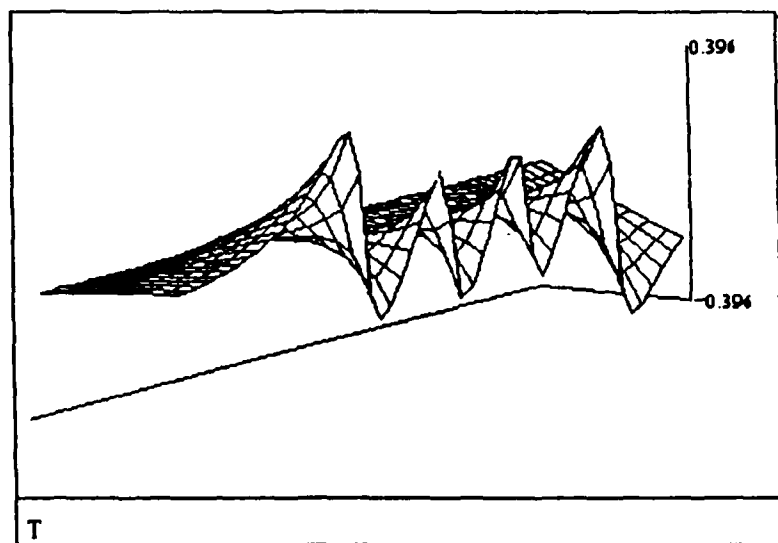
Figure 7 Surface plots of B_z and B_r used in MAGIC calculations.
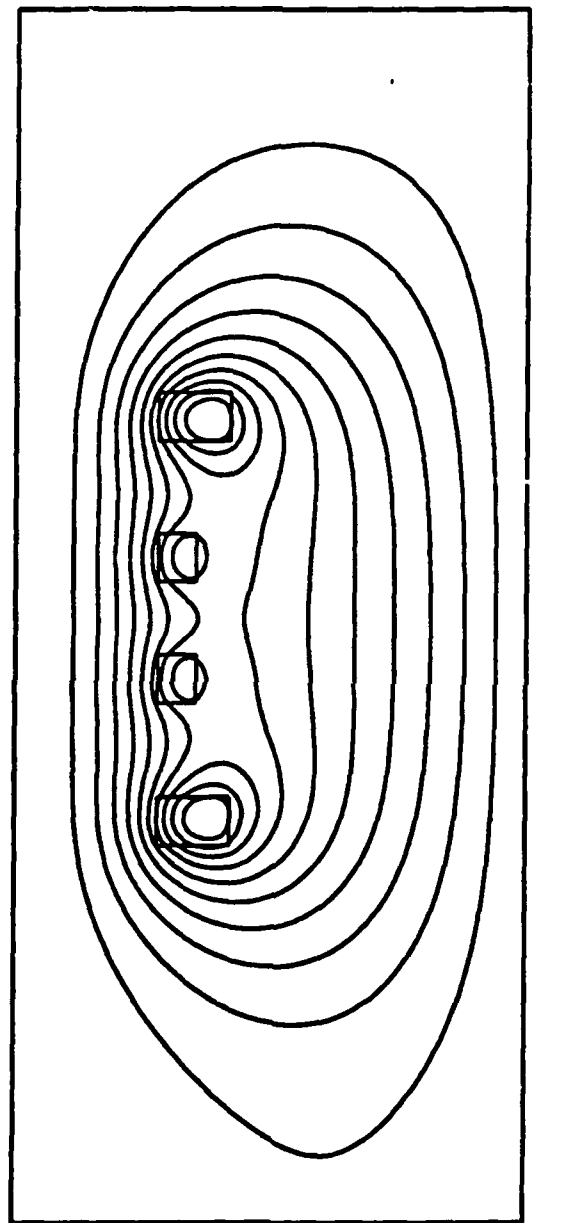
RKA MAGNET (7/1/92)   CYCLE = 370

Figure 8 Sample magnetic flux contour plot from POISSON.

a)   t=0.5 ms

b)   t=3.5 ms

c)   t=22.0 ms
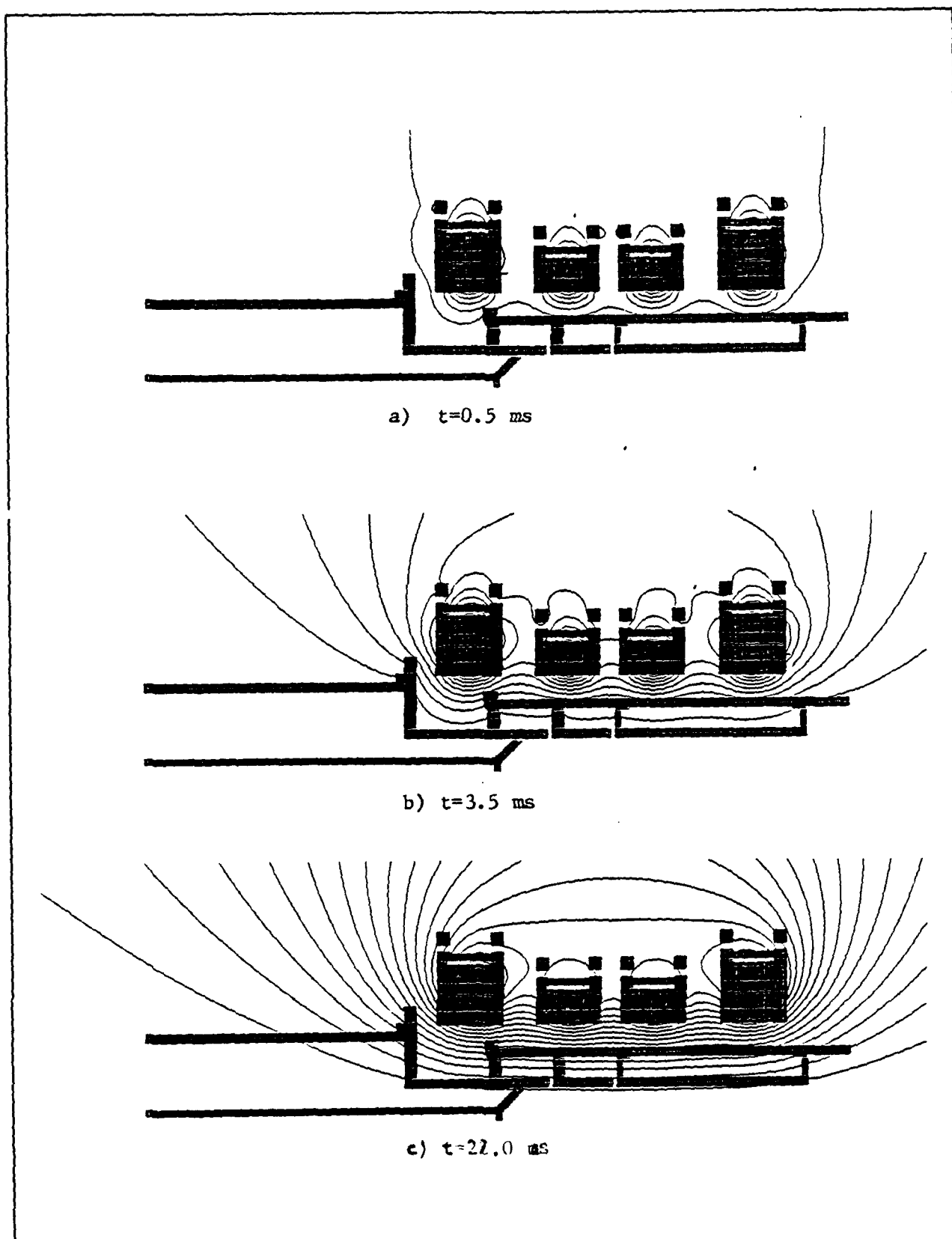
Figure 9 Magnetic flux snapshots from MAGDIF.
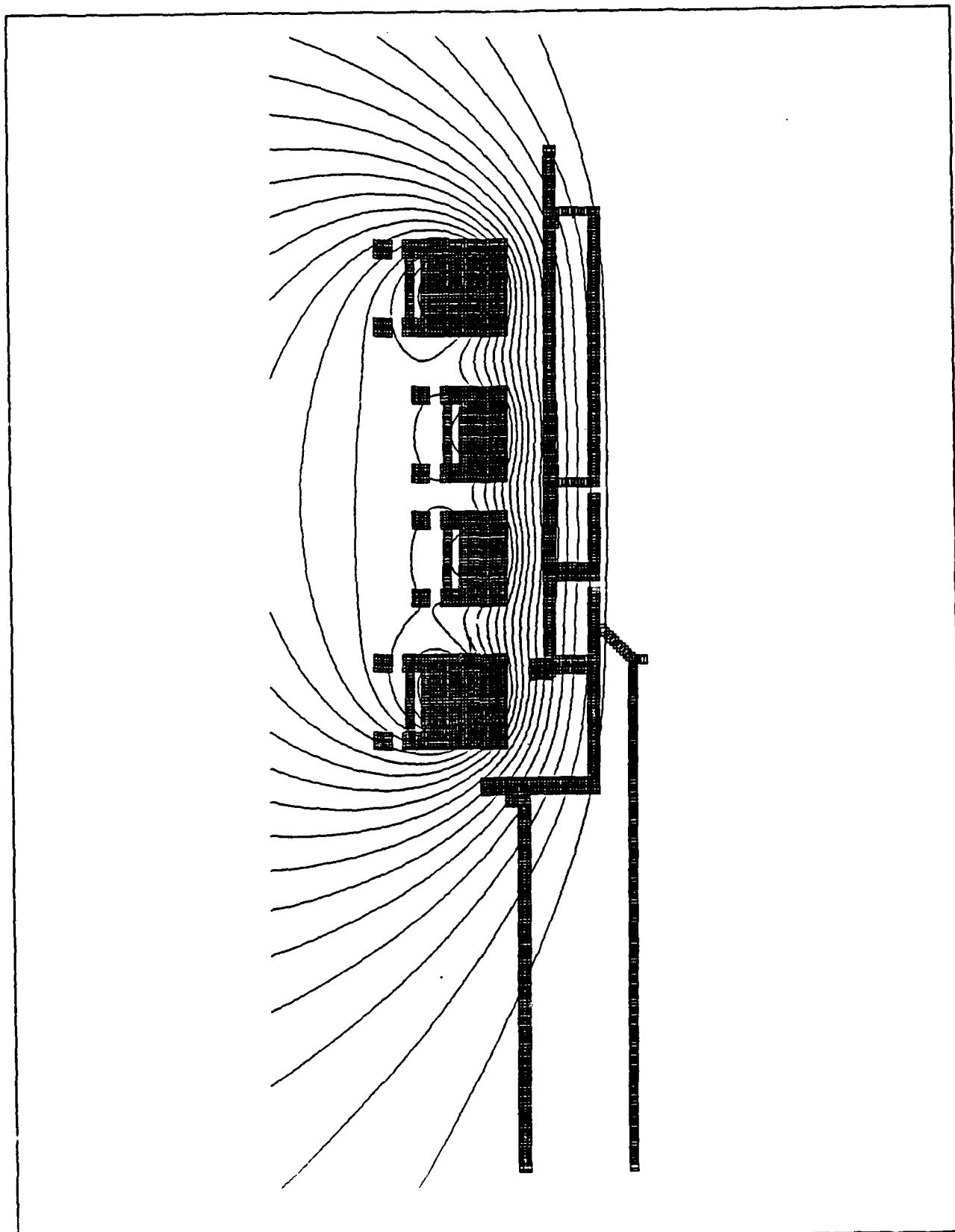
Figure 10 Steady state result from MAGDIF.
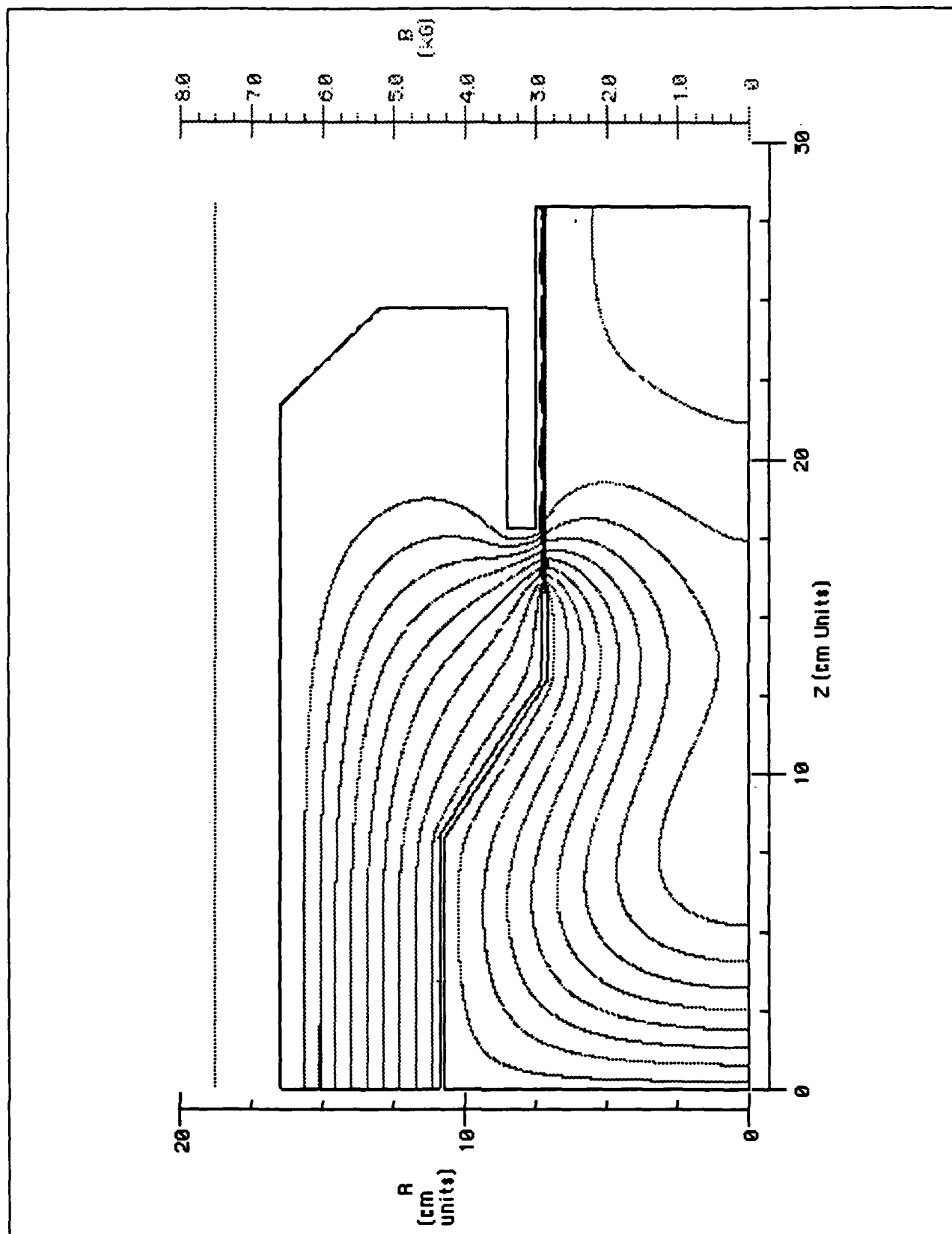
Figure 11 Sample result of electron emission in a uniform magnetic field from EGUN.

17

3.4 RKA

The one-dimensional (1-D) buncher code RKA was written to allow rapid simulation of the amplifier gap space and drift spaces is based on the theory of Solymar (Ref. 25). This code propagates the electron beam through a single modulating gap, with a specified voltage, frequency, and gap extent. The beam space charge is an input parameter which is calculated following the formalism of Reference 26. The user must provide as parameters the voltage applied at the gap, and the space charge reduction factor or plasma reduction factor (PRF). One postulates an applied voltage on the first gap, and the code provides the beam modulation through the drift·space following the gap. The output data file may then be used as input to any subsequent modulating gaps (which may be either externally or self-excited). This program allows for any number of modulating gaps to be used to modulate the electron beam by changing $\alpha=V_{rf}/V_{diode}$, nrun to 1, and renaming the output data file to be the input data file for the subsequent simulation (see Appendix E).

A simulation for the predicted beam modulation and optimum phase bunching of the electron beam kinetic energy for the final experimental configuration and parameters are shown below (Figs. 12 and 13). The table of input values yielded the graphical results of two RKA simulations. The first begins at the input to the first gap and concludes at the z coordinate of the second gap. The output of the first simulation was used as input for the second simulation. The second gap voltage is initially chosen to give the desired maximum modulation coefficient. If this value is unrealistic in amplitude, then one must redesign the experiment to remove this problem.
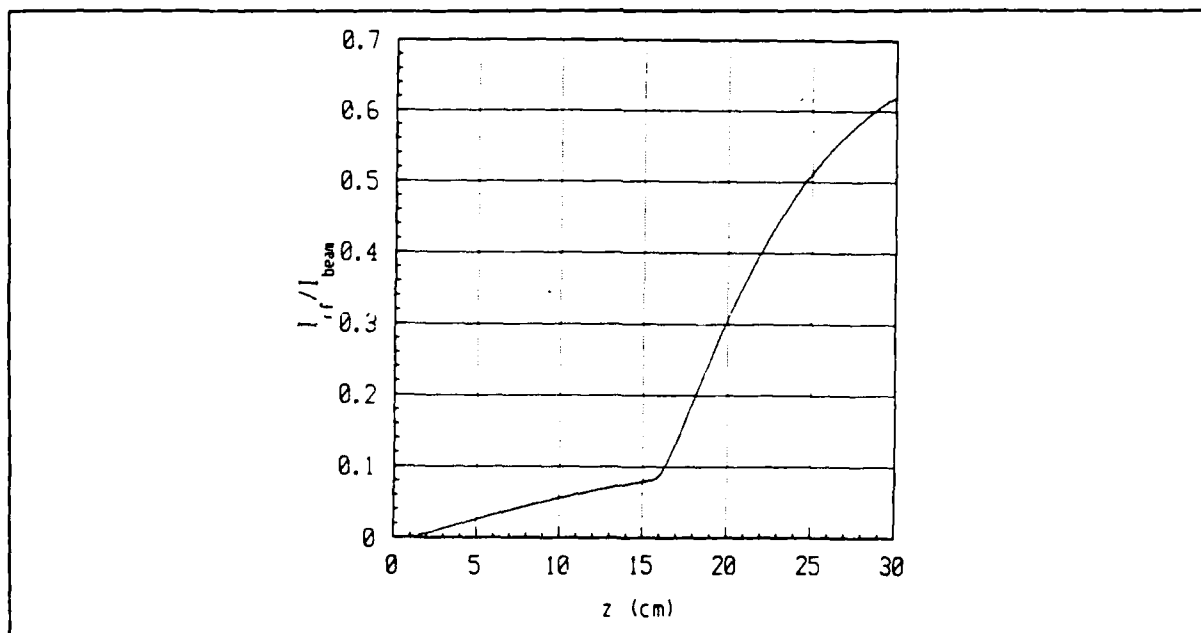
Figure 12 RKA result of modulation coefficient versus axial drift distance.

18
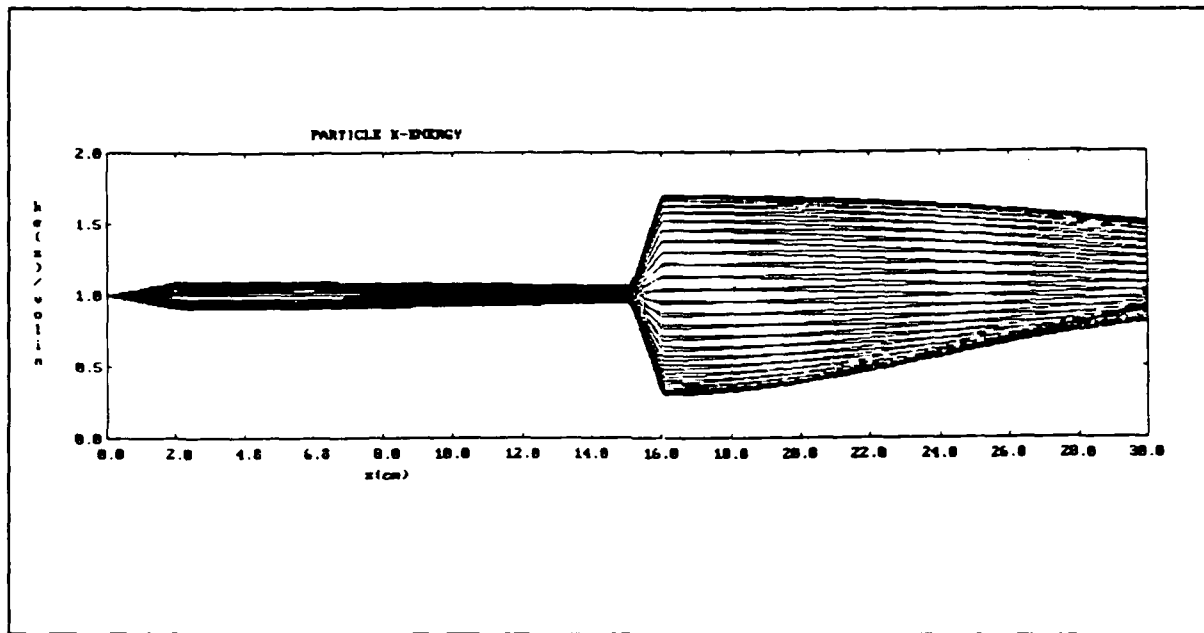
Figure 13 Sample result from RKA showing kinetic energy phase bunching versus drift distance.

TABLE 1. Sample RKA input data

Diode Voltage	400 kV	Gap size	2.0 cm
Diode Current	16 kA	Drift space	13.0 cm
Drift wall radii	7.65 cm	First gap voltage	40 kV
Outer beam radii	7.10 cm	Second gap voltage	280 kV
Inner beam radii	6.60 cm		

That this code is very versatile and allows one to rapidly try any sequence of modulation cavities, drift distances, and applied/inauced modulating voltages. The main limitation is that the applied voltage α is that voltage actually at the position of the beam, not the voltage developed in the gap. This may be a difficult value to estimate. The value of the PRF is not determined self-consistently as the beam is modulated. These issues are minor, because excellent agreement with MAGIC has been obtained.

3.5 MAGIC

The particle-in-cell (PIC) code MAGIC has been used to model the electron beam dynamics of an intense annular electron beam propagated through an RKA system. MAGIC is a 2½-D, fully electromagnetic and relativistic, self-consistent PIC code (Ref. 23). The major limitation is that one spatial dimension must be assumed ignorable, or that any motion is isotropic in that dimension. For this project this limitation is avoided by the azimuthal symmetry of the device. To investigate if any azimuthal dynamics occur, one would have to employ a full 3-D code such as SOS or ISIS.

MAGIC has been used to simulate the propagation of the electron beam through the RKA without an applied voltage on the first gap. This demonstrated that the ABA simulation did not self-oscillate. The simulation was an injection run with a uniform axial magnetic field of 8 kG. The injection simulation allows one to complete the simulation much quicker, however the accuracy may be suspect as self-consistency is sacrificed. The simulations typically only match the first 60 ns of the 300 ns pulse. This is due to the inherent problem of numerical noise generated by the finite differencing employed to solve the system of differential equations. This problem is not only with MAGIC but with all finite difference technique codes. The limitation on problem time also impacts the ability to simulate other physics, such as plasma production on grounded surfaces or self-ionization of background gas. These phenomena typically occur on a much longer time scale than one can simulate with present computer systems.

A problem occurred in trying to complete an emission simulation employing the original cathode. The technique of gridding the problem space causes "stair-stepping" on slanted lines. This causes enhanced emission from the corners of the jagged lines. If one tries to increase the number of mesh points to allow better replication of the "real" system, problems arise in execution speed because of the number of mesh points. These issues are being raised, because they limit ones ability to make the code predictive instead of a qualitative guide.

A uniform axial magnetic field was used in the initial simulations. Clearly that does not accurately reflect the magnetic field generated by the pulse field coils. MAGNET was used to generate a series of radial contours of the axial and radial magnetic fields as functions of axial coordinate. These contours were then put in matrix form and read into MAGIC. This allows simulation of the magnetic focusing used in the new "Friedman/Fazio" cathode (Refs. 6,13). The curving magnetic flux lines are crucial to demonstrating that the full 16 kA of electron beam current goes into the amplifier and not away from the region of interest. The matrices for B_z and B_r are shown below:

20

B$_z$ (Tesla) =

0.3863	0.3854	0.3825	0.3772	0.3689	0.3566	0.3393	0.3158	0.2855
0.4353	0.4347	0.4328	0.429	0.4225	0.4121	0.3957	0.3712	0.3368
0.4867	0.4866	0.4862	0.485	0.4821	0.4759	0.4635	0.441	0.4039
0.5383	0.5389	0.5405	0.5431	0.5458	0.5473	0.5441	0.5299	0.4949
0.5875	0.5888	0.5929	0.5999	0.6099	0.6226	0.6359	0.6424	0.6234
0.6314	0.6334	0.6396	0.6508	0.6681	0.6938	0.7303	0.7776	0.8135
0.6676	0.6699	0.6773	0.6909	0.713	0.7479	0.8046	0.9031	1.091
0.6944	0.6968	0.7041	0.7174	0.739	0.7734	0.8298	0.9306	1.14
0.7123	0.7142	0.72	0.7304	0.7464	0.7702	0.8047	0.8513	0.8903
0.7228	0.724	0.7276	0.7335	0.7415	0.7508	0.7588	0.7575	0.7269
0.7284	0.7289	0.7304	0.7321	0.7328	0.73	0.7188	0.6909	0.6344
0.7318	0.7319	0.7318	0.7309	0.7273	0.718	0.6976	0.6583	0.5917
0.7347	0.7346	0.7342	0.7326	0.7285	0.7191	0.6994	0.6609	0.5924
0.7378	0.7379	0.7378	0.7374	0.7361	0.7325	0.7236	0.7012	0.6445
0.7408	0.7411	0.7418	0.7433	0.7461	0.7514	0.7613	0.7766	0.777
0.743	0.7433	0.7446	0.7473	0.7529	0.7645	0.7898	0.8489	1.011
0.7438	0.7441	0.7452	0.7476	0.7525	0.7626	0.7844	0.8331	0.9409
0.7434	0.7435	0.7438	0.7445	0.7457	0.7477	0.7507	0.7511	0.7241
0.7426	0.7424	0.7419	0.7406	0.7377	0.7311	0.7167	0.6846	0.6166
0.7423	0.742	0.7411	0.7388	0.7339	0.7234	0.7017	0.6589	0.5822
0.7429	0.7428	0.7421	0.7405	0.7368	0.7289	0.7118	0.6757	0.6042
0.7442	0.7443	0.7444	0.7446	0.7448	0.7448	0.7433	0.7343	0.6931
0.7453	0.7456	0.7466	0.7487	0.753	0.7617	0.78	0.8186	0.8854
0.7454	0.7458	0.7471	0.7499	0.7557	0.7677	0.7941	0.8571	1.048
0.744	0.7443	0.7452	0.7472	0.7509	0.7581	0.7723	0.7982	0.824
0.7415	0.7416	0.7418	0.742	0.7417	0.7402	0.735	0.7188	0.6686
0.7386	0.7386	0.7383	0.7372	0.7338	0.7256	0.7077	0.6713	0.6034
0.7357	0.7358	0.7358	0.7349	0.7315	0.7222	0.7018	0.6622	0.5945
0.7323	0.7328	0.7341	0.7356	0.7358	0.7321	0.7193	0.6892	0.6304
0.7268	0.728	0.7313	0.7368	0.7439	0.7515	0.7566	0.7509	0.7152
0.7168	0.7186	0.7242	0.734	0.7492	0.7713	0.8023	0.8418	0.8678
0.6996	0.7019	0.709	0.7221	0.7432	0.7767	0.8312	0.9269	1.111
0.6735	0.6758	0.6833	0.697	0.7192	0.7545	0.8124	0.915	1.126
0.6381	0.6401	0.6465	0.658	0.6761	0.7031	0.7424	0.7957	0.8433
0.5947	0.5961	0.6005	0.6079	0.6188	0.6329	0.6486	0.6587	0.6432
0.5457	0.5464	0.5483	0.5513	0.5548	0.5573	0.5556	0.543	0.5088
0.494	0.494	0.4938	0.493	0.4906	0.4851	0.4734	0.4514	0.414
0.4424	0.4418	0.44	0.4364	0.4303	0.4201	0.4039	0.3794	0.3444
0.3929	0.392	0.3891	0.3839	0.3757	0.3635	0.3461	0.3224	0.2915
0.3469	0.3458	0.3424	0.3365	0.3276	0.315	0.2982	0.2766	0.25
0.3052	0.304	0.3005	0.2945	0.2857	0.2737	0.2582	0.2392	0.2167
0.268	0.2669	0.2635	0.2578	0.2495	0.2385	0.2248	0.2084	0.1894
0.2353	0.2343	0.2311	0.2258	0.2184	0.2086	0.1967	0.1826	0.1667
0.2068	0.2058	0.203	0.1983	0.1916	0.1832	0.1728	0.1609	0.1475
0.1819	0.1811	0.1786	0.1745	0.1687	0.1614	0.1526	0.1424	0.1312
0.1605	0.1597	0.1576	0.154	0.149	0.1427	0.1352	0.1266	0.1172
0.1419	0.1413	0.1394	0.1363	0.132	0.1267	0.1203	0.113	0.105
0.1258	0.1253	0.1237	0.121	0.1174	0.1128	0.1074	0.1012	0.09447
0.1119	0.1115	0.1101	0.1078	0.1047	0.1008	0.0962	0.09097	0.08524
0.09986	0.09947	0.09829	0.09636	0.09371	0.09038	0.08646	0.08201	0.07713
0.08938	0.08904	0.08804	0.08639	0.08413	0.08129	0.07794	0.07415	0.06999

B$_r$ (Tesla) =

0	-0.024	-0.048	-0.073	-0.098	-0.12	-0.15	-0.18	-0.2
0	-0.025	-0.051	-0.078	-0.11	-0.14	-0.17	-0.2	-0.24
0	-0.026	-0.053	-0.082	-0.11	-0.15	-0.19	-0.23	-0.28
0	-0.026	-0.052	-0.082	-0.11	-0.15	-0.2	-0.26	-0.33
0	-0.024	-0.049	-0.076	-0.11	-0.15	-0.2	-0.27	-0.37
0	-0.02	-0.042	-0.065	-0.092	-0.13	-0.17	-0.25	-0.4
0	-0.016	-0.032	-0.049	-0.067	-0.088	-0.12	-0.16	-0.3
0	-0.011	-0.022	-0.031	-0.039	-0.043	-0.04	-0.017	0.087
0	-0.0067	-0.013	-0.016	-0.015	-0.0064	0.019	0.078	0.21
0	-0.0036	-0.0061	-0.006	-0.0011	0.013	0.041	0.095	0.18
0	-0.0019	-0.0029	-0.0019	0.0029	0.014	0.034	0.067	0.11
0	-0.0014	-0.0023	-0.0023	-0.00066	0.0031	0.0098	0.02	0.035
0	-0.0015	-0.003	-0.0047	-0.007	-0.011	-0.019	-0.033	-0.05
0	-0.0016	-0.0036	-0.0064	-0.011	-0.021	-0.041	-0.078	-0.14
0	-0.0014	-0.0031	-0.0058	-0.011	-0.02	-0.042	-0.091	-0.2
0	-0.00076	-0.0016	-0.0027	-0.0045	-0.0079	-0.015	-0.036	-0.12
0	-1.8e-005	0.0002	0.001	0.0033	0.0087	0.022	0.057	0.18
0	0.00044	0.0013	0.0033	0.0077	0.018	0.04	0.088	0.19
0	0.00038	0.0011	0.0027	0.0062	0.014	0.029	0.059	0.11
0	-7.6e-005	-0.00011	-5.1e-005	0.00023	0.00096	0.0025	0.0055	0.0097
0	-0.00058	-0.0015	-0.0031	-0.0063	-0.013	-0.026	-0.05	-0.087
0	-0.00074	-0.0019	-0.0042	-0.009	-0.019	-0.041	-0.087	-0.18

0	-0.00039	-0.0011	-0.0026	-0.0058	-0.013	-0.03	-0.072	-0.2
0	0.00034	0.00068	0.0011	0.0016	0.0027	0.0053	0.013	0.049
0	0.0011	0.0024	0.0046	0.0086	0.017	0.036	0.083	0.21
0	0.0014	0.0032	0.0059	0.011	0.021	0.041	0.082	0.15
0	0.0015	0.003	0.0048	0.0076	0.013	0.023	0.041	0.066
0	0.0014	0.0025	0.0027	0.0018	-0.00064	-0.0048	-0.011	-0.021
0	0.0019	0.003	0.0021	-0.0021	-0.012	-0.03	-0.06	-0.1
0	0.0035	0.0059	0.0058	0.00092	-0.012	-0.04	-0.091	-0.17
0	0.0065	0.012	0.015	0.014	0.0042	-0.022	-0.082	-0.21
0	0.011	0.021	0.03	0.037	0.039	0.032	0.0021	-0.12
0	0.015	0.031	0.047	0.064	0.084	0.11	0.15	0.27
0	0.02	0.041	0.063	0.09	0.12	0.17	0.25	0.4
0	0.024	0.048	0.075	0.11	0.15	0.2	0.28	0.38
0	0.026	0.052	0.082	0.11	0.15	0.2	0.26	0.33
0	0.026	0.053	0.082	0.11	0.15	0.19	0.24	0.28
0	0.026	0.052	0.079	0.11	0.14	0.17	0.21	0.24
0	0.024	0.048	0.074	0.1	0.13	0.15	0.18	0.2
0	0.022	0.044	0.067	0.089	0.11	0.13	0.15	0.17
0	0.02	0.039	0.059	0.079	0.098	0.12	0.13	0.15
0	0.017	0.035	0.052	0.069	0.085	0.099	0.11	0.12
0	0.015	0.03	0.045	0.059	0.073	0.085	0.096	0.1
0	0.013	0 026	0.039	0.051	0.063	0.073	0.082	0.09
0	0.012	0.023	0.034	0.044	0.054	0.063	0.071	0.077
0	0.01	0.02	0.029	0.038	0.047	0.054	0.061	0.066
0	0.0086	0.017	0.025	0.033	0.04	0.047	0.052	0.057
0	0.0074	0.015	0.022	0.029	0.035	0.04	0.045	0.049
0	0.0064	0.013	0.019	0.025	0.03	0.035	0.039	0.043
0	0.0056	0.011	0.016	0.021	0.026	0.03	0.034	0.037
0	0.0049	0.0097	0.014	0.019	0.023	0.027	0.03	0.033

where each row is for a different axial position and each column reflects a
different radial contour. The spacing for the data in the matrices is $\Delta z = 1$
cm and $\Delta r = 0.5$ cm.

Additional physics dealt with imposing the proper voltage on the first gap.
One then observes the beam modulation build up as the beam propagates through
the ABA, and the induced voltage developed on the idler cavity. MAGIC employs
a command called "antenna" which specifies a current density on a wire dipole
model. To compare experiment and simulation would require calibrating the
amplitude to know the power required from the external oscillator. Instead,
we monitor the rf mode, the voltage on the modulation gap and infer the same
voltage from an electric field probe in the cavity. This indicates whether
the input cavity is driven with sufficient power to modulate the electron
beam. Sample plots from MAGIC of the voltage on the first and second gap are
shown (Figs. 14 and 15).

The drop in voltage (Fig. 14) is due to beam loading of the modulating gap.
This effect has been seen by Fazio, and will be discussed later. The
amplitude of the voltage on the second gap corresponds well with the assumed
voltage used in the second gap of the RKA simulations. A representative plot
(Fig. 16) of the beam modulation based on simulations with MAGIC and RKA is
shown. Note the qualitative and quantitative agreement.
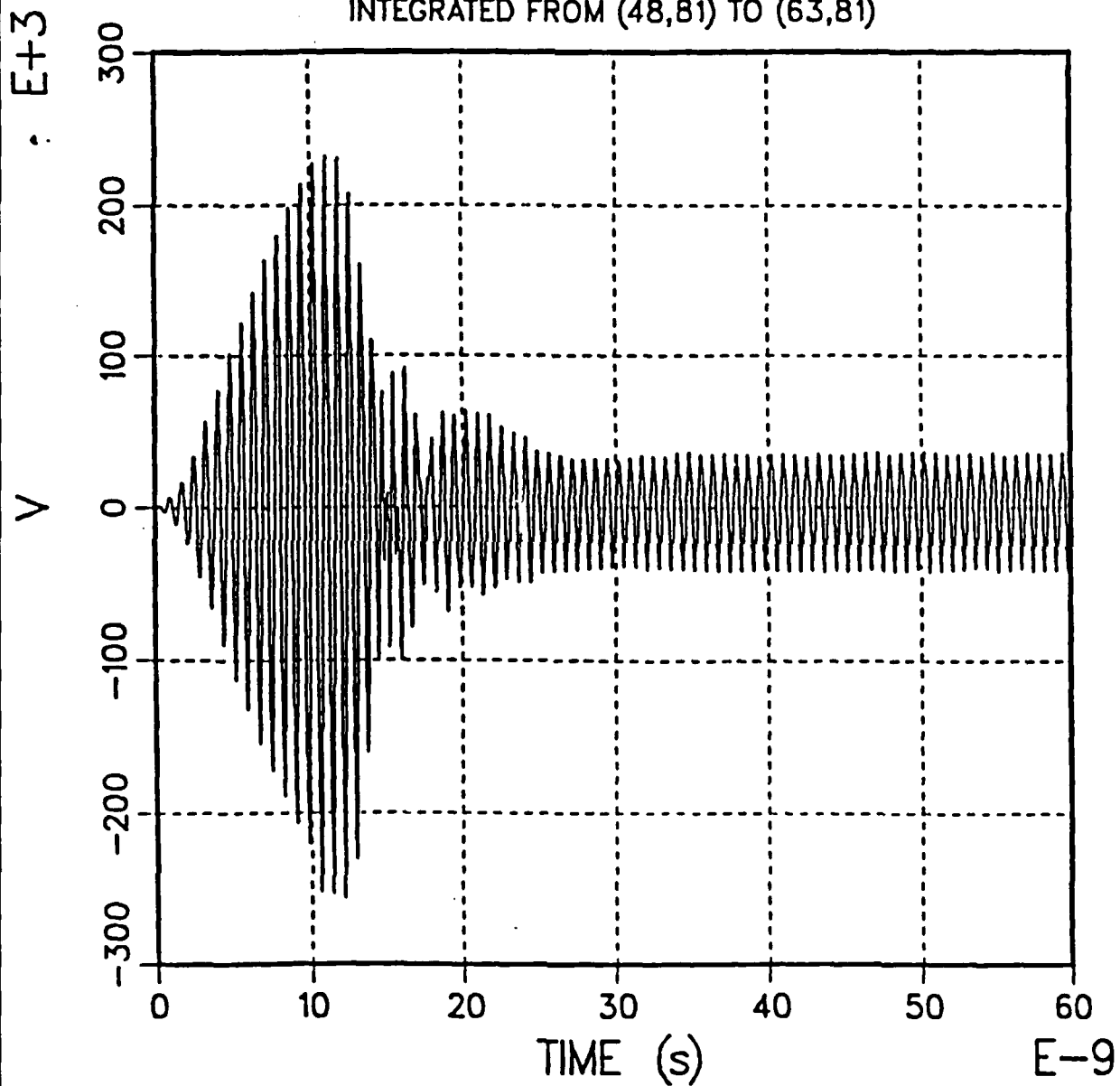
Figure 14 Time variation of modulation gap voltage from MAGIC.
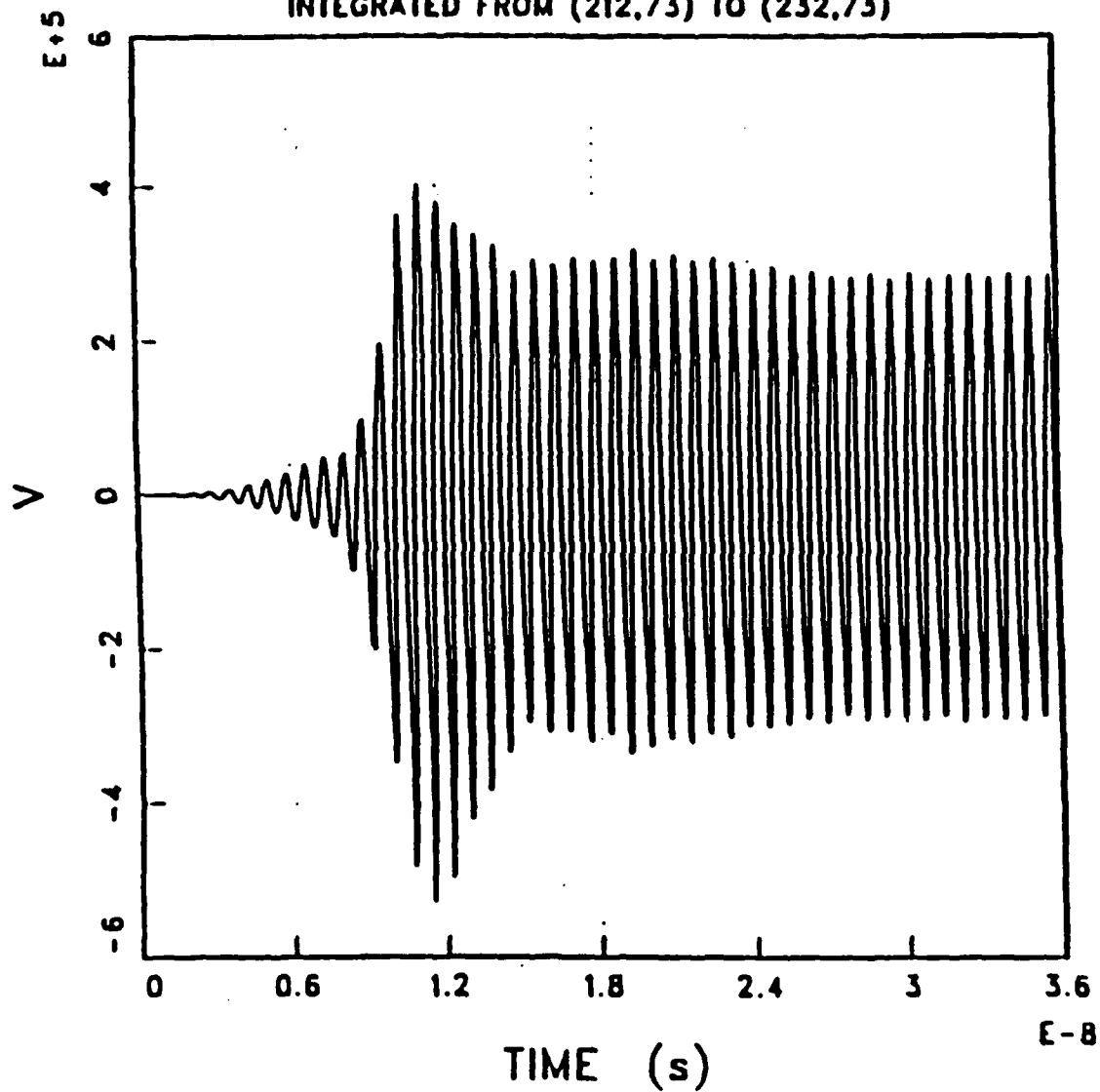
Figure 15 Time variation of idler gap voltage from MAGIC.
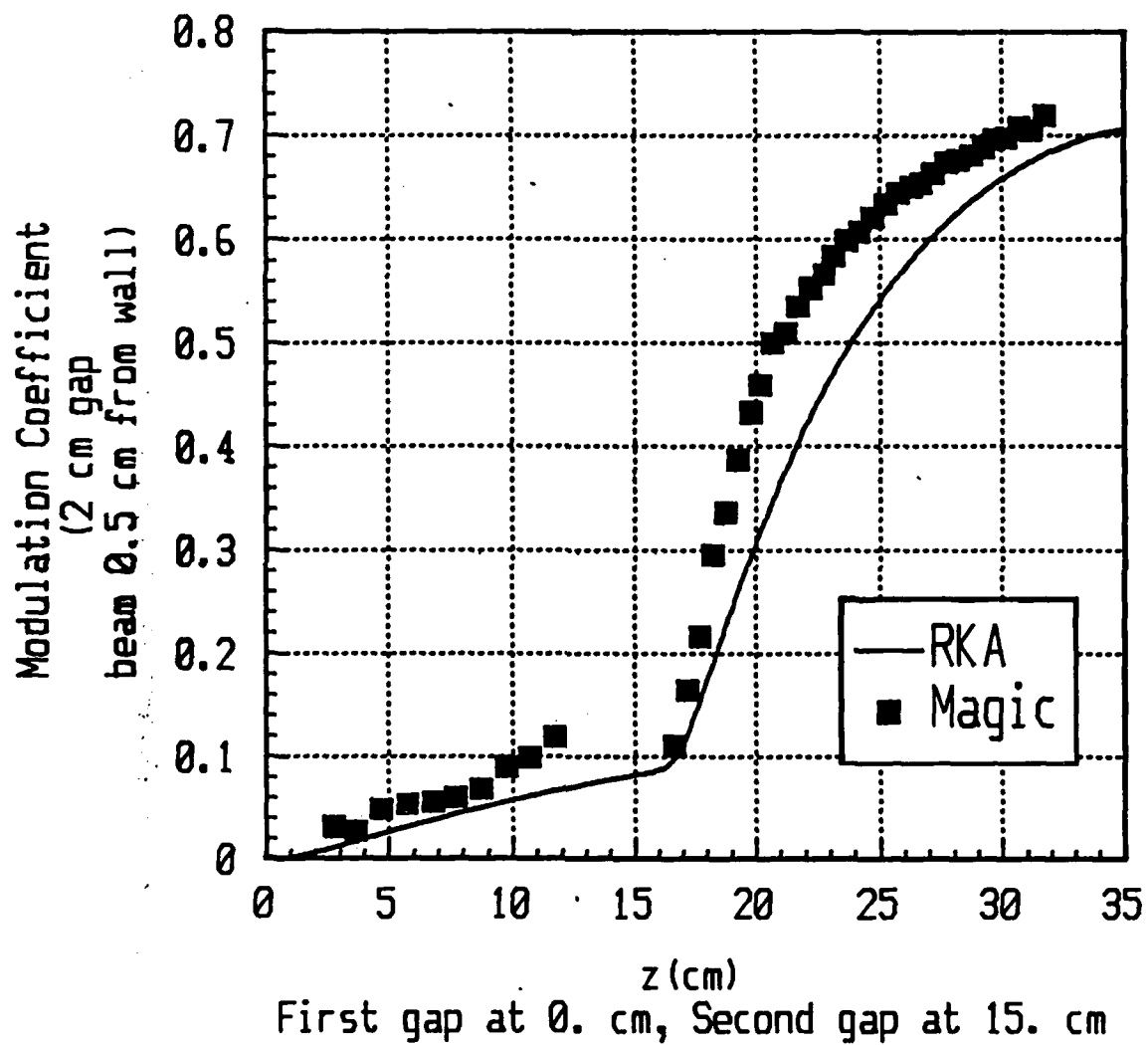
Figure 16 Comparison of MAGIC and RKA results of axial variation of beam modulation.

4.0 EXPERIMENTAL RESULTS

4.1 OSCILLATOR COUPLING/BEAM LOADING

To develop the modulating voltage across the modulating gap, a signal from an external oscillatoris requied. A 500-kW, 2-μsec magnetron, which is tunable from 1.25 GHz to 1.35 GHz was employed. We use a 12-dB isolator on the output of the magnetron to reduce the reflected signal coupling into the magnetron. A dual waveguide loop coupler is used to monitor the input power to the cavity and the reflected power from the B-dot coupling loop in the modulating cavity. These monitors are used both in cold tests and experiments with the electron beam. The difference in the two waveguide power monitors should time correlate with power detected in the cavity by the E-dot probe.

In principle one could construct a B-dot loop in the cavity with the proper cross sectional area and conductor size to match the waveguide impedance. In practice, this is very difficult because the mode within the cavity must be known to determine the area required to match the real part of the impedance, and adjusting the size of the conductor used in forming the loop to cancel the reactive impedance is impractical. Also, this impedance match must be done for each frequency used in the amplifier. A solution was to use a double stub tuner which could easily be adjusted outside the experimental system regardless of the frequency of operation. We chose a double stub tuner over a single stub tuner simply due to our inability to place the tuner at a maximum in the line standing wave ratio (SWR) pattern.

Figures 17 and 18 show data for the reflection and transmission characteristics of the B-dot coupling loop into the modulation cavity. The reflection is shown by the S_{11} parameter, and the transmission is shown by the S_{21} parameter from the network analyzer. The calibration procedure used standard 50 Ω RG-214 cable to connect the analyzer to the experiment. The device under test included a type-N to WR-650 adapter, a section of WR-650 waveguide with a dielectric plate used to make an air-vacuum interface, another WR-650 to vacuum coaxial line, the double stub tuner, the coupling loop within the cavity, and the E-dot cavity probe. This allows the observed reflection to be the composite of all the connections in the transmission line. The transmission coefficient (Fig. 18) included all the effective areas of the coupling loop and the E-dot probe. The reflection was typically viewed on a Smith Chart, where a match to input was shown as an intersection with the origin of the chart.

While it is trivial to use the double stub tuner to match the B-dot coupling loop to the 50 Ω waveguide impedance at the cavity frequency, we have observed, as has Fazio (Ref. 13), that matching the cold test cavity frequency does not provide optimum matching during the presence of the electron beam. In fact, one must view the cold cavity impedance as shunted by the electron beam impedance. This combined load, which is dominated by the lower electron beam impedance, must be matched to the waveguide/B-dot launcher. This parallel impedance causes a slightly different matching condition for the B-dot coupler into the modulation cavity. Two methods may be employed to compensate for this beam loading of the cavity. First, the double stub tuner may be properly adjusted for this new optimum frequency. Secondly, if the cavity has a lower beam loaded Q, adjust the frequency of the magnetron by a few MHz until the double stub tuner provides a match to the loaded cavity.

The reader should recall that the modulating cavity voltage observed in the MAGIC simulations also shows this beam loading. The voltage drop, which occurs after the 10-ns delay to fill the cavity, is a manifestation of electron beam loading.
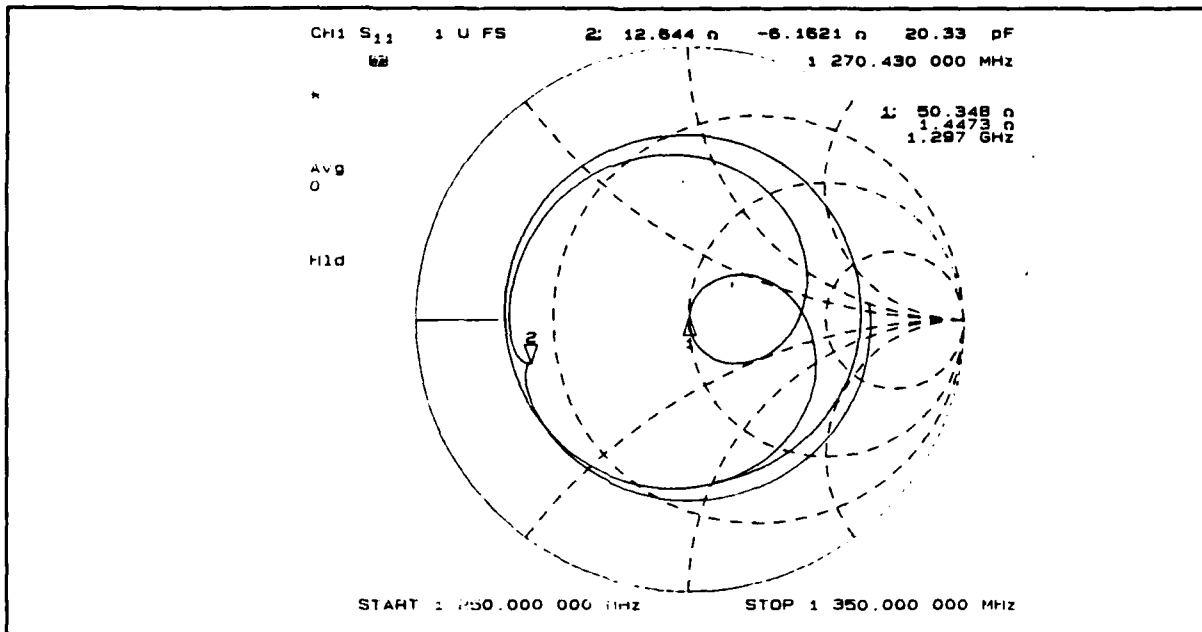
Figure 17 Results of modulation cavity cold tests showing impedance matching of waveguide to cavity.
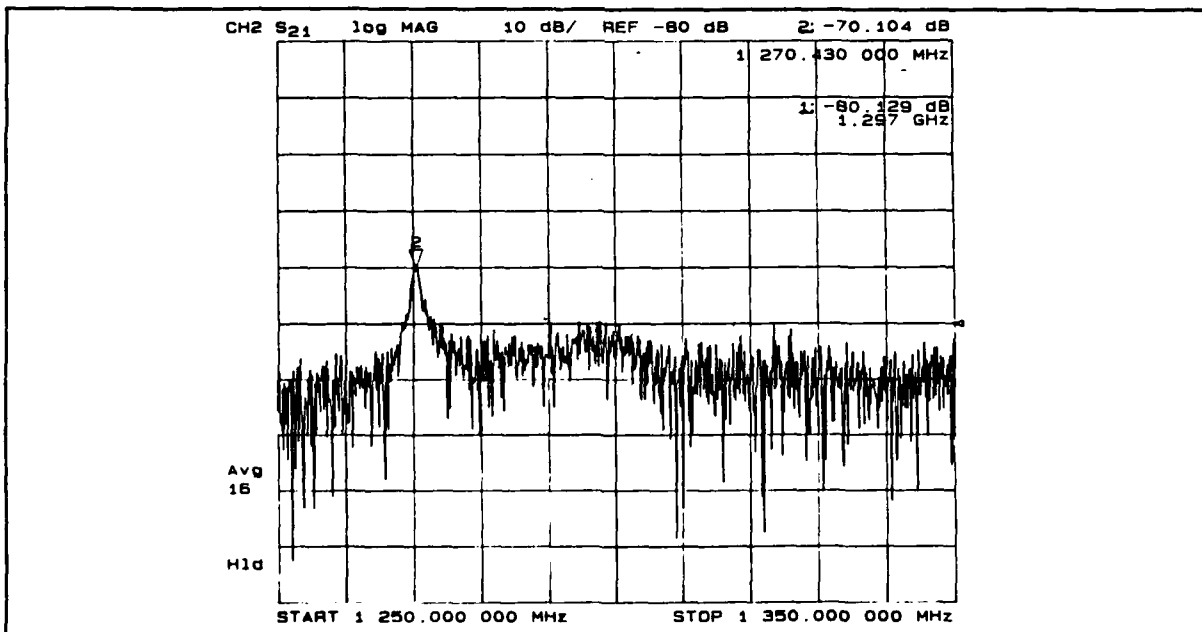
Figure 18 Results of coupling coefficient from cavity E-dot probe when impedance matching is satisfied.

27

4.2 BEAM PROPAGATION

One of the first experiments to be completed in this type of project is the generation and propagation of an intense electron beam through the microwave circuit and extractor region of the amplifier. To generate an intense, or high power, electron beam requires that the product of the beam voltage and current be large, typically on the order of a few GW of power. This requirement specifies the voltage or impedance of the electron beam. A constraint is that the electron beam current must be below the space charge limiting current for the beam cross section in the beamline of the vacuum vessel. For this experiment with a 7.65-cm radius beam line, and the electron beam between 6.6 to 7.1 cm, one finds that the space charge limiting current is 22 kA for a 400-kV electron beam. As the beam modulation grows or as the beam passes by the modulation and idler gaps, the space charge limiting current condition is violated. However, the transit time of the gaps is small compared to the rf wavelength, therefore the potential for self-oscillation or reflection of electrons is minimized.

A series of experiments were conducted with both cathode geometries to demonstrate the propagation of the electron beam through the microwave circuit. The original cathode in a uniform magnetic field, the modulating cavity and the diagnostic package with an inserted graphite witness plate were used to image the electron beam at various axial positions. The A-K gap in this configuration is simply the radial separation of the cathode and wall. The beam propagated for a maximum of 55 cm. The witness plate showed a time integrated image of the electron beam which was of 5-mm uniform thickness, and the image inner radius matched the outer radius of the original cathode (Fig.19). The only occasion which the witness plate showed a thicker image was when the plate was a few centimeters from the cathode. The thickening of the beam pattern was due to the psuedo-ground formed by the graphite plate.
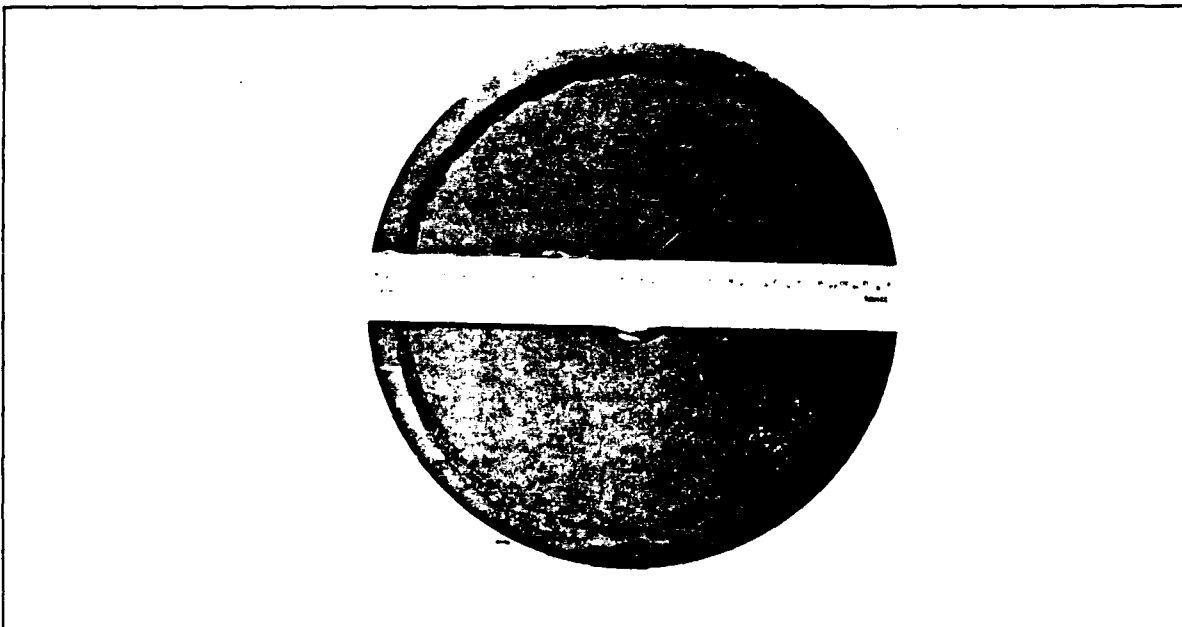
Figure 19 Sample of graphite witness plate data for uniform field propagation.

28
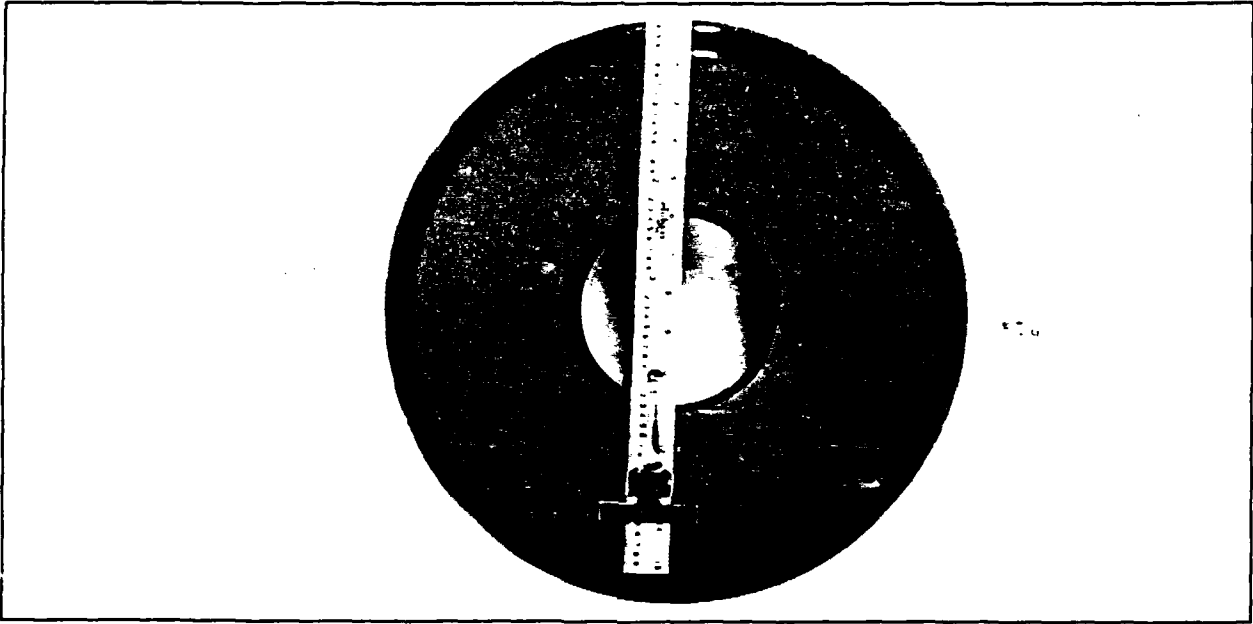
Figure 20 Sample data from the graphite witness plate for converging magnetic field propagation.

A second series of experiments was done with the second cathode located in both a converging and uniform magnetic field. In this geometry the A-K gap is primarily axial, but there is a small radial separation. The beam is propagated through the modulating gap, idler gap, and the diagnostic package. The total axial distance is 65 to 70 cm. Recall the magnetic field coils are only deemed uniform for about 50 cm. These experiments dealt with varying the position of the cathode in the portion of the magnetic field where the field changes from mainly B_r to B_z and the size of the A-K gap. The goal was to determine the proper positions to get the 16 kA beam through the beamline, and to have the witness plate indicate that the beam has the desired thickness and radius (Fig. 20). This set of experiments also provided a check on the accuracy of the B-dot probe array calibrations, and the azimuthal uniformity of the electron beam.

The position of the cathode, in order to provide the proper witness plate pattern was about 6 cm further from the anode than anticipated. This also required fabrication of an anode extension of 4 cm such that the A-K gap remained at about 2 cm. Sample data are shown in Figure 21 for the case of a 3-cm anode extension, 3-cm A-K gap, and the magnets in the original position. Notice that the current diagnostics indicate about 2 kA of current loss, however the witness plate indicates that the beam is several mm from the wall. Inspection of the "cathode end" of the anode found several burn marks indicating beam scrape-off at the anode. The B-dots of the diagnostic package agree with the exit Rogowskii indicating no additional loss as the beam travels through the structure.

29
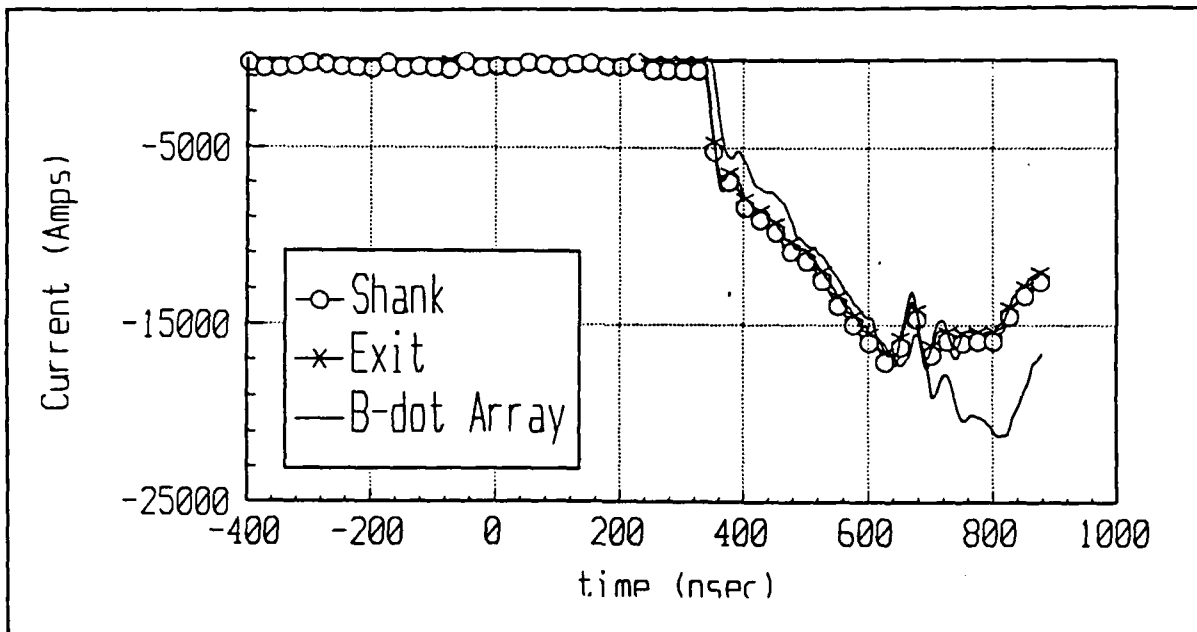
Figure 21 Samples of beam current data recorded by various diagnostics at different axial positions.

4.3 BEAM MODULATION

While using the original cathode system, there was a brief opportunity to attempt to modulate the electron beam. The data are not definitive nor quantitative. However, these data are good indicators of the ability to compensate for the electron beam loading, and this is a valid technique to modulate the electron beam.

As stated above, first a cold test calibration was completed, determining the cold resonant frequency, the transfer function for the cavity E-dot probe against the waveguide loop coupler monitoring the magnetron, and the relationship between the E-dot probe and the modulation gap voltage.

Then a series of electron beam pulses where the magnetron frequency was varied by 1- or 2- MHz steps from the cold cavity frequency. Observations included the following:

    1) A correlation between the time of the reduction of the reflected magnetron power during the time of the electron beam pulse (Fig. 22).

    2) An observation of signals from a line of the B-dot array. The signal amplitude varied with axial position. The results are not quantitative because the probe areas were not known at the time (Fig. 23). The data do show that the double stub tuner allows coupling of rf power into the cavity.

This series of experiments indicates a viable technique to modulate the electron beam and that the electron beam can carry the modulation to the idler cavity.

30
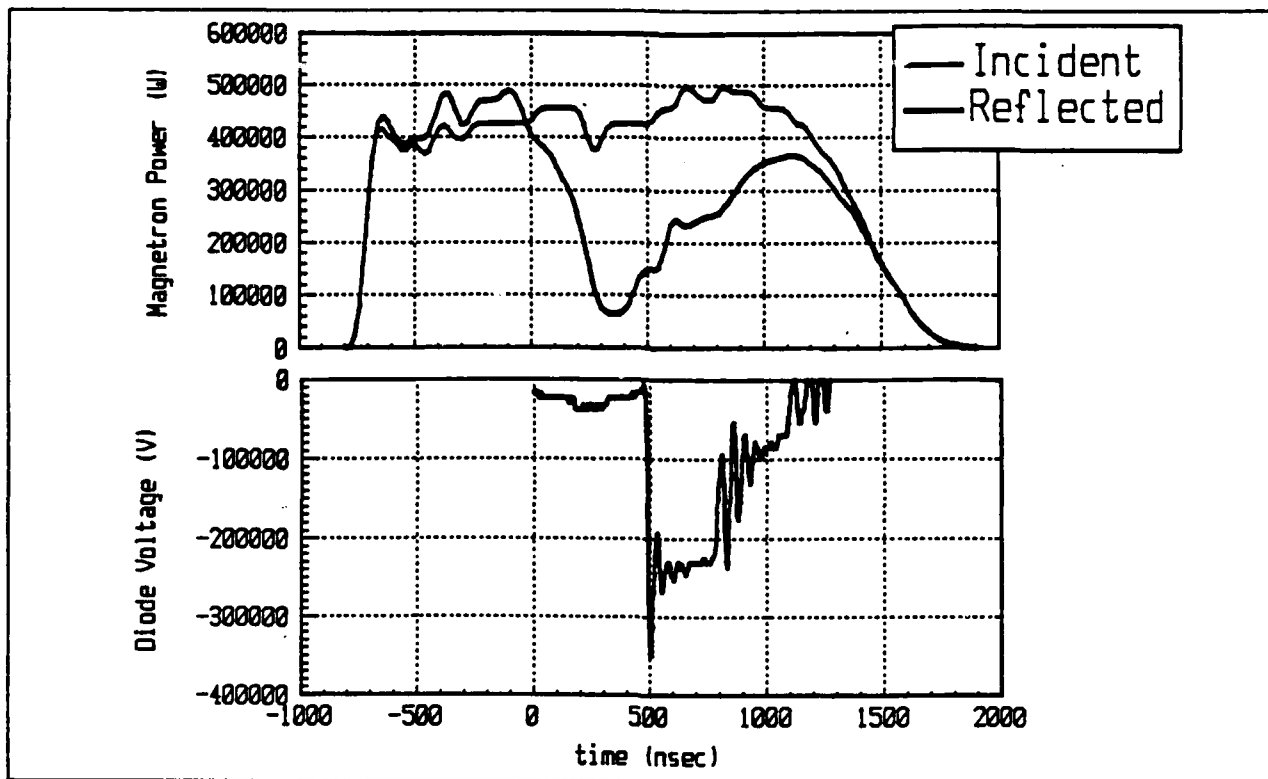
Figure 22 Overcoupled data showing reduction in reflected power during the duration of the electron beam pulse.
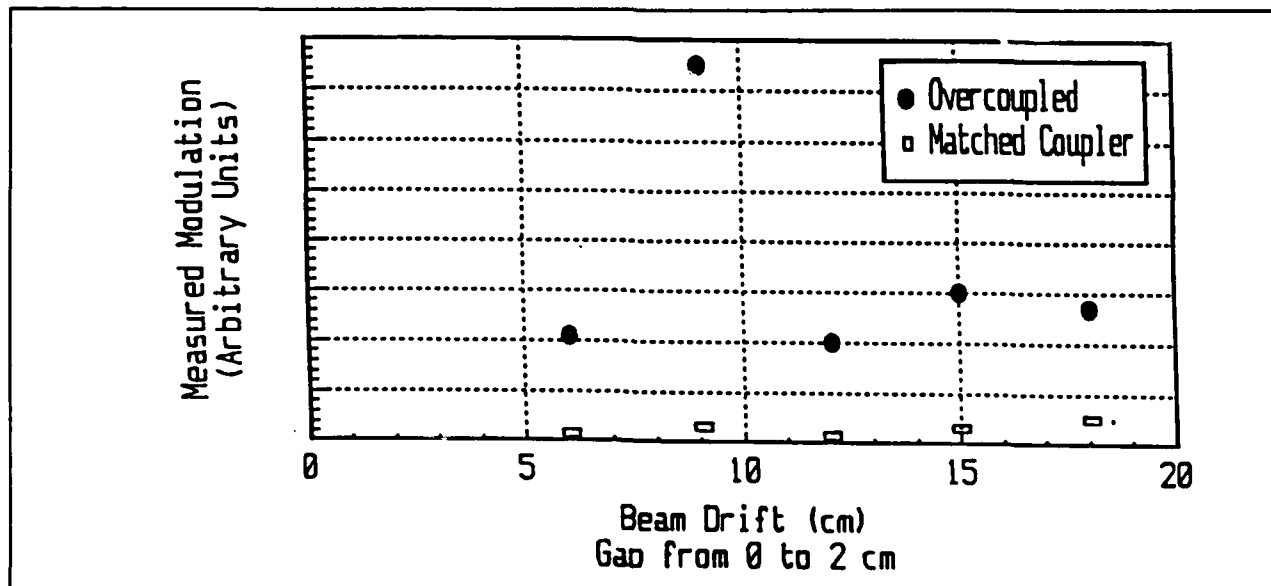
Figure 23 Axial variation of beam modulation data from the B-dot probe array.

5.0 FUTURE PLANS

There are three main projects which will be conducted in the near future: validation of the diagnostics; adding the idler cavity to validate the calculated beam modulation coefficient and beam propagation; and the design and construction of an efficient rf extractor.

5.1 VALIDATION OF DIAGNOSTICS

The various E-dot and B-dot probes have been independently calibrated, however, the interpretation of the data is yet to be validated. For instance in Section 4 we discussed the radial E-dot probe data as an indicator for the modulating gap voltage. However, our only cross check is to measure the beam modulation as the beam propagates past the modulating gap. Later on it may be useful to try and use a streak camera to validate the depth of the beam modulation at various axial positions.

5.2 IDLER CAVITY

The addition of the idler cavity requires an accurate determination of the axial drift distance to reach the peak of the beam modulation. This axial position may allow a flexibility of 1 or 2 cm in the exact position of the idler gap. The other question to be addressed is the formation of a virtual cathode in the idler gap due to the larger currents present in the modulated electron beam, and the larger vacuum wall radius. There are the options of adjusting the extent of the axial gap and tuning the idler cavity by the addition of volume displacements. These adjustments must be done self-consistently to achieve the largest beam modulation at the extractor position.

5.3 THE Rf EXTRACTOR

The rf extractor technique is presently undefined. Only certain axial positions allow one to extract the maximum rf power, due to the phase bunching of the electron beam. The research plan is to begin with the design of Fazio (Fig. 24). Again the idea is to validate or improve calculational techniques that one might employ in other HPM sources. We will simulate this rf extractor with several different computational tools, such as MAGIC and finite element codes like Hewlett-Packard's High Frequency Structure Simulator code. Each type of code brings different physics to the problem and allows one to focus on special issues. We will be looking at the modulated beam electron distribution function, the voltage generated on the rf extractor, the power coupled out by the extractor, and the difference in the input electron beam power and the remaining beam power following the rf extractor. Again, one can see that self-consistency checks are used whenever possible to ensure the accuracy of the calculations. These are the same checks that will be used experimentally if possible. The problem to be addressed has best been stated by Dr. Keith Kato: "Anyone can modulate an electron beam, but no one has been able to extract rf power." Finally, the rf extractor must incorporate an electron beam dump which does not cause problems in the rf extractor efficiency such as secondary electrons or plasma formation.

This research project has identified several limitations in the way HPM sources, specifically amplifiers, are developed. These limitations are being addressed for future HPM source requirements so that one may more quickly move from a concept or requirement to an operational source. One limitation that deserves additional comment is the material properties of the metal used to construct the microwave circuit. Plasma production, secondary electron emission, multipactoring, etc. are unavailable qualities of the conductors used in the simulations. Possibly these qualities will be included in future codes which will use massively parallel computers.

32
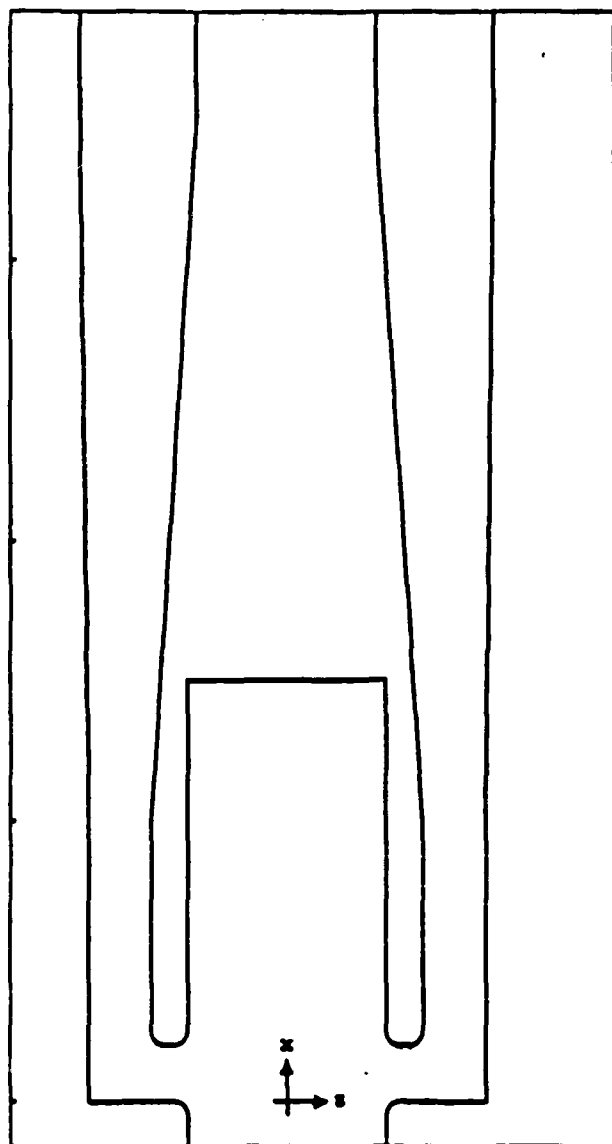
$f = 1300 \text{ MHz}$

$Q = 4$

Figure 24 RKA extractor design of Fazio.

REFERENCES

1. Friedman, M., and Herndon, M., "Emission of coherent radiation from a relativistic electron beam propagating in a spatially modulated field", Phys.Fluids, 16(11), ppgs 1982-1995, Nov. 1973

2. Friedman, M. and Serlin, V., "Modulation of Intense Relativistic Electron Beams by an External Microwave Source", Phys.Rev.Lett., 55(26), ppgs 2860-2863, 23 Dec. 1985

3. Friedman, M., Serlin, V., Drobot, A., Mondelli, A., "High-power Modulated Intense Relativistic Electron Sources with Applications to RF Generation and Controlled Thermonuclear Fusion", IEEE Trans. Plasma Science, 14(3), 3 June 1986

4. Friedman, M., Krall, J., Lau, Y.Y., Serlin, V., "Externally modulated intense relativistic electron beams", J.Appl.Phys., 64(7), ppgs 201-214, 1 October 1988, ppgs 3353-3379

5. Friedman, M., Krall, J., Lau, Y.Y., Serlin, V., "Efficient generation of multigigawatt rf power by a klystronlike amplifier", Rev. Sci. Instrum., 61(1), ppgs. 171-181, January 1990

6. Lau, Y.Y., Friedman, M., Krall, J., Serlin, V., "Relativistic Klystron Amplifiers Driven by Modulated Intense Relativistic Electron Beams", IEEE Trans. Plasma Sci., 18(3), ppgs 553-569, June 1990

7. Krall, J. and Lau, Y.Y, "Modulation of an intense beam by an external microwave source: Theory and Simulation", Appl.Phys.Lett., 52(6), ppgs 431-433, 8 Feb. 1988

8. Colombant, D.G. and Lau, Y.Y., "Nonlinear Beam Loading and Dynamical Limiting Currents in a High-Power Microwave Gap", Phys.Rev.Lett., 64(19), ppgs 2320-2323, 7 May 1990

9. Lau, Y.Y. and Chernin, D., "A review of the ac space-charge effect in electron-circuit interactions", Phys.Fluids B, 4(11), ppgs 3473-3497, Nov. 1992

10. Levine, J.S., Cooksey, N.J., Harteneck, B.D., Parks, C.W., Pomeroy, S.R., "A Relativistic Klystron Amplifier at High Average Power", Proc. of IEEE ICOPS, paper 3P8, 7-9 June 1993

11. Rickel, D.G., Fazio, M.V., Carlsten, B.E., Faehl, R.J., Haynes, W.B., Kwan, T.J.T., Stringfield, R.M., "Experimental Progress on a Microsecond Pulse-Length Relativistic Klystron Amplifier", Proc. of the SPIE, vol 1629, ppgs 51-56, Jan 1992

12. Carlsten, B.E., Fazio, M.V., Faehl, R.J., Kwan, T.J.T., Rickel, D.G., Stringfield, R.M., "Theory and modeling of a Relativistic Klystron Amplifier with high space charge for microsecond applications", Proc. of the SPIE, vol 1629, ppgs 57-68, Jan 1992

13. Fazio, M.V., "Long Pulse Relativistic Klystron High Power Microwave Source Research", LA-UR-92-744, Los Alamos National Laboratory, NM, 12 Feb. 1992

14. Fazio, M.V., Carlsten, B.E., Faehl, R.J., Haynes, W.B., Hoeberling, R.F., Kwan, T.J.T., Rickel, D.G., Stringfield, R.M., Vanhaaften, F.W., Wasierski, R.F., Erickson, A., Rust, K., "The Experimental and Theoretical Development of a One Gigawatt, Repetitively Pulse, One Microsecond Pulse Length, High Current Relativistic Klystron and Modulator", <u>Proc. of the 9th International Conf. on High Power Particle Beams</u>, Washington, D.C., 25-29 May 1992

15. Rickel, D.G., Carlsten, B.E., Fazio, M.V., Faehl, R.J., Kwan, T.J.T., Stringfield, R.M., Wasierski, R.F., "Development of a Long-Pulse 1.3 GHz Relativistic Klystron Amplifier", <u>IEEE Trans. on Plasma Sci</u>., 20(3), ppgs 373-382, June 1992

16. Fazio, M.V., Haynes, W.B., Carlsten, B.E., Faehl, R.J., Kwan, T.J.T., Stringfield, R.M., Wasierski, R.F., "Experimental Progress on a One Microsecond, One Kilojoule per pulse L-Band Relativistic Klystron", <u>Proc. of the SPIE</u>, 16-23 Jan 1993

17. Kato, K.G., Crouch, D.D., Sar, D.R., Speciale, R.A., Carlsten, B.E., Fazio, M.V., Haynes, B., Stringfield, R.M., "Recent Experimental results from a long pulse J-band relativistic klystron amplifier developmental effort", <u>Proc. of the SPIE</u>, Jan 1994

18. Kato, K.G., Crouch, D.D., Sar, D.R., Speciale, R.A., Carlsten, B.E., Fazio, M.V., Kwan, T.J.T., Stringfield, R.M., "Experimental results from a J-band relativistic klystron amplifier developmental effort", <u>Proc. of the SPIE</u>, Jan 1994

19. Granatstein, V.L. and Alexeff, I., (eds), <u>High-Power Microwave Sources</u>, Artech House, 1987

20. Benford,J and Swegle,J, (eds.), <u>High-Power Microwaves</u>, Artech House, 1991

21. Burkhart, S., "Coaxial E-field Probe for High-Power Microwave Measurements", <u>IEEE Trans. on Microwave Theory and Techniques</u>, 33(3), 3 March 1985, ppgs. 262-265

22. Los Alamos Accelerator Code Group, <u>Users Manual for the POISSON/ Group of Codes</u> and <u>Reference Manual for the POISSON/ Group of Codes</u>, LA-UR-87-115 and 126, Los Alamos National Laboratory, NM, 1987

23. Goplen, B., Ludeking, L., Smithe, D., Warren, G., <u>The MAGIC Users manual</u>, MRC/WDC-R-282, Mission Research Corporation, Alexandria, VA., 1991

24. Hermannsfeldt, W.B., <u>Electron Trajectory Program</u>, SLAC-226, Stanford Linear Accelerator Group, Stanford, CA, 1979

25. Solymar, L., "Exact Solution of the One-Dimensional (klystron) Solution to Finite Gaps", <u>Journal of Electronics and Control</u>, vol. 11 , ppgs 361-383, 1961

26. Branch, G.M. and Mihran T.G., "Plasma Frequency Reduction Factors in Electron Beams", <u>IRE Trans.-Electron Devices</u>, April, 1955, ppgs 3-11

APPENDICES

A. Determination of B-dot probe areas

The calibration technique employed to determine the effective area of any probe must include consideration of the nature of the result desired. For example, when calibrating B-dot probes one may wish information as either a current diagnostic or microwave power diagnostic. At first glance one might believe that these calibrations would yield the same result, but it will be shown that the nature of the data obtained makes the calibration techniques differ. Please note that the following calculations use MKS units.

First, consider a B-dot probe used to couple a microwave signal to a crystal diode detector. The crystal detector provides the time variation of the root mean square (RMS) power collected by the probe. For the time being ignore the fact that typically some amount of attenuation is required to keep from overdriving the crystal. The RMS power coupled to a coaxial cable is:

$$P_{RMS} = \frac{V^2}{2 \, Z_{LINE}} \tag{1}$$

where V is the voltage induced by the B-dot loop and Z_{LINE} is typically 50Ω. The factor of ½ (which is the RMS time average factor) is the crucial difference in the calibration analysis.

The V is related to the B_θ by Faraday's Law:

$$V = A_{probe} \, \frac{dB_\theta}{dt}$$
$$= A_{probe} \, \omega \, B_\theta \tag{2}$$

where A_{probe} is the parameter to be found, and B_θ is the magnetic field generated by the "Tin Man" calibration line when powered by continuous wave (CW) oscillator at a frequency $f=\omega/(2\,\pi)$.

One may relate B_θ to the current (I) or power (P_{in}) used to drive "Tin Man" as:

$$B_\theta = \frac{\mu_0 \, I}{2\pi b} \tag{3}$$

$$I = \sqrt{2 \, \frac{P_{in}}{Z_{TIN \, MAN}}} \tag{4}$$

where $Z_{TIN \, MAN}$ is also 50Ω, b is radius of the outer conductor.

Now solving the above equations for A_{probe},

36

$$A_{probe} = \frac{2\pi b}{\omega \mu_0} \sqrt{Z_{LINE} Z_{TIN\ MAN}} \sqrt{\frac{P_{out}}{P_{in}}} \tag{5}$$

where P_{out}/P_{in} may be easily determined with a network analyzer such as an Hewlett-Packard 8510. The data are obtained as attenuation versus frequency, and the area may be determined from Equation 5.

Equation 2 also allows determination of the coefficient between the voltage generated on a 50-Ω coaxial cable by a B-dot probe due to passage of a current pulse. This current pulse may be generated by either an electron beam or a "short shot" from a pulse source. Essentially this technique is looking for the time variation of a current pulse, and employs observation of the time derivative of the current pulse as follows:

$$\frac{dI}{dt} = C\ V(t) \tag{6}$$

where C is a coefficient which depends on the probe area and position. Using Ampere's Law with Faraday's Law one finds that from C one may get A_{probe} as follows:

$$A_{probe} = \frac{2\pi r}{C\mu_0} \tag{7}$$

where C is determined by comparison with other current pulse diagnostics (i.e. current viewing resistors or previously calibrated Rogowskii coils) and for this application r = b as in Equation 5.

Now one would like to find that Equation 5 and Equation 7 yield the same answers for the effective area for the B-dot probes. However, the ratio of Equation 7 to Equation 5 is found to equal $\sqrt{2}$. This difference is the result of the nature of the data provided by the B-dot probe.

B. SUPERFISH INPUT

Data file for the RKA geometry, input to AUTOMESH:

```
X RKA SINGLE CAVITY(3/24/92)
 $REG NREG=4, DX=0.5, DY=0.5, XMAX=45.0, YMAX=15.0, MAT=1, NPOINT=5,
NDRIVE=1, IBOUND=1, $END
 $PO X=0.0, Y=0.0, $END
 $PO X=0.0, Y=15.0, $END
 $PO X=45.0, Y=15.0, $END
 $PO X=45.0, Y=0.0, $END
 $PO X=0.0, Y=0.0, $END
 $REG NPOINT=11, MAT=0, $END
 $PO X=0.0, Y=7.5, $END
 $PO X=12.0, Y=7.5, $END
 $PO X=12.0, Y=14.5, $END
 $PO X=25.0, Y=14.5, $END
 $PO X=25.0, Y=8.5, $END
 $PO X=13.5, Y=8.5, $END
 $PO X=13.5, Y=7.5, $END
 $PO X=45.0, Y=7.5, $END
 $PO X=45.0, Y=15.0, $END
 $PO X=0.0, Y=15.0, $END
 $PO X=0.0, Y=7.5, $END
 $REG NPOINT=8, MAT=0, $END
 $PO X=0.0, Y=0.0, $END
 $PO X=0.0, Y=1.0, $END
 $PO X=2.0, Y=1.0, $END
 $PO X=6.0, Y=6.5, $END
 $PO X=6.0, Y=6.0, $END
 $PO X=2.5, Y=1.0, $END
 $PO X=2.5, Y=0.0, $END
 $PO X=0.0, Y=0.0, $END
 $REG NPOINT=1, $END
 $PO X=12.0, Y=14.50, $END
```

CON input for LATTICE:

```
*19 1 *21 1 0 0 0 s
```

This sets cylindrical symmetry, and allows for Neumann boundary conditions on the left and right surfaces of the problem. This choice is required when no conducting surface matches the left/right edges.

PSFPLOT input to plot geometry and mesh:

in response to (num, itri, nphi, inap, nswxy)

0,0,0,0,0   to plot problem geometry, and

0,1,0,0,0   to plot triangular mesh used to solve problem.

CON input for :

*65 initial frequency guess to find a specific mode s;

*62 nsteps *63 Δk^2 *65 initial frequency(f_0) s.

f_1 - final frequency of search range

$$\Delta k^2 = (\frac{2\pi}{c})^2 \frac{(f_1^2 - f_0^2)}{(nsteps - 1)} \tag{8}$$

PSFPLOT input to plot electric field contours:

in response to (num, itri, nphi, inap, nswxy)

1,0,#,0,0 where # specifies the number of electric field contours to plot.

Input for SHY to specify normalized electric field amplitude:

*42 kmin *43 ktop *44 lmin *45 lmax *74 ascale

where kmin/kmax and lmin/lmax specify the left/right axial and lower/upper radial mesh points for the electric field amplitude. Notice that if lmin=lmax then the normalized E_z is found along the contour from kmin to kmax. Also, if kmin=kmax then the normalized E_r is found along the contour from lmin to lmax. One must then select the proper value from the listed normalized field amplitudes for the desired mesh coordinate. The parameter ascale may be set to 1.0 if the absolute value is not required, or any other normalizing value may be used to properly scale the electric field.

C. MAGNET INPUT

MAGNET was originally written by John Freeman of Sandia National Laboratory. The code was later modified by several users as the code was ported to other platforms such as PCs.

One may use CDFMAG to input the geometry and current for each winding in the coil, or write a short FORTRAN program to generate the input deck. The format of each line is critical, but is documented within the code. Basically, the format is:

#; for the total number of lines in the data file
r(in.), left z(in.), right z(in.), # turns, I (Amps); this line is repeated # times. The code MAGNET does require the inputs of dimensions in inches, this is a minor irritant and has not been updated. The following geometry list is from a short Fortran program. Other techniques are possible to create the file, as long as the format of the line is followed.

For the RKA magnets #=550

Sample MAGNET input for the RKA coils:

```
    550


Coil 1
    8.737500E+00    6.560000E+00    9.560000E+00    1    1.000000E+00
    8.762500E+00    6.560000E+00    9.560000E+00    1    1.000000E+00
    8.787499E+00    6.560000E+00    9.560000E+00    1    1.000000E+00
    8.812499E+00    6.560000E+00    9.560000E+00    1    1.000000E+00
    8.837499E+00    6.560000E+00    9.560000E+00    1    1.000000E+00
    8.862498E+00    6.560000E+00    9.560000E+00    1    1.000000E+00
    8.887498E+00    6.560000E+00    9.560000E+00    1    1.000000E+00
    8.912498E+00    6.560000E+00    9.560000E+00    1    1.000000E+00
    8.937497E+00    6.560000E+00    9.560000E+00    1    1.000000E+00
    8.962497E+00    6.560000E+00    9.560000E+00    1    1.000000E+00
    8.987496E+00    6.560000E+00    9.560000E+00    1    1.000000E+00
    9.012496E+00    6.560000E+00    9.560000E+00    1    1.000000E+00
    9.037496E+00    6.560000E+00    9.560000E+00    1    1.000000E+00
    9.062495E+00    6.560000E+00    9.560000E+00    1    1.000000E+00
    9.087495E+00    6.560000E+00    9.560000E+00    1    1.000000E+00
    9.112494E+00    6.560000E+00    9.560000E+00    1    1.000000E+00
    9.137494E+00    6.560000E+00    9.560000E+00    1    1.000000E+00
    9.162494E+00    6.560000E+00    9.560000E+00    1    1.000000E+00
    9.187493E+00    6.560000E+00    9.560000E+00    1    1.000000E+00
    9.212493E+00    6.560000E+00    9.560000E+00    1    1.000000E+00
    9.237493E+00    6.560000E+00    9.560000E+00    1    1.000000E+00
    9.262492E+00    6.560000E+00    9.560000E+00    1    1.000000E+00
    9.287492E+00    6.560000E+00    9.560000E+00    1    1.000000E+00
    9.312491E+00    6.560000E+00    9.560000E+00    1    1.000000E+00
    9.337491E+00    6.560000E+00    9.560000E+00    1    1.000000E+00
    9.362491E+00    6.560000E+00    9.560000E+00    1    1.000000E+00
    9.387490E+00    6.560000E+00    9.560000E+00    1    1.000000E+00
    9.412490E+00    6.560000E+00    9.560000E+00    1    1.000000E+00
    9.437490E+00    6.560000E+00    9.560000E+00    1    1.000000E+00
    9.462489E+00    6.560000E+00    9.560000E+00    1    1.000000E+00
    9.487489E+00    6.560000E+00    9.560000E+00    1    1.000000E+00
    9.512488E+00    6.560000E+00    9.560000E+00    1    1.000000E+00
    9.537488E+00    6.560000E+00    9.560000E+00    1    1.000000E+00
    9.562488E+00    6.560000E+00    9.560000E+00    1    1.000000E+00
    9.587487E+00    6.560000E+00    9.560000E+00    1    1.000000E+00
    9.612487E+00    6.560000E+00    9.560000E+00    1    1.000000E+00
    9.637486E+00    6.560000E+00    9.560000E+00    1    1.000000E+00
    9.662486E+00    6.560000E+00    9.560000E+00    1    1.000000E+00
    9.687486E+00    6.560000E+00    9.560000E+00    1    1.000000E+00
    9.712485E+00    6.560000E+00    9.560000E+00    1    1.000000E+00
    9.737485E+00    6.560000E+00    9.560000E+00    1    1.000000E+00
    9.762485E+00    6.560000E+00    9.560000E+00    1    1.000000E+00
    9.787484E+00    6.560000E+00    9.560000E+00    1    1.000000E+00
    9.812484E+00    6.560000E+00    9.560000E+00    1    1.000000E+00
    9.837483E+00    6.560000E+00    9.560000E+00    1    1.000000E+00
    9.862483E+00    6.560000E+00    9.560000E+00    1    1.000000E+00
    9.887483E+00    6.560000E+00    9.560000E+00    1    1.000000E+00
```

```
9.912482E+00    6.560000E+00    9.560000E+00    1    1.000000E+00
9.937482E+00    6.560000E+00    9.560000E+00    1    1.000000E+00
9.962481E+00    6.560000E+00    9.560000E+00    1    1.000000E+00
9.987481E+00    6.560000E+00    9.560000E+00    1    1.000000E+00
1.001248E+01    6.560000E+00    9.560000E+00    1    1.000000E+00
1.003748E+01    6.560000E+00    9.560000E+00    1    1.000000E+00
1.006248E+01    6.560000E+00    9.560000E+00    1    1.000000E+00
1.008748E+01    6.560000E+00    9.560000E+00    1    1.000000E+00
1.011248E+01    6.560000E+00    9.560000E+00    1    1.000000E+00
1.013748E+01    6.560000E+00    9.560000E+00    1    1.000000E+00
1.016248E+01    6.560000E+00    9.560000E+00    1    1.000000E+00
1.018748E+01    6.560000E+00    9.560000E+00    1    1.000000E+00
1.021248E+01    6.560000E+00    9.560000E+00    1    1.000000E+00
1.023748E+01    6.560000E+00    9.560000E+00    1    1.000000E+00
1.026248E+01    6.560000E+00    9.560000E+00    1    1.000000E+00
1.028748E+01    6.560000E+00    9.560000E+00    1    1.000000E+00
1.031248E+01    6.560000E+00    9.560000E+00    1    1.000000E+00
1.033748E+01    6.560000E+00    9.560000E+00    1    1.000000E+00
1.036248E+01    6.560000E+00    9.560000E+00    1    1.000000E+00
1.038748E+01    6.560000E+00    9.560000E+00    1    1.000000E+00
1.041247E+01    6.560000E+00    9.560000E+00    1    1.000000E+00
1.043747E+01    6.560000E+00    9.560000E+00    1    1.000000E+00
1.046247E+01    6.560000E+00    9.560000E+00    1    1.000000E+00
1.048747E+01    6.560000E+00    9.560000E+00    1    1.000000E+00
1.051247E+01    6.560000E+00    9.560000E+00    1    1.000000E+00
1.053747E+01    6.560000E+00    9.560000E+00    1    1.000000E+00
1.056247E+01    6.560000E+00    9.560000E+00    1    1.000000E+00
1.058747E+01    6.560000E+00    9.560000E+00    1    1.000000E+00
1.061247E+01    6.560000E+00    9.560000E+00    1    1.000000E+00
1.063747E+01    6.560000E+00    9.560000E+00    1    1.000000E+00
1.066247E+01    6.560000E+00    9.560000E+00    1    1.000000E+00
1.068747E+01    6.560000E+00    9.560000E+00    1    1.000000E+00
1.071247E+01    6.560000E+00    9.560000E+00    1    1.000000E+00
1.073747E+01    6.560000E+00    9.560000E+00    1    1.000000E+00
1.076247E+01    6.560000E+00    9.560000E+00    1    1.000000E+00
1.078747E+01    6.560000E+00    9.560000E+00    1    1.000000E+00
1.081247E+01    6.560000E+00    9.560000E+00    1    1.000000E+00
1.083747E+01    6.560000E+00    9.560000E+00    1    1.000000E+00
1.086247E+01    6.560000E+00    9.560000E+00    1    1.000000E+00
1.088747E+01    6.560000E+00    9.560000E+00    1    1.000000E+00
1.091247E+01    6.560000E+00    9.560000E+00    1    1.000000E+00
1.093747E+01    6.560000E+00    9.560000E+00    1    1.000000E+00
1.096247E+01    6.560000E+00    9.560000E+00    1    1.000000E+00
1.098747E+01    6.560000E+00    9.560000E+00    1    1.000000E+00
1.101247E+01    6.560000E+00    9.560000E+00    1    1.000000E+00
1.103747E+01    6.560000E+00    9.560000E+00    1    1.000000E+00
1.106246E+01    6.560000E+00    9.560000E+00    1    1.000000E+00
1.108746E+01    6.560000E+00    9.560000E+00    1    1.000000E+00
1.111246E+01    6.560000E+00    9.560000E+00    1    1.000000E+00
1.113746E+01    6.560000E+00    9.560000E+00    1    1.000000E+00
1.116246E+01    6.560000E+00    9.560000E+00    1    1.000000E+00
1.118746E+01    6.560000E+00    9.560000E+00    1    1.000000E+00
1.121246E+01    6.560000E+00    9.560000E+00    1    1.000000E+00
1.123746E+01    6.560000E+00    9.560000E+00    1    1.000000E+00
1.126246E+01    6.560000E+00    9.560000E+00    1    1.000000E+00
1.128746E+01    6.560000E+00    9.560000E+00    1    1.000000E+00
1.131246E+01    6.560000E+00    9.560000E+00    1    1.000000E+00
1.133746E+01    6.560000E+00    9.560000E+00    1    1.000000E+00
1.136246E+01    6.560000E+00    9.560000E+00    1    1.000000E+00
1.138746E+01    6.560000E+00    9.560000E+00    1    1.000000E+00
1.141246E+01    6.560000E+00    9.560000E+00    1    1.000000E+00
1.143746E+01    6.560000E+00    9.560000E+00    1    1.000000E+00
1.146246E+01    6.560000E+00    9.560000E+00    1    1.000000E+00
1.148746E+01    6.560000E+00    9.560000E+00    1    1.000000E+00
1.151246E+01    6.560000E+00    9.560000E+00    1    1.000000E+00
1.153746E+01    6.560000E+00    9.560000E+00    1    1.000000E+00
1.156246E+01    6.560000E+00    9.560000E+00    1    1.000000E+00
1.158746E+01    6.560000E+00    9.560000E+00    1    1.000000E+00
1.161246E+01    6.560000E+00    9.560000E+00    1    1.000000E+00
1.163746E+01    6.560000E+00    9.560000E+00    1    1.000000E+00
1.166246E+01    6.560000E+00    9.560000E+00    1    1.000000E+00
1.168746E+01    6.560000E+00    9.560000E+00    1    1.000000E+00
1.171245E+01    6.560000E+00    9.560000E+00    1    1.000000E+00
1.173745E+01    6.560000E+00    9.560000E+00    1    1.000000E+00
1.176245E+01    6.560000E+00    9.560000E+00    1    1.000000E+00
1.178745E+01    6.560000E+00    9.560000E+00    1    1.000000E+00
1.181245E+01    6.560000E+00    9.560000E+00    1    1.000000E+00
1.183745E+01    6.560000E+00    9.560000E+00    1    1.000000E+00
```

```
1.186245E+01    6.560000E+00    9.560000E+00    1    1.000000E+00
1.188745E+01    6.560000E+00    9.560000E+00    1    1.000000E+00
1.191245E+01    6.560000E+00    9.560000E+00    1    1.000000E+00
1.193745E+01    6.560000E+00    9.560000E+00    1    1.000000E+00
1.196245E+01    6.560000E+00    9.560000E+00    1    1.000000E+00
1.198745E+01    6.560000E+00    9.560000E+00    1    1.000000E+00
1.201245E+01    6.560000E+00    9.560000E+00    1    1.000000E+00
1.203745E+01    6.560000E+00    9.560000E+00    1    1.000000E+00
1.206245E+01    6.560000E+00    9.560000E+00    1    1.000000E+00
1.208745E+01    6.560000E+00    9.560000E+00    1    1.000000E+00
1.211245E+01    6.560000E+00    9.560000E+00    1    1.000000E+00
1.213745E+01    6.560000E+00    9.560000E+00    1    1.000000E+00
1.216245E+01    6.560000E+00    9.560000E+00    1    1.000000E+00
1.218745E+01    6.560000E+00    9.560000E+00    1    1.000000E+00
1.221245E+01    6.560000E+00    9.560000E+00    1    1.000000E+00
1.223745E+01    6.560000E+00    9.560000E+00    1    1.000000E+00
1.226245E+01    6.560000E+00    9.560000E+00    1    1.000000E+00
1.228745E+01    6.560000E+00    9.560000E+00    1    1.000000E+00
1.231245E+01    6.560000E+00    9.560000E+00    1    1.000000E+00
1.233745E+01    6.560000E+00    9.560000E+00    1    1.000000E+00
1.236244E+01    6.560000E+00    9.560000E+00    1    1.000000E+00
1.238744E+01    6.560000E+00    9.560000E+00    1    1.000000E+00
1.241244E+01    6.560000E+00    9.560000E+00    1    1.000000E+00
1.243744E+01    6.560000E+00    9.560000E+00    1    1.000000E+00
1.246244E+01    6.560000E+00    9.560000E+00    1    1.000000E+00
1.248744E+01    6.560000E+00    9.560000E+00    1    1.000000E+00
1.251244E+01    6.560000E+00    9.560000E+00    1    1.000000E+00
1.253744E+01    6.560000E+00    9.560000E+00    1    1.000000E+00
1.256244E+01    6.560000E+00    9.560000E+00    1    1.000000E+00
1.258744E+01    6.560000E+00    9.560000E+00    1    1.000000E+00
1.261244E+01    6.560000E+00    9.560000E+00    1    1.000000E+00
1.263744E+01    6.560000E+00    9.560000E+00    1    1.000000E+00
1.266244E+01    6.560000E+00    9.560000E+00    1    1.000000E+00
1.268744E+01    6.560000E+00    9.560000E+00    1    1.000000E+00
1.271244E+01    6.560000E+00    9.560000E+00    1    1.000000E+00
1.273744E+01    6.560000E+00    9.560000E+00    1    1.000000E+00
1.276244E+01    6.560000E+00    9.560000E+00    1    1.000000E+00
1.278744E+01    6.560000E+00    9.560000E+00    1    1.000000E+00
1.281244E+01    6.560000E+00    9.560000E+00    1    1.000000E+00
1.283744E+01    6.560000E+00    9.560000E+00    1    1.000000E+00
1.286244E+01    6.560000E+00    9.560000E+00    1    1.000000E+00
1.288744E+01    6.560000E+00    9.560000E+00    1    1.000000E+00
1.291244E+01    6.560000E+00    9.560000E+00    1    1.000000E+00
1.293744E+01    6.560000E+00    9.560000E+00    1    1.000000E+00
1.296244E+01    6.560000E+00    9.560000E+00    1    1.000000E+00
1.298744E+01    6.560000E+00    9.560000E+00    1    1.000000E+00
1.301243E+01    6.560000E+00    9.560000E+00    1    1.000000E+00
1.303743E+01    6.560000E+00    9.560000E+00    1    1.000000E+00
1.306243E+01    6.560000E+00    9.560000E+00    1    1.000000E+00
1.308743E+01    6.560000E+00    9.560000E+00    1    1.000000E+00
1.311243E+01    6.560000E+00    9.560000E+00    1    1.000000E+00
1.313743E+01    6.560000E+00    9.560000E+00    1    1.000000E+00
1.316243E+01    6.560000E+00    9.560000E+00    1    1.000000E+00
1.318743E+01    6 560000E+00    9.560000E+00    1    1.000000E+00
1.321243E+01    6.560000E+00    9.560000E+00    1    1.000000E+00

Coil 2
8.737500E+00    1.536000E+01    1.836000E+01    1    1.000000E+00
8.762500E+00    1.536000E+01    1.836000E+01    1    1.000000E+00
8.787499E+00    1.536000E+01    1.836000E+01    1    1.000000E+00
8.812499E+00    1.536000E+01    1.836000E+01    1    1.000000E+00
8.837499E+00    1.536000E+01    1.836000E+01    1    1.000000E+00
8.862498E+00    1.536000E+01    1.836000E+01    1    1.000000E+00
8.887498E+00    1.536000E+01    1.836000E+01    1    1.000000E+00
8.912498E+00    1.536000E+01    1.836000E+01    1    1.000000E+00
8.937497E+00    1.536000E+01    1.836000E+01    1    1.000000E+00
8.962497E+00    1.536000E+01    1.836000E+01    1    1.000000E+00
8.987496E+00    1.536000E+01    1.836000E+01    1    1.000000E+00
9.012496E+00    1.536000E+01    1.836000E+01    1    1.000000E+00
9.037496E+00    1.536000E+01    1.836000E+01    1    1.000000E+00
9.062495E+00    1.536000E+01    1.836000E+01    1    1.000000E+00
9.087495E+00    1.536000E+01    1.836000E+01    1    1.000000E+00
9.112494E+00    1.536000E+01    1.836000E+01    1    1.000000E+00
9.137494E+00    1.536000E+01    1.836000E+01    1    1.000000E+00
9.162494E+00    1.536000E+01    1.836000E+01    1    1.000000E+00
9.187493E+00    1.536000E+01    1.836000E+01    1    1.000000E+00
9.212493E+00    1.536000E+01    1.836000E+01    1    1.000000E+00
9.237493E+00    1.536000E+01    1.836000E+01    1    1.000000E+00
```

```
    9.262492E+00    1.536000E+01    1.836000E+01    1    1.000000E+00
    9.287492E+00    1.536000E+01    1.836000E+01    1    1.000000E+00
    9.312491E+00    1.536000E+01    1.836000E+01    1    1.000000E+0C
    9.337491E+00    1.536000E+01    1.836000E+01    1    1.000000E+00
    9.362491E+00    1.536000E+01    1.836000E+01    1    1.000000E+00
    9.387490E+00    1.536000E+01    1.836000E+01    1    1.000000E+00
    9.412490E+00    1.536000E+01    1.836000E+01    1    1.000000E+00
    9.437490E+00    1.536000E+01    1.836000E+01    1    1.000000E+00
    9.462489E+00    1.536000E+01    1.836000E+01    1    1.000000E+00
    9.487489E+00    1.536000E+01    1.836000E+01    1    1.000000E+00
    9.512488E+00    1.536000E+01    1.836000E+01    1    1.000000E+00
    9.537488E+00    1.536000E+01    1.836000E+01    1    1.000000E+00
    9.562488E+00    1.536000E+01    1.836000E+01    1    1.000000E+00
    9.587487E+00    1.536000E+01    1.836000E+01    1    1.000000E+00
    9.612487E+00    1.536000E+01    1.836000E+01    1    1.000000E+00
    9.637486E+00    1.536000E+01    1.836000E+01    1    1.000000E+00
    9.662486E+00    1.536000E+01    1.836000E+01    1    1.000000E+00
    9.687486E+00    1.536000E+01    1.836000E+01    1    1.000000E+00
    9.712485E+00    1.536000E+01    1.836000E+01    1    1.000000E+00
    9.737485E+00    1.536000E+01    1.836000E+01    1    1.000000E+00
    9.762485E+00    1.536000E+01    1.836000E+01    1    1.000000E+00
    9.787484E+00    1.536000E+01    1.836000E+01    1    1.000000E+00
    9.812484E+00    1.536000E+01    1.836000E+01    1    1.000000E+00
    9.837483E+00    1.536000E+01    1.836000E+01    1    1.000000E+00
    9.862483E+00    1.536000E+01    1.836000E+01    1    1.000000E+00
    9.887483E+00    1.536000E+01    1.836000E+01    1    1.000000E+00
    9.912482E+00    1.536000E+01    1.836000E+01    1    1.000000E+00
    9.937482E+00    1.536000E+01    1.836000E+01    1    1.000000E+00
    9.962481E+00    1.536000E+01    1.836000E+01    1    1.000000E+00
    9.987481E+00    1.536000E+01    1.836000E+01    1    1.000000E+00
    1.001248E+01    1.536000E+01    1.836000E+01    1    1.000000E+00
    1.003748E+01    1.536000E+01    1.836000E+01    1    1.000000E+00
    1.006248E+01    1.536000E+01    1.836000E+01    1    1.000000E+00
    1.008748E+01    1.536000E+01    1.836000E+01    1    1.000000E+00
    1.011248E+01    1.536000E+01    1.836000E+01    1    1.000000E+00
    1.013748E+01    1.536000E+01    1.836000E+01    1    1.000000E+00
    1.016248E+01    1.536000E+01    1.836000E+01    1    1.000000E+00
    1.018748E+01    1.536000E+01    1.836000E+01    1    1.000000E+00
    1.021248E+01    1.536000E+01    1.836000E+01    1    1.000000E+00
    1.023748E+01    1.536000E+01    1.836000E+01    1    1.000000E+00
    1.026248E+01    1.536000E+01    1.836000E+01    1    1.000000E+00
    1.028748E+01    1.536000E+01    1.836000E+01    1    1.000000E+00
    1.031248E+01    1.536000E+01    1.836000E+01    1    1.000000E+00
    1.033748E+01    1.536000E+01    1.836000E+01    1    1.000000E+00
    1.036248E+01    1.536000E+01    1.836000E+01    1    1.000000E+00
    1.038748E+01    1.536000E+01    1.836000E+01    1    1.000000E+00
    1.041247E+01    1.536000E+01    1.836000E+01    1    1.000000E+00
    1.043747E+01    1.536000E+01    1.836000E+01    1    1.000000E+00
    1.046247E+01    1.536000E+01    1.836000E+01    1    1.000000E+00
    1.048747E+01    1.536000E+01    1.836000E+01    1    1.000000E+00
    1.051247E+01    1.536000E+01    1.836000E+01    1    1.000000E+00
    1.053747E+01    1.536000E+01    1.836000E+01    1    1.000000E+00
    1.056247E+01    1.536000E+01    1.836000E+01    1    1.000000E+00
    1.058747E+01    1.536000E+01    1.836000E+01    1    1.000000E+00
    1.061247E+01    1.536000E+01    1.836000E+01    1    1.000000E+00
    1.063747E+01    1.536000E+01    1.836000E+01    1    1.000000E+00
    1.066247E+01    1.536000E+01    1.836000E+01    1    1.000000E+00
    1.068747E+01    1.536000E+01    1.836000E+01    1    1.000000E+00
    1.071247E+01    1.536000E+01    1.836000E+01    1    1.000000E+00
    1.073747E+01    1.536000E+01    1.836000E+01    1    1.000000E+00
    1.076247E+01    1.536000E+01    1.836000E+01    1    1.000000E+00
    1.078747E+01    1.536000E+01    1.836000E+01    1    1.000000E+00
    1.081247E+01    1.536000E+01    1.836000E+01    1    1.000000E+00
    1.083747E+01    1.536000E+01    1.836000E+01    1    1.000000E+00
    1.086247E+01    1.536000E+01    1.836000E+01    1    1.000000E+00
    1.088747E+01    1.536000E+01    1.836000E+01    1    1.000000E+00
    1.091247E+01    1.536000E+01    1.836000E+01    1    1.000000E+00
    1.093747E+01    1.536000E+01    1.836000E+01    1    1.000000E+00
    1.096247E+01    1.536000E+01    1.836000E+01    1    1.000000E+00
    1.098747E+01    1.536000E+01    1.836000E+01    1    1.000000E+00
    1.101247E+01    1.536000E+01    1.836000E+01    1    1.000000E+00
    1.103747E+01    1.536000E+01    1.836000E+01    1    1.000000E+00
    1.106246E+01    1.536000E+01    1.836000E+01    1    1.000000E+00
    1.108746E+01    1.536000E+01    1.836000E+01    1    1.000000E+00

Coil 3
    8.737500E+00    2.286000E+01    2.586000E+01    1    1.000000E+00
    8.762500E+00    2.286000E+01    2.586000E+01    1    1.000000E+00
```

```
8.787499E+00    2.286000E+01    2.586000E+01    1    1.000000E+00
8.812499E+00    2.286000E+01    2.586000E+01    1    1.000000E+00
8.837499E+00    2.286000E+01    2.586000E+01    1    1.000000E+00
8.862498E+00    2.286000E+01    2.586000E+01    1    1.000000E+00
8.887498E+00    2.286000E+01    2.586000E+01    1    1.000000E+00
8.912498E+00    2.286000E+01    2.586000E+01    1    1.000000E+00
8.937497E+00    2.286000E+01    2.586000E+01    1    1.000000E+00
8.962497E+00    2.286000E+01    2.586000E+01    1    1.000000E+00
8.987496E+00    2.286000E+01    2.586000E+01    1    1.000000E+00
9.012496E+00    2.286000E+01    2.586000E+01    1    1.000000E+00
9.037496E+00    2.286000E+01    2.586000E+01    1    1.000000E+00
9.062495E+00    2.286000E+01    2.586000E+01    1    1.000000E+00
9.087495E+00    2.286000E+01    2.586000E+01    1    1.000000E+00
9.112494E+00    2.286000E+01    2.586000E+01    1    1.000000E+00
9.137494E+00    2.286000E+01    2.586000E+01    1    1.000000E+00
9.162494E+00    2.286000E+01    2.586000E+01    1    1.000000E+00
9.187493E+00    2.286000E+01    2.586000E+01    1    1.000000E+00
9.212493E+00    2.286000E+01    2.586000E+01    1    1.000000E+00
9.237493E+00    2.286000E+01    2.586000E+01    1    1.000000E+00
9.262492E+00    2.286000E+01    2.586000E+01    1    1.000000E+00
9.287492E+00    2.286000E+01    2.586000E+01    1    1.000000E+00
9.312491E+00    2.286000E+01    2.586000E+01    1    1.000000E+00
9.337491E+00    2.286000E+01    2.586000E+01    1    1.000000E+00
9.362491E+00    2.286000E+01    2.586000E+01    1    1.000000E+00
9.387490E+00    2.286000E+01    2.586000E+01    1    1.000000E+00
9.412490E+00    2.286000E+01    2.586000E+01    1    1.000000E+00
9.437490E+00    2.286000E+01    2.586000E+01    1    1.000000E+00
9.462489E+00    2.286000E+01    2.586000E+01    1    1.000000E+00
9.487489E+00    2.286000E+01    2.586000E+01    1    1.000000E+00
9.512488E+00    2.286000E+01    2.586000E+01    1    1.000000E+00
9.537488E+00    2.286000E+01    2.586000E+01    1    1.000000E+00
9.562488E+00    2.286000E+01    2.586000E+01    1    1.000000E+00
9.587487E+00    2.286000E+01    2.586000E+01    1    1.000000E+00
9.612487E+00    2.286000E+01    2.586000E+01    1    1.000000E+00
9.637486E+00    2.286000E+01    2.586000E+01    1    1.000000E+00
9.662486E+00    2.286000E+01    2.586000E+01    1    1.000000E+00
9.687486E+00    2.286000E+01    2.586000E+01    1    1.000000E+00
9.712485E+00    2.286000E+01    2.586000E+01    1    1.000000E+00
9.737485E+00    2.286000E+01    2.586000E+01    1    1.000000E+00
9.762485E+00    2.286000E+01    2.586000E+01    1    1.000000E+00
9.787484E+00    2.286000E+01    2.586000E+01    1    1.000000E+00
9.812484E+00    2.286000E+01    2.586000E+01    1    1.000000E+00
9.837483E+00    2.286000E+01    2.586000E+01    1    1.000000E+00
9.862483E+00    2.286000E+01    2.586000E+01    1    1.000000E+00
9.887483E+00    2.286000E+01    2.586000E+01    1    1.000000E+00
9.912482E+00    2.286000E+01    2.586000E+01    1    1.000000E+00
9.937482E+00    2.286000E+01    2.586000E+01    1    1.000000E+00
9.962481E+00    2.286000E+01    2.586000E+01    1    1.000000E+00
9.987481E+00    2.286000E+01    2.586000E+01    1    1.000000E+00
1.001248E+01    2.286000E+01    2.586000E+01    1    1.000000E+00
1.003748E+01    2.286000E+01    2.586000E+01    1    1.000000E+00
1.006248E+01    2.286000E+01    2.586000E+01    1    1.000000E+00
1.008748E+01    2.286000E+01    2.586000E+01    1    1.000000E+00
1.011248E+01    2.286000E+01    2.586000E+01    1    1.000000E+00
1.013748E+01    2.286000E+01    2.586000E+01    1    1.000000E+00
1.016248E+01    2.286000E+01    2.586000E+01    1    1.000000E+00
1.018748E+01    2.286000E+01    2.586000E+01    1    1.000000E+00
1.021248E+01    2.286000E+01    2.586000E+01    1    1.000000E+00
1.023748E+01    2.286000E+01    2.586000E+01    1    1.000000E+00
1.026248E+01    2.286000E+01    2.586000E+01    1    1.000000E+00
1.028748E+01    2.286000E+01    2.586000E+01    1    1.000000E+00
1.031248E+01    2.286000E+01    2.586000E+01    1    1.000000E+00
1.033748E+01    2.286000E+01    2.586000E+01    1    1.000000E+00
1.036248E+01    2.286000E+01    2.586000E+01    1    1.000000E+00
1.038748E+01    2.286000E+01    2.586000E+01    1    1.000000E+00
1.041247E+01    2.286000E+01    2.586000E+01    1    1.000000E+00
1.043747E+01    2.286000E+01    2.586000E+01    1    1.000000E+00
1.046247E+01    2.286000E+01    2.586000E+01    1    1.000000E+00
1.048747E+01    2.286000E+01    2.586000E+01    1    1.000000E+00
1.051247E+01    2.286000E+01    2.586000E+01    1    1.000000E+00
1.053747E+01    2.286000E+01    2.586000E+01    1    1.000000E+00
1.056247E+01    2.286000E+01    2.586000E+01    1    1.000000E+00
1.058747E+01    2.286000E+01    2.586000E+01    1    1.000000E+00
1.061247E+01    2.286000E+01    2.586000E+01    1    1.000000E+00
1.063747E+01    2.286000E+01    2.586000E+01    1    1.000000E+00
1.066247E+01    2.286000E+01    2.586000E+01    1    1.000000E+00
1.068747E+01    2.286000E+01    2.586000E+01    1    1.000000E+00
1.071247E+01    2.286000E+01    2.586000E+01    1    1.000000E+00
```

```
1.073747E+01    2.286000E+01    2.586000E+01    1    1.000000E+00
1.076247E+01    2.286000E+01    2.586000E+01    1    1.000000E+00
1.078747E+01    2.286000E+01    2.586000E+01    1    1.000000E+00
1.081247E+01    2.286000E+01    2.586000E+01    1    1.000000E+00
1.083747E+01    2.286000E+01    2.586000E+01    1    1.000000E+00
1.086247E+01    2.286000E+01    2.586000E+01    1    1.000000E+00
1.088747E+01    2.286000E+01    2.586000E+01    1    1.000000E+00
1.091247E+01    2.286000E+01    2.586000E+01    1    1.000000E+00
1.093747E+01    2.286000E+01    2.586000E+01    1    1.000000E+00
1.096247E+01    2.286000E+01    2.586000E+01    1    1.000000E+00
1.098747E+01    2.286000E+01    2.586000E+01    1    1.000000E+00
1.101247E+01    2.286000E+01    2.586000E+01    1    1.000000E+00
1.103747E+01    2.286000E+01    2.586000E+01    1    1.000000E+00
1.106246E+01    2.286000E+01    2.586000E+01    1    1.000000E+00
1.108746E+01    2.286000E+01    2.586000E+01    1    1.000000E+00

Coil 4
8.737500E+00    3.156000E+01    3.456000E+01    1    1.000000E+00
8.762500E+00    3.156000E+01    3.456000E+01    1    1.000000E+00
8.787499E+00    3.156000E+01    3.456000E+01    1    1.000000E+00
8.812499E+00    3.156000E+01    3.456000E+01    1    1.000000E+00
8.837499E+00    3.156000E+01    3.456000E+01    1    1.000000E+00
8.862498E+00    3.156000E+01    3.456000E+01    1    1.000000E+00
8.887498E+00    3.156000E+01    3.456000E+01    1    1.000000E+00
8.912498E+00    3.156000E+01    3.456000E+01    1    1.000000E+00
8.937497E+00    3.156000E+01    3.456000E+01    1    1 000000E+00
8.962497E+00    3.156000E+01    3.456000E+01    1    1.000000E+00
8.987496E+00    3.156000E+01    3.456000E+01    1    1.000000E+00
9.012496E+00    3.156000E+01    3.456000E+01    1    1.000000E+00
9.037496E+00    3.156000E+01    3.456000E+01    1    1.000000E+00
9.062495E+00    3.156000E+01    3.456000E+01    1    1.000000E+00
9.087495E+00    3.156000E+01    3.456000E+01    1    1.000000E+00
9.112494E+00    3.156000E+01    3.456000E+01    1    1.000000E+00
9.137494E+00    3.156000E+01    3.456000E+01    1    1.000000E+00
9.162494E+00    3.156000E+01    3.456000E+01    1    1.000000E+00
9.187493E+00    3.156000E+01    3.456000E+01    1    1.000000E+00
9.212493E+00    3.156000E+01    3.456000E+01    1    1.000000E+00
9.237493E+00    3.156000E+01    3.456000E+01    1    1.000000E+00
9.262492E+00    3 156000E+01    3.456000E+01    1    1.000000E+00
9.287492E+00    3.156000E+01    3.456000E+01    1    1.000000E+00
9.312491E+00    3.156000E+01    3.456000E+01    1    1.000000E+00
9.337491E+00    3.156000E+01    3.456000E+01    1    1.000000E+00
9.362491E+00    3.156000E+01    3.456000E+01    1    1.000000E+00
9.387490E+00    3.156000E+01    3.456000E+01    1    1.000000E+00
9.412490E+00    3.156000E+01    3.456000E+01    1    1.000000E+00
9.437490E+00    3.156000E+01    3.456000E+01    1    1.000000E+00
9.462489E+00    3.156000E+01    3.456000E+01    1    1.000000E+00
9.487489E+00    3.156000E+01    3.456000E+01    1    1.000000E+00
9.512488E+00    3.156000E+01    3.456000E+01    1    1.000000E+00
9.537488E+00    3.156000E+01    3.456000E+01    1    1.000000E+00
9.562488E+00    3.156000E+01    3.456000E+01    1    1.000000E+00
9.587487E+00    3.156000E+01    3.456000E+01    1    1.000000E+00
9.612487E+00    3.156000E+01    3.456000E+01    1    1.000000E+00
9.637486E+00    3.156000E+01    3.456000E+01    1    1.000000E+00
9.662486E+00    3.156000E+01    3.456000E+01    1    1.000000E+00
9.687486E+00    3.156000E+01    3.456000E+01    1    1.000000E+00
9.712485E+00    3.156000E+01    3.456000E+01    1    1.000000E+00
9.737485E+00    3.156000E+01    3.456000E+01    1    1.000000E+00
9.762485E+00    3.156000E+01    3.456000E+01    1    1.000000E+00
9.787484E+00    3.156000E+01    3.456000E+01    1    1.000000E+00
9.812484E+00    3.156000E+01    3.456000E+01    1    1.000000E+00
9.837483E+00    3.156000E+01    3.456000E+01    1    1.000000E+00
9.862483E+00    3.156000E+01    3.456000E+01    1    1.000000E+00
9.887483E+00    3.156000E+01    3.456000E+01    1    1.000000E+00
9.912482E+00    3.156000E+01    3.456000E+01    1    1.000000E+00
9.937482E+00    3.156000E+01    3.456000E+01    1    1.000000E+00
9.962481E+00    3.156000E+01    3.456000E+01    1    1.000000E+00
9.987481E+00    3.156000E+01    3.456000E+01    1    1.000000E+00
1.001248E+01    3.156000E+01    3.456000E+01    1    1.000000E+00
1.003748E+01    3.156000E+01    3.456000E+01    1    1.000000E+00
1.006248E+01    3.156000E+01    3.456000E+01    1    1.000000E+00
1.008748E+01    3.156000E+01    3.456000E+01    1    1.000000E+00
1.011248E+01    3.156000E+01    3.456000E+01    1    1.000000E+00
1.013748E+01    3.156000E+01    3.456000E+01    1    1.000000E+00
1.016248E+01    3.156000E+01    3.456000E+01    1    1.000000E+00
1.018748E+01    3.156000E+01    3.456000E+01    1    1.000000E+00
1.021248E+01    3.156000E+01    3.456000E+01    1    1.000000E+00
1.023748E+01    3.156000E+01    3.456000E+01    1    1.000000E+00
```

```
1.026248E+01    3.156000E+01    3.456000E+01    1    1.000000E+00
1.028748E+01    3.156000E+01    3.456000E+01    1    1.000000E+00
1.031248E+01    3.156000E+01    3.456000E+01    1    1.000000E+00
1.033748E+01    3.156000E+01    3.456000E+01    1    1.000000E+00
1.036248E+01    3.156000E+01    3.456000E+01    1    1.000000E+00
1.038748E+01    3.156000E+01    3.456000E+01    1    1.000000E+00
1.041247E+01    3.156000E+01    3.456000E+01    1    1.000000E+00
1.043747E+01    3.156000E+01    3.456000E+01    1    1.000000E+00
1.046247E+01    3.156000E+01    3.456000E+01    1    1.000000E+00
1.048747E+01    3.156000E+01    3.456000E+01    1    1.000000E+00
1.051247E+01    3.156000E+01    3.456000E+01    1    1.000000E+00
1.053747E+01    3.156000E+01    3.456000E+01    1    1.000000E+00
1.056247E+01    3.156000E+01    3.456000E+01    1    1.000000E+00
1.058747E+01    3.156000E+01    3.456000E+01    1    1.000000E+00
1.061247E+01    3.156000E+01    3.456000E+01    1    1.000000E+00
1.063747E+01    3.156000E+01    3.456000E+01    1    1.000000E+00
1.066247E+01    3.156000E+01    3.456000E+01    1    1.000000E+00
1.068747E+01    3.156000E+01    3.456000E+01    1    1.000000E+00
1.071247E+01    3.156000E+01    3.456000E+01    1    1.000000E+00
1.073747E+01    3.156000E+01    3.456000E+01    1    1.000000E+00
1.076247E+01    3.156000E+01    3.456000E+01    1    1.000000E+00
1.078747E+01    3.156000E+01    3.456000E+01    1    1.000000E+00
1.081247E+01    3.156000E+01    3.456000E+01    1    1.000000E+00
1.083747E+01    3.156000E+01    3.456000E+01    1    1.000000E+00
1.086247E+01    3.156000E+01    3.456000E+01    1    1.000000E+00
1.088747E+01    3.156000E+01    3.456000E+01    1    1.000000E+00
1.091247E+01    3.156000E+01    3.456000E+01    1    1.000000E+00
1.093747E+01    3.156000E+01    3.456000E+01    1    1.000000E+00
1.096247E+01    3.156000E+01    3.456000E+01    1    1.000000E+00
1.098747E+01    3.156000E+01    3.456000E+01    1    1.000000E+00
1.101247E+01    3.156000E+01    3.456000E+01    1    1.000000E+00
1.103747E+01    3.156000E+01    3.456000E+01    1    1.000000E+00
1.106246E+01    3.156000E+01    3.456000E+01    1    1.000000E+00
1.108746E+01    3.156000E+01    3.456000E+01    1    1.000000E+00
1.111246E+01    3.156000E+01    3.456000E+01    1    1.000000E+00
1.113746E+01    3.156000E+01    3.456000E+01    1    1.000000E+00
1.116246E+01    3.156000E+01    3.456000E+01    1    1.000000E+00
1.118746E+01    3.156000E+01    3.456000E+01    1    1.000000E+00
1.121246E+01    3.156000E+01    3.456000E+01    1    1.000000E+00
1.123746E+01    3.156000E+01    3.456000E+01    1    1.000000E+00
1.126246E+01    3.156000E+01    3.456000E+01    1    1.000000E+00
1.128746E+01    3.156000E+01    3.456000E+01    1    1.000000E+00
1.131246E+01    3.156000E+01    3.456000E+01    1    1.000000E+00
1.133746E+01    3.156000E+01    3.456000E+01    1    1.000000E+00
1.136246E+01    3.156000E+01    3.456000E+01    1    1.000000E+00
1.138746E+01    3.156000E+01    3.456000E+01    1    1.000000E+00
1.141246E+01    3.156000E+01    3.456000E+01    1    1.000000E+00
1.143746E+01    3.156000E+01    3.456000E+01    1    1.000000E+00
1.146246E+01    3.156000E+01    3.456000E+01    1    1.000000E+00
1.148746E+01    3.156000E+01    3.456000E+01    1    1.000000E+00
1.151246E+01    3.156000E+01    3.456000E+01    1    1.000000E+00
1.153746E+01    3.156000E+01    3.456000E+01    1    1.000000E+00
1.156246E+01    3.156000E+01    3.456000E+01    1    1.000000E+00
1.158746E+01    3.156000E+01    3.456000E+01    1    1.000000E+00
1.161246E+01    3.156000E+01    3.456000E+01    1    1.000000E+00
1.163746E+01    3.156000E+01    3.456000E+01    1    1.000000E+00
1.166246E+01    3.156000E+01    3.456000E+01    1    1.000000E+00
1.168746E+01    3.156000E+01    3.456000E+01    1    1.000000E+00
1.171245E+01    3.156000E+01    3.456000E+01    1    1.000000E+00
1.173745E+01    3.156000E+01    3.456000E+01    1    1.000000E+00
1.176245E+01    3.156000E+01    3.456000E+01    1    1.000000E+00
1.178745E+01    3.156000E+01    3.456000E+01    1    1.000000E+00
1.181245E+01    3.156000E+01    3.456000E+01    1    1.000000E+00
1.183745E+01    3.156000E+01    3.456000E+01    1    1.000000E+00
1.186245E+01    3.156000E+01    3.456000E+01    1    1.000000E+00
1.188745E+01    3.156000E+01    3.456000E+01    1    1.000000E+00
1.191245E+01    3.156000E+01    3.456000E+01    1    1.000000E+00
1.193745E+01    3.156000E+01    3.456000E+01    1    1.000000E+00
1.196245E+01    3.156000E+01    3.456000E+01    1    1.000000E+00
1.198745E+01    3.156000E+01    3.456000E+01    1    1.000000E+00
1.201245E+01    3.156000E+01    3.456000E+01    1    1.000000E+00
1.203745E+01    3.156000E+01    3.456000E+01    1    1.000000E+00
1.206245E+01    3.156000E+01    3.456000E+01    1    1.000000E+00
1.208745E+01    3.156000E+01    3.456000E+01    1    1.000000E+00
1.211245E+01    3.156000E+01    3.456000E+01    1    1.000000E+00
1.213745E+01    3.156000E+01    3.456000E+01    1    1.000000E+00
1.216245E+01    3.156000E+01    3.456000E+01    1    1.000000E+00
1.218745E+01    3.156000E+01    3.456000E+01    1    1.000000E+00
```

```
1.221245E+01    3.156000E+01    3.456000E+01    1    1.000000E+00
1.223745E+01    3.156000E+01    3.456000E+01    1    1.000000E+00
1.226245E+01    3.156000E+01    3.456000E+01    1    1.000000E+00
1.228745E+01    3.156000E+01    3.456000E+01    1    1.000000E+00
1.231245E+01    3.156000E+01    3.456000E+01    1    1.000000E+00
1.233745E+01    3.156000E+01    3.456000E+01    1    1.000000E+00
1.236244E+01    3.156000E+01    3.456000E+01    1    1.000000E+00
1.238744E+01    3.156000E+01    3.456000E+01    1    1.000000E+00
1.241244E+01    3.156000E+01    3.456000E+01    1    1.000000E+00
1.243744E+01    3.156000E+01    3.456000E+01    1    1.000000E+00
1.246244E+01    3.156000E+01    3.456000E+01    1    1.000000E+00
1.249744E+01    3.156000E+01    3.456000E+01    1    1.000000E+00
1.251244E+01    3.156000E+01    3.456000E+01    1    1.000000E+00
1.253744E+01    3.156000E+01    3.456000E+01    1    1.000000E+00
1.256244E+01    3.156000E+01    3.456000E+01    1    1.000000E+00
1.258744E+01    3.156000E+01    3.456000E+01    1    1.000000E+00
1.261244E+01    3.156000E+01    3.456000E+01    1    1.000000E+00
1.263744E+01    3.156000E+01    3.456000E+01    1    1.000000E+00
1.266244E+01    3.156000E+01    3.456000E+01    1    1.000000E+00
1.268744E+01    3.156000E+01    3.456000E+01    1    1.000000E+00
1.271244E+01    3.156000E+01    3.456000E+01    1    1.000000E+00
1.273744E+01    3.156000E+01    3.456000E+01    1    1.000000E+00
1.276244E+01    3.156000E+01    3.456000E+01    1    1.000000E+00
1.278744E+01    3.156000E+01    3.456000E+01    1    1.000000E+00
1.281244E+01    3.156000E+01    3.456000E+01    1    1.000000E+00
1.283744E+01    3.156000E+01    3.456000E+01    1    1.000000E+00
1.286244E+01    3.156000E+01    3.456000E+01    1    1.000000E+00
1.288744E+01    3.156000E+01    3.456000E+01    1    1.000000E+00
1.291244E+01    3.156000E+01    3.456000E+01    1    1.000000E+00
1.293744E+01    3.156000E+01    3.456000E+01    1    1.000000E+00
1.296244E+01    3.156000E+01    3.456000E+01    1    1.000000E+00
1.298744E+01    3.156000E+01    3.456000E+01    1    1.000000E+00
1.301243E+01    3.156000E+01    3.456000E+01    1    1.000000E+00
1.303743E+01    3.156000E+01    3.455000E+01    1    1.000000E+00
1.306243E+01    3.156000E+01    3.456000E+01    1    1.000000E+00
1.308743E+01    3.156000E+01    3.456000E+01    1    1.000000E+00
1.311243E+01    3.156000E+01    3.456000E+01    1    1.000000E+00
1.313743E+01    3.156000E+01    3.456000E+01    1    1.000000E+00
1.315243E+01    3.156000E+01    3.456000E+01    1    1.000000E+00
1.318743E+01    3.156000E+01    3.456000E+01    1    1.000000E+00
1.321243E+01    3.156000E+01    3.456000E+01    1    1.000000E+00
```

Sample geometry input for POISSON:

```
RKA MAGNET (7/1/92)
$REG NREG=5,XMAX=80.0,DX=1.,YMIN=0.,YMAX=190.,NPOINT=5,$END
$PO X=0.0, Y=0., $END
$PO X=80.0, Y=0.0, $END
$PO X=80.0, Y=190.0, $END
$PO X=0.0, Y=190.0, $END
$PO X=0.0, Y=0.0, $END
$REG MAT=1, CUR=3.40E5, NPOINT=5, $END
$PO X=22.19, Y=59.10, $END
$PO X=33.56, Y=59.10, $END
$PO X=33.56, Y=66.72, $END
$PO X=22.19, Y=66.72, $END
$PO X=22.19, Y=59.10, $END
$REG MAT=1, CUR=1.80E5, NPOINT=5, $END
$PO X=22.19, Y=81.45, $END
$PO X=28.16, Y=81.45, $END
$PO X=28.16, Y=89.07, $END
$PO X=22.19, Y=89.07, $END
$PO X=22.19, Y=81.45, $END
$REG MAT=1, CUR=1.80E5, NPOINT=5, $END
$PO X=22.19, Y=100.50, $END
$PO X=28.16, Y=100.50, $END
$PO X=28.16, Y=108.12, $END
$PO X=22.19, Y=108.12, $END
```

47

```
$PO X=22.19, Y=100.50, $END
$REG MAT=1, CUR=3.40E5, NPOINT=5, $END
$PO X=22.19, Y=122.60, $END
$PO X=33.56, Y=122.60, $END
$PO X=33.56, Y=130.22, $END
$PO X=22.19, Y=130.22, $END
$PO X=22.19, Y=122.60, $END
```

One then goes through LATTICE and POISSON, no extra CON variable must be set except *19 1 s. PSFPLOT is used as in .

Sample 2-D grid input for the magnetic diffusion code MAGDIF:

Note: An index of 4 indicates the stainless steel, an index of 5 indicates turns for the larger coil, an index of 6 indicates the turns for a smaller coil, and an index of 0 indicates free space.

```
*aba outline 3/24/92
 $inp nr=120 nz=428 dr=0.0050 dz=0.0050
  npas=4 nact=2 sigma=7.854,1.,1.,1.745,0.2629,0.3480,1.,1.,1.,
  amu=100000.,1.,1.,1.,1.,1.,1.,1.,1.
 $end
```

```
0000000000000000000000000000000000000000000000000000000000000000000000000000000000000000000000000000000000000000000000000000000000
0000000000000000000000000000000000000000000000000000000000000000000000000000000000000000000000000000000000000000000000000000000000
0000000000000000000000000000000000000000000000000000000000000000000000000000000000000000000000000000000000000000000000000000000000
0000000000000000000000000000000000000000000000000000000000000000000000000000000000000000000000000000000000000000000000000000000000
0000000000000000000000000000000000000000000000000000000000000000000000000000000000000000000000000000000000000000000000000000000000
0000000000000000000000000000000000000000000000000000000000000000000000000000000000000000000000000000000000000000000000000000000000
0000000000000000000000000000000000000000000000000000000000000000000000000000000000000000000000000000000000000000000000000000000000
0000000000000000000000000000000000000000000000000000000000000000000000000000000000000000000000000000000000000000000000000000000000
0000000000000000000000000000000000000000000000000000000000000000000000000000000000000000000000000000000000000000000000000000000000
0000000000000000000000000000000000000000000000000000000000000000000000000000000000000000000000000000000000000000000000000000000000
0000000000000000000000000000000000000000000000000000000000000000000000000000000000000000000000000000000000000000000000000000000000
0000000000000000000000000000000000000000000000000000000000000000000000000000000000000000000000000000000000000000000000000000000000
0000000000000000000000000000000000000000000000000000000000000000000000000000000000000000000000000000000000000000000000000000000000
0000000000000000000000000000000000000000000000000000000000000000000000000000000000000000000000000000000000000000000000000000000000
0000000000000000000000000000000000000000000000000000000000000000000000000000000000000000000000000000000000000000000000000000000000
0000000000000000000000000000000000000000000000000000000000000000000000000000000000000000000000000000000000000000000000000000000000
0000000000000000000000000000000000000000000000000000000000000000000000000000000000000000000000000000000000000000000000000000000000
0000000000000000000000000000000000000000000000000000000000000000000000000000000000000000000000000000000000000000000000000000000000
0000000000000000000000000000000000000000000000000000000000000000000000000000000000000000000000000000000000000000000000000000000000
0000000000000000000000000000000000000000000000000000000000000000000000000000000000000000000000000000000000000000000000000000000000
0000000000000000000000000000000000000000000000000000000000000000000000000000000000000000000000000000000000000000000000000000000000
0000000000000000000000000000000000000000000000000000000000000000000000000000000000000000000000000000000000000000000000000000000000
0000000000000000000000000000000000000000000000000000000000000000000000000000000000000000000000000000000000000000000000000000000000
0000000000000000000000000000000000000000000000000000000000000000000000000000000000000000000000000000000000000000000000000000000000
0000000000000000000000000000000000000000000000000000000000000000000000000000000000000000000000000000000000000000000000000000000000
0000000000000000000000000000000000000000000000000000000000000000000000000000000000000000000000000000000000000000000000000000000000
0000000000000000000000000000000000000000000000000000000000000000000000000000000000000000000000000000000000000000000000000000000000
0000000000000000000000000000000000000000000000000000000000000000000000000000000000000000000000000000000000000000000000000000000000
0000000000000000000000000000000000000000000000000000000000000000000000000000000000000000000000000000000000000000000000000000000000
0000000000000000000000000000000000000000000000000000000000000000000000000000000000000000000000000000000000000000000000000000000000
0000000000000000000000000000000000000000000000000000000000000000000000000000000000000000000000000000000000000000000000000000000000
0000000000000000000000000000000000000000000000000000000000000000000000000000000000000000000000000000000000000000000000000000000000
0000000000000000000000000000000000000000000000000000000000000000000000000000000000000000000000000000000000000000000000000000000000
0000000000000000000000000000000000000000000000000000000000000000000000000000000000000000000000000000000000000000000000000000000000
0000000000000000000000000000000000000000000000000000000000000000000000000000000000000000000000000000000000000000000000000000000000
0000000000000000000000000000000000000000000000000000000000000000000000000000000000000000000000000000000000000000000000000000000000
0000000000000000000000000000000000000000000000000000000000000000000000000000000000000000000000000000000000000000000000000000000000
0000000000000000000000000000000000000000000000000000000000000000000000000000000000000000000000000000000000000000000000000000000000
0000000000000000000000000000000000000000000000000000000000000000000000000000000000000000000000000000000000000000000000000000000000
0000000000000000000000000000000000000000000000000000000000000000000000000000000000000000000000000000000000000000000000000000000000
0000000000000000000000000000000000000000000000000000000000000000000000000000000000000000000000000000000000000000000000000000000000
0000000000000000000000000000000000000000000000000000000000000000000000000000000000000000000000000000000000000000000000000000000000
0000000000000000000000000000000000000000000000000000000000000000000000000000000000000000000000000000000000000000000000000000000000
0000000000000000000000000000000000000000000000000000000000000000000000000000000000000000000000000000000000000000000000000000000000
0000000000000000000000000000000000000000000000000000000000000000000000000000000000000000000000000000000000000000000000000000000000
0000000000000000000000000000000000000000000000000000000000000000000000000000000000000000000000000000000000000000000000000000000000
0000000000000000000000000000000000000000000000000000000000000000000000000000000000000000000000000000000000000000000000000000000000
0000000000000000000000000000000000000000000000000000000000000000000000000000000000000000000000000000000000000000000000000000000000
0000000000000000000000000000000000000000000000000000000000000000000000000000000000000000000000000000000000000000000000000000000000
0000000000000000000000000000000000000000000000000000000000000000000000000000000000000000000000000000000000000000000000000000000000
0000000000000000000000000000000000000000000000000000000000000000000000000000000000000000000000000000000000000000000000000000000000
0000000000000000000000000000000000000000000000000000000000000000000000000000000000000000000000000000000000000000000000000000000000
0000000000000000000000000000000000000000000000000000000000000000000000000000000000000000000000000000000000000000000000000000000000
0000000000000000000000000000000000000000000000000000000000000000000000000000000000000000000000000000000000000000000000000000000000
0000000000000000000000000000000000000000000000000000000000000000000000000000000000000000000000000000000000000000000000000000000000
0000000000000000000000000000000000000000000000000000000000000000000000000000000000000000000000000000000000000000000000000000000000
000400000000000003000000000000000000000044000000000000000000000000000000000000000000000000000000000000000000000000000000000000000
000400000000000003000000000000000000000044000000000000000000000000000003000000000000000000000000000000000000000000000000000000000
000400000000000000000000000000000000000044000000000000000000000000000000000000000000000000000000000000000000000000000000000000000
000400000000000000000000000000000000000044000000000000000000000000000000000000000000000000000000000000000000000000000000000000000
000400000000000000000000000000000000000044000000000000000000000000000000000000000000000000000000000000000000000000000000000000000
000400000000000000000000000000000000000044000000000000000000000000000000000000000000000000000000000000000000000000000000000000000
000400000000000000000000000000000000000044000000000000000000000000000000000000000000000000000000000000000000000000000000000000000
000400000000000000000000000000000000000044000000000000000000000000000000000000000000000000000000000000000000000000000000000000000
000400000000000000000000000000000000000044000000000000000000000000000000000000000000000000000000000000000000000000000000000000000
000400000000000000000000000000000000000044000000000000000000000000000000000000000000000000000000000000000000000000000000000000000
000400000000000000000000000000000000000044000000000000000000000000000000000000000000000000000000000000000000000000000000000000000
000400000000000000000000000000000000000044000000000000000000000000000000000000000000000000000000000000000000000000000000000000000
000400000000000000000000000000000000000044000000000000000000000000000000000000000000000000000000000000000000000000000000000000000
000400000000000000000000000000000000000044000000000000000000000000000000000000000000000000000000000000000000000000000000000000000
```

This is a copy of the inputs which the codes prompts the user. We use a text file which was piped into the code.

```
&inp ntmax=50,dt=5.00e-4, cmax=0.0025, eps=1.e-8,
 nout=1 &end
&inp mode=3 &end
&inp mode=0 &end
```

D. EGUN INPUT

Note that the line format is very important when defining the problem geometry. Comments are placed within the input file, and indicated by (* ... *). However the comments must be removed prior to using the input file.

(* General definitions and gridding for the problem *)
Big RKA Diode / Kyle H Setup 11/16/93 B = 7.5 kG E = 400 kV
RLIM ZLIM POTN   POT(POTN)   LSTPOT MI MAGSEG
495 840   4   0.0,4.0E05,0.0,0.0   2   3   -1
(* Axial magnetic field for each axial mesh point on axis, normalized to MAGMLT. The values begin at mesh point -6 and goes to ZLIM+7. Notice that 1.0 is used to denote every tenth value. This helps in keeping track of the magnetic field values. The data are actually input as one column, however it is shown here in multi-column form. *)

1.	1.	1.	1.	1.
1.	1.	1.	1.	1.0
1.	1.0	1.	1.	1.
1.	1.	1.	1.	1.
1.	1.	1.	1.	1.
1.	1.	1.0	1.	1.
1.	1.	1.	1.	1.
1.	1.	1.	1.	1.
1.	1.	1.	1.0	1.
1.0	1.	1.	1.	1.
1.	1.	1.	1.	1.
1.	1.	1.	1.	1.0
1.	1.0	1.	1.	1.
1.	1.	1.	1.	1.
1.	1.	1.	1.	1.
1.	1.	1.0	1.	1.
1.	1.	1.	1.	1.
1.	1.	1.	1.	1.
1.	1.	1.	1.0	1.
1.0	1.	1.	1.	1.
1.	1.	1.	1.	1.
1.	1.	1.	1.	1.0
1.	1.0	1.	1.	1.
1.	1.	1.	1.	1.
1.	1.	1.	1.	1.
1.	1.	1.0	1.	1.
1.	1.	1.	1.	1.
1.	1.	1.	1.	1.
1.	1.	1.	1.0	1.
1.0	1.	1.	1.	1.
1.	1.	1.	1.	1.
1.	1.	1.	1.	1.0
1.	1.0	1.	1.	1.
1.	1.	1.	1.	1.
1.	1.	1.0	1.	1.
1.	1.	1.	1.	1.
1.	1.	1.	1.	1.
1.	1.	1.	1.0	1.
1.0	1.	1.	1.	1.
1.	1.	1.	1.	1.
1.	1.	1.	1.	1.0
1.	1.0	1.	1.	1.
1.	1.	1.	1.	1
1.	1.	1.	1.	1.
1.	1.	1.0	1.	1.
1.	1.	1.	1.	1.

1.	1.	1.0	1.	1.
1.	1.	1.	1.	1.
1.	1.0	1.	1.	1.
1.	1.	1.	1.	1.
1.0	1.	1.	1.	1.
1.	1.	1.	1.	1.0
1.	1.	1.	1.	1.
1.	1.	1.	1.0	1.
1.	1.	1.	1.	1.
1.	1.	1.0	1.	1.
1.	1.0	1.	1.	1.
1.	1.	1.	1.	1.
1.0	1.	1.	1.	1.
1.	1.	1.	1.	1.0
1.	1.	1.	1.	1.
1.	1.	1.	1.0	1.
1.	1.	1.0	1.	1.
1.	1.	1.	1.	1.
1.	1.0	1.	1.	1.
1.	1.	1.	1.	1.
1.0	1.	1.	1.	1.
1.	1.	1.	1.	1.0
1.	1.	1.	1.0	1.
1.	1.	1.	1.	1.
1.	1.	1.0	1.	1.
1.	1.0	1.	1.	1.
1.	1.	1.	1.	1.
1.0	1.	1.	1.	1.0
1.	1.	1.	1.	1.
1.	1.	1.	1.0	1.
1.	1.	1.	1.	1.
1.	1.	1.0	1.	1.
1.	1.0	1.	1.	1.
1.0	1.	1.	1.	1.0
1.	1.	1.	1.	1.
1.	1.	1.	1.0	1.
1.	1.	1.	1.	1.
1.	1.	1.	1.	1.
1.	1.	1.0	1.	1.
1.	1.0	1.	1.	1.
1.	1.	1.	1.	1.
1.0	1.	1.	1.	1.0
1.	1.	1.	1.	1.
1.	1.	1.	1.0	1.
1.	1.	1.0	1.	1.
1.	1.	1.	1.	1.
1.	1.	1.	1.	1.
1.	1.	1.	1.	1.0
1.	1.	1.	1.0	1.
1.	1.	1.	1.	1.
1.	1.	1.	1.	1.
1.	1.	1.	1.	1.

1.	1.	1.0	1.	1.
1.	1.	1.	1.	1.
1.	1.0	1.	1.	1.
1.	1.	1.	1.	1.
1.0	1.	1.	1.	1.
1.	1.	1.	1.	1.0
1.	1.	1.	1.	1.
1.	1.	1.	1.0	1.
1.	1.	1.	1.	1.
1.	1.	1.0	1.	1.
1.	1.	1.	1.	1.
1.	1.0	1.	1.	1.
1.	1.	1.	1.	1.
1.0	1.	1.	1.	1.0
1.	1.	1.	1.	1.
1.	1.	1.	1.0	1.
1.	1.	1.	1.	1.
1.	1.	1.0	1.	1.
1.	1.	1.	1.	1.
1.	1.0	1.	1.	1.
1.0	1.	1.	1.	1.0
1.	1.	1.	1.	1.
1.	1.	1.	1.0	1.
1.	1.	1.	1.	1.
1.	1.	1.0	1.	1.
1.	1.	1.	1.	1.
1.	1.0	1.	1.	1.
1.	1.	1.	1.	1.
1.0	1.	1.	1.	1.0
1.	1.	1.	1.	1.
1.	1.	1.	1.0	1.
1.	1.	1.	1.	1.
1.	1.	1.0	1.	1.
1.	1.	1.	1.	1.
1.	1.0	1.	1.	1.
1.	1.	1.	1.	1.0
1.0	1.	1.	1.	1.
1.	1.	1.	1.0	1.
1.	1.	1.0	1.	1.
1.	1.	1.	1.	1.
1.	1.0	1.	1.	1.
1.	1.	1.	1.	1.
1.	1.	1.	1.	1.0
1.	1.	1.	1.	1.
1.	1.	1.	1.0	1.
1.	1.	1.0	1.	1.
1.	1.	1.	1.	1.
1.	1.0	1.	1.	1.
1.	1.	1.	1.	1.
1.0	1.	1.	1.	1.
1.	1.	1.	1.0	1.0
1.	1.	1.	1.	1.
1.	1.	1.0	1.	1.
1.	1.	1.	1.	1.
1.	1.	1.	1.	1.
1.	1.	1.	1.	1.
1.	1.	1.	1.0	1.
1.	1.	1.	1.	
1.	1.	1.0	1.	
1.	1.	1.	1.	

4	0	1	0.0	-0.99
4	50	1	2.0	-0.99
4	320	1	2.0	-0.99
4	321	1	0.01	-0.99
4	321	2	0.01	2.00
4	321	10	0.01	2.00
4	321	239	0.01	2.00
4	321	240	0.01	0.01
4	313	250	0.75	0.10
4	213	390	0.01	-0.01
4	213	391	0.01	2.00
4	213	425	0.01	2.00
4	213	473	0.01	2.00
4	213	474	0.01	2.00
1	214	475	2.00	-0.99
1	215	475	2.00	-0.99
1	216	475	2.00	-0.99
1	217	475	2.00	-0.99
1	218	475	2.00	-0.99
1	219	475	2.00	-0.99
4	220	474	-0.99	2.00
4	220	473	-0.99	2.00
4	220	425	-0.99	2.00
4	220	391	-0.99	2.00
4	220	390	-0.99	-0.01
4	320	251	-0.25	-0.90
4	328	240	-0.99	0.01
4	328	239	-0.99	2.00
4	328	10	-0.99	2.00
4	328	1	-0.99	2.00
0	329	0	0.00	0.00
0	330	0	2.00	0.00
0	450	0	2.00	0.00
0	493	0	2.00	0.00
2	494	0	0.99	0.00
2	494	1	0.99	2.00
2	494	200	0.99	2.00
2	494	653	0.99	2.00
2	494	654	0.99	0.01
2	441	700	0.22	0.10
2	389	744	0.99	0.01
2	388	744	2.00	0.01
2	275	744	2.00	0.01
2	256	744	2.00	0.01
2	255	744	-0.01	0.01
2	255	743	-0.01	2.00
2	255	650	-0.01	2.00
2	255	535	-0.01	2.00
2	255	534	-0.01	2.00
2	254	533	2.00	0.99
2	253	533	2.00	0.99
2	235	533	2.00	0.99
2	226	533	2.00	0.99
2	225	533	2.00	0.99
2	224	534	0.99	2.00
2	224	600	0.99	2.00
2	224	839	0.99	2.00
2	224	840	0.99	0.00
0	223	840	2.00	0.00
0	150	840	2.00	0.00
0	0	840	0.00	0.00
0	0	800	0.00	2.00

```
   0    0    2         0.00      2.00
   888
   UNIT    MAXRAY   STEP   NS   SPC  MASS  ZEND   VION    SAVE
   0.000333    27    0.1   13   0.6   0.0   840  -1.E8      0
   START   AV  AVR   RC    ZC   DENS  SURFACE MAGMLT MAGORD
  'GENERAL'  0  1.0 213.01 476.01  5000.0   1   7500.0     2
```

E. RKA INPUT

The Mathematica calculations for the space charge reduction factor are discussed first. The equations are:

```
bsn/: bsn[(x_) , (y_)] :=
    (Pi*Sqrt[x*y]*(BesselY[0, y]*BesselJ[0, x] - BesselY[0, x]*BesselJ[0, y]))/
    2

Bsn/: Bsn[(x_) , (y_)] :=
    (Pi*Sqrt[x*y]*(BesselY[1, y]*BesselJ[1, x] - BesselY[1, x]*BesselJ[1, y]))/
     2

btn/: btn[(x_) , (y_)] :=
    (BesselY[0, y]*BesselJ[0, x] - BesselY[0, x]*BesselJ[0, y])/
    (BesselY[0, y]*BesselJ[1, x] - BesselY[1, x]*BesselJ[0, y])

btnh/: btnh[(x_) , (y_)] :=
    (BesselK[0, x]*BesselI[0, y] - BesselK[0, y]*BesselI[0, x])/
    (BesselK[0, y]*BesselI[1, x] + BesselK[1, x]*BesselI[0, y])

g/: g[x_] := x^(-2) + (BesselI[0, c]/BesselI[1, c])*((btn[x b , x c])^(-1) -
      btnh[a , b]/btn[x c , x b])/x^1 -
    (BesselI[0, c]*Bsn[x b , x c]*btnh[a , b])/(BesselI[1, c]*bsn[x b , x c])

f1/: f1[x_] := 1 + 2*x*a1 + x^2*((1 + a1^2) - a2^2) + 2*x^3*a1 + x^4*a1^2

f2/: f2[x_] := (1 + 2*x*a1 + x^2*((1 + a1^2) - a2^2)) - 2*x^3*a1 + x^4*a1^2

f3/: f3[x_] := 1 - 2*x*a1 + x^2*((1 + a1^2) - a2^2) + 2*x^3*a1 + x^4*a1^2

f4/: f4[x_] := (1 - 2*x*a1 + x^2*((1 + a1^2) - a2^2)) - 2*x^3*a1 + x^4*a1^2
```

The value of x when g[x]= 0 is used to determine the space charge reduction factor. The problem is restricted to an annular electron beam in a hollow pipe. The values of the radii a (wall inner radius), b (beam outer radius), c (beam inner radius) must be multiplied by $\gamma_0 = \omega/(\beta c)$ and then used in the equation for g.

To find the root within an x-range can be achieved by:

```
FindRoot[g[x_],{x,xstart,xmin,xmax}].
```

You may plot g[x] to verify that there is a root by using:

```
Plot[g[x],{x,xmin,xmax}].
```

This value of x is then used for the variable a2, while $a1=f_b/(f\sqrt{\gamma})$ where f_b is the beam plasma frequency and f is the rf frequency. The roots of f1, f2, f3, and f4 are then found for x in the range 0 to 1. This final value of x is the plasma reduction factor (PRF) or space-charge reduction factor required by RKA.

For example, consider the case of a 300 kV, 10 kA beam in a pipe of radius a = 7.65 cm, and beam position b = 6.6 cm and c = 6.0 cm. One finds the following set of inputs for the function g[x]:

γ_0 = 0.3441 cm^{-1} for a frequency of 1.3 GHz

a = 2.6325
b = 2.2712
c = 2.0647

g[x]= 0 yields x= 2.2063 which is then used for a2.

Now a1 = 1.8775 yields from f4[x]= 0 that the PRF = 0.248849. This is due to f1[x] never crossing the x-axis. Also f2 and f3 are not physical because of the crossed +/- signs. That is the signs should both be + or -, but not mixed.

RKA may now be run to determine the beam modulation as a function of the axial position z. A sample deck for the above PRF is listed below:

```
&param
ti=0.0,tf=1.0,nt=51,
xi=0.000005,xf=30.000001,mx=151,
d=1.56,f0=1300.0e+6,alpha=0.050,
volin=0.300,i0=10.0e+3,rin=6.0,rout=6.6,prf=0.248849,
nharm=2,norbit=50,
nxint=5,
yubhrm=1.0,nhrmint=4,
ylborb=0.0,yuorb=5.0,norbint=5,
ylbvel=0.0,yubvel=1.5,nvelint=5,
ylbke=0.0,yubke=2.5,nkeint=5,
nequil=1,epslon=1.e-5,
nrun=0
/
```

One finds that a maximum beam modulation of 10% occurs after propagating 15 cm, 13.44 cm past the 1.56-cm modulating gap. Using this modulated beam as input to another cavity is accomplished by renaming the generated file RESTART.OUT as RESTART.IN, changing nrun=1, changing alpha to reflect the voltage induced in the second gap, and changing xi and xf for the positions of the second gap and drift space.

F. MAGIC INPUT

Below is a sample input deck for the PIC code MAGIC. The plots discussed in section 3 can be found in the input listing.

```
TITLE "field(400kV 16kA) cavity2cellshorter ant8e6 ";

COMMENT " Relativistic Klystron Amplifier with cup cathode";
COMMENT " MAGIC Jun 1993 SPARC10   SIMULATION FOR KYLE HENDRICKS ";
COMMENT " LAST CHANGED   25 Jun 93   LESTER BOWERS (14Apr93)";
comment " /usr12/home/les/magic/rka04/in04rka   incup";

DEFINE PI       3.14159;  DEFINE C      2.9979e+8;  DEFINE bz       .6    ;
DEFINE COURNT  .7      ;  DEFINE TSIM      59.e-9;  DEFINE DUMP  29.E-9;
define bi     16.E3    ;  DEFINE RAMP      10.e-9;  define delay  5.e-9;
define bv    400.      ;  DEFINE AMPT     8.0e+6;  DEFINE F      1.3E+9;
DEFINE ANTRAMP 2.E-9 ;    DEFINE ROUND     1.e-7;  define cavity  2    ;
define dz       .001 ;    define dr       .001  ;  define bkv=bv*1000.;


terminate warning ;    define on  = 1 ;    define off = 0 ;
define idump              = off ;
define iflux              = off ;
define irange             = off ;
define ivector            = off ;
define icontour           = off ;
define iantenna           =  on ;
define idisplay           =  on ;
define iobserve           =  on ;
define iphasespace        =  on ;
define iperspective       = off ;
define ihighqfilter       = off ;
define iemission_beam     = off ;
define iemission_field    =  on ;


define z0       .0       ;   c  start of        rka     ;
define z1       .1       ;   c  end   of        shank   ;
define z2       .2025    ;   c  end   of        slant   ;
define z3       .213     ;   c  tip   of        cathode;
define z4       .23      ;   c  tip   of        anode   ;
define z5       .267     ;   c  end   of        a-k gap;
define z6       .377     ;   c  start of first  cavity ;
define z7       .387     ;   c  start of first  gap     ;
define z8       .407     ;   c  end   of first  cavity ;
define z9       .527     ;   c  start of last   cavity ;
define z10      .537     ;   c  start of last   gap     ;
define z11      .557     ;   c  end   of last   cavity ;
define z12      .66      ;   c  end   of        rka     ;
define zm   = z12    ;
define ngz      12       ;


define r0       .0       ;      c  center line    ;
define r1       .07      ;      c  cathode tip     ;
define r2       .074     ;      c  cathode tip     ;
define r3       .076     ;      c  anode inside    ;
define r4       .086     ;      c  cavity bottom ;
define r5       .107     ;      c  cathode shank ;
define r6       .111     ;      c  cathode shank ;
define r7       .107     ;      c  cavity top      ;
define r8       .135     ;      c  anode break     ;
define r9       .16      ;      c  anode outside ;
define rm   = r9     ;
define ngr      9        ;
```

```
function nxgrid(dxtotal,dxfirst,dxlast)=2.*dxtotal/(dxfirst+dxlast);

define zspect1  3.0  ;    define zspect2  1.  ;    define zspect3 3.0  ;
dzsum1 = z4 ;    dzsum2 = z11-z4 ;    dzsum3 = zm-z11 ;
define dzfirst1 = zspect1*dz  ;        define dzlast1 = dz          ;
define dzfirst2 = dz          ;        define dzlast2 = dz          ;
define dzfirst3 = dz          ;        define dzlast3 = zspect3*dz ;
define ndz1 = nxgrid(dzsum1,dzfirst1,dzlast1);
define ndz2 = nxgrid(dzsum2,dzfirst2,dzlast2);
define ndz3 = nxgrid(dzsum3,dzfirst3,dzlast3);
define i0 2 ;    define im = i0 + ndz1 + ndz2 + ndz3 ;


define aspect1 3.  ; drsum1 = r1 ;
define aspect2 1.  ; drsum2 = r7-r1 ;
define aspect3 3.  ; drsum3 = rm-r7 ;
define drfirst3 = dr           ;    define drlast3 = aspect3*dr;
define drfirst2 = dr           ;    define drlast2 = dr        ;
define drfirst1 = aspect1*dr ;    define drlast1 = dr        ;
define ndr1 = nxgrid(drsum1,drfirst1,drlast1);
define ndr2 = nxgrid(drsum2,drfirst2,drlast2);
define ndr3 = nxgrid(drsum3,drfirst3,drlast3);
define k0  2 ;    define km = k0 + ndr1 + ndr2 + ndr3 ;


DEFINE BAREA   = PI*( R4**2 - R2**2 )      ;
define bgamma  = bv/511. + 1.              ;
define bbeta   = sqrt( 1. - 1./bgamma**2 ) ;
DEFINE BVEL    = C*BBETA                    ;
DEFINE GAMV    = BGAMMA*BVEL                ;
define bj      = bi/barea                   ;
define wavelen = 100.*c/f                   ;
define rbeamavg= .5*(r1+r2)                 ;
define twopir  = 2.*pi*rbeamavg             ;
define temp1   = (bgamma**.66667 - 1.)**1.5;
define temp2   = log(r3/rbeamavg)           ;
define scli    = 8.55*temp1/temp2          ;        c  kA ;


system cylinder-theta;
x1grid function im i0   z0
                                ndz1 dzfirst1 dzsum1
                                ndz2 dzfirst2 dzsum2
                                ndz3 dzfirst3 dzsum3   ;

x2grid function km k0   r0       ndr1 drfirst1 drsum1
                                ndr2 drfirst2 drsum2
                                ndr3 drfirst3 drsum3   ;

do i 1,ngz,1 ;
   engrid x1 i'i' z'i' full ;
enddo ;
do k 1,ngr,1 ;
   engrid x2 k'k' r'k' full ;
enddo ;
z8_z6=z8-z6; r7_r4=r7-r4; z8_z7=z8-z7; r4_r3=r4-r3; z11_z9=z11-z9;
ungrid x1 x1i6 i6 full ; ungrid x1 x1i8 i8 full ; cavln1=x1i8-x1i6 ;
ungrid x1 x1i11 i11 full ; ungrid x1 x1i9 i9 full ; cavln2=x1i11-x1i9 ;
ungrid x2 x2k4 k4 full ; ungrid x2 x2k7 k7 full ; cavhit=x2k7-x2k4 ;
ungrid x1 x1i7 i7 full ; stubln=x1i8-x1i7 ;
ungrid x2 x2k3 k3 full ; stubht=x2k4-x2k3 ;

   conductor cavities anti-align
            i4  km   i5  k8   i5  k4   i4  k4   i4  k3
            i7  k3   i7  k4   i6  k4   i6  k7   i8  k7


                              60
```

```
                i8   k3    i10 k3    i10 k4    i9 k4    i9 k7
                i11 k7    i11 k3    im  k3    im  km    i0 km ;

conductor shank            align    i0 k6  i1 k6 ;
conductor cathode          align    i3 k1  i3 k2  i2 k2  i1 k6 ;
conductor noemit           align    i2 k0  i2 k1  i3 k1 ;

define dt = 2.*cournt/c*sqrt(1./(1./dz**2+1./dr**2)) ;
define fnyquist = 1./(2.*dt) ;
define ndt = tsim/dt + round ;
if ( ihighqfilter .eq. on ) then ;
    define cratio = 4*cournt*cournt ;
z   define gaa    = .85 ;
    define gaa    = 1. - 1./(sqrt(3.)*(1.+2.*cournt)) ;
    define alpha1 = .5*gaa/cratio ;
    define alpha2 = 1. - alpha1 ;
    define alpha3 = 0. ;
    define iters  = 4  ;
    define tau1   = 1. ;
    define tau2   = .5 ;
z   define tau3   = .25*(-3.+sqrt(17.)) ;
z   define tau4   = .25*(-3.-sqrt(17.)) ;
    define tau3   = .2807764 ;
    define tau4   = -1.7807764 ;
    fields all biased ndt dt alpha1 alpha2 alpha3 iters tau1 tau2 tau3 tau4 ;
else ;
    fields all biased ndt dt;
endif ;
lookback fields all 1. 1. anti-align im k0 im k3 ;
symmetry axial align i0 k0 im k0 ;
define dmaxnorm 1.e-4 ;
define nppc 2 ;
define mts  1 ;
define t2 = delay + ramp ;
define temp .05 ;
if ( iemission_beam .eq. on ) then ;
    function rho data 4    0. 0. delay 0. t2 bj tsim bj ;
    emit annular bb ;
    emission annular electron nppc mts
            beam    rho
            spacing random dmaxnorm random
            thermal gamv temp ;
endif;
if ( iemission_field .eq. on ) then ;
    define threshold 1.5e7 ;
    define breakdown 1.    ;
    emit annular cathode ;
    emission annular electron nppc mts
            field   breakdown threshold 0. 0. 0.
            spacing random dmaxnorm random
            energy 1.e4 ;
function sph = 1. ;
function voltramp data 4    0. 0.  delay 0.  t2 bkv   tsim bkv ;
voltage fields tm voltramp sph 1. 0. 1. align i0 k6 i0 km ;
endif;
CURRENTS LCC NO NO 0. 1. ;
FORCES .5 1. 1. ;
KINEMATICS ELECTRON 1 YES NO YES EM 1 1 ;

DEFINE 1k7 = k7-1;  DEFINE OMEGA = 2.*PI*F ;
define mz1 = im-1;  define k21    = k2-1    ;
if ( iantenna .eq. on ) then ;
```

```
      FUNCTION "TFUN(T) = MIN(T/ANTRAMP,1.)*AMPT*SIN(OMEGA*T)" ;
      antenna tfun null null e1  I6 I8 1k7 1k7 ;
endif;
c bexternal bz .0 .0 ;
preset b1rd read MAGDATZ surface extmag ascii modify replace ;
preset b2rd read MAGDATR surface extmag ascii modify replace ;

if ( idump .eq. on ) then ;
   DUMP FORMAT ASCII ;
   DUMP TYPE     BOUNDARY ;
   DUMP TYPE   PHASESPACE ;
   DUMP TYPE PERSPECTIVE ;
   DUMP TYPE      CONTOUR ;
   DUMP TYPE      OBSERVE ;
   DUMP TYPE       VECTOR ;
   DUMP TYPE        RANGE ;
   DUMP TYPE         FLUX ;
   DUMP TYPE         GRID ;
   DUMP TYPE    PARTICLES ;
endif ;
DEFINE FQN .05E9 ;   DEFINE FQX 5.9E9 ;
output meta  ;
output color ;
if ( idisplay .eq. on ) then;
   display integer   i0    im   k0    km nogrid ;   c  full device         ;
   display    real  .36  .43  .04 .13          ;   c  first  cavity  ;
   display    real  .50  .57  .04 .13          ;   c  second cavity  ;
   display    real  .19  .29  .05 .15          ;   c  a-k gap         ;
   display    real  .09  .22  .02 .15          ;   c  cathode             ;
endif;
c TAGGING .8 ;

DEFINE NT 3 ;  DEFINE FREQMAX = 1./(2.*NT*DT) ;
DEFINE NSNAP = MAX(1,DUMP/DT) ;   DEFINE NSTWO = 2*NSNAP ;
TIMER CHECK PERIODIC 300 99999 600 ;
TIMER ENE-T PERIODIC    0 99999    2 ;
TIMER SPIT  PERIODIC NSNAP 99999 NSNAP ;
TIMER FLX-T DISCRETE 50 ;
TIMER RPUT  PERIODIC NSTWO 99999 NSTWO ;
COURANT SEARCH ;
DIAGNOSE COURANT   1 0 1 ;
DIAGNOSE SPACING   1 0 0 ;
DIAGNOSE CONDUCTOR 1 0 1 ;
STATISTICS CHECK ;

if ( irange .eq. on ) then ;
c                      across bottom of cavity gap ;
  range spit 1 field e1 i4 k5 i5 k5 ;
  range spit 1 field b2rd i0 k1 im k1 ;
  range spit 1 field b1rd i0 k1 im k1 ;
endif ;
   trajectory 99999 spit 1 electron z0 zm  r0 rm ;
if (icontour .eq. on) then;
  contour spit field e1  i0 im  k0 km boundary yes ;
  contour spit field e2  i0 im  K0 km boundary yes ;
endif;

if (iperspective .eq. on) then;
  perspective rput field e1 i0 im k0 km 1 1 ;
  perspective spit field b1rd i0 im k0 km 1 1 ;
  perspective spit field b2rd i0 im k0 km 1 1 ;
endif;
```

```
            if (iphasespace .eq. on) then;
               phasespace spit
                       axes x1 p1
                       axis x .0 zm .1
                       axis y -.75e9 .75e9 ;
            endif;

            if (ivector .eq. on) then;
              vector spit field e1 e2
                   scale log 1
                   number 60 30
                   axis x z0   zm  .1
                   axis y r0   rm  .05 ;
            endif;

            energy ene-t i0 im k0 km ;

            if (iobserve .eq. on) then;
            define kf 5 ;
            c observe energy voltage 1 0 interval nt fft kf ;
                         c window frequency fqn fqx ;
            observe energy electric 0 1 interval nt   ;
            observe energy lookback 1 0 interval nt fft kf
                         window frequency fqn fqx ;
            c   E/M field energy ;
            observe energy em 0 1 INTERVAL NT  ;
            c   E/M field energy rate ;
            OBSERVE ENERGY em 0 0 INTERVAL NT fft kf
                         WINDOW FREQUENCY FQN FQX ;
            c   B_theta one cell from the end and 1 cell below Rbo ;
            observe field b3 mz1 k21 mz1 k21 interval nt fft kF
                         window frequency fqn fqx ;
            c   voltages - first gap ;
            observe field e1 i7 k3 i8 k3 interval nt fft kf
                         window frequency fqn fqx ;
            c   voltages - second gap ;
            observe field e1 i10 k3 i11 k3 interval nt fft kf
                         window frequency fqn fqx ;
            define midgap1=(i7+i8)/2 ; define midcav1=(i8+i6)/2 ;
            c   Ez field in the middle of the gap on top of the beam ;
            observe field e1 midgap1 k2 midgap1 k2 interval nt fft kf
                         window frequency fqn fqx ;
            c   Ez field at the middle botom of gap ;
            observe field e1 midgap1 k3 midgap1 k3 interval nt fft kf
                         window frequency fqn fqx ;
            c   Er field midcavity one cell below the top ;
            observe field e2 midcav1 1k7 midcav1 1k7 interval nt fft kf
                         window frequency fqn fqx ;
            c voltage on exit ;
            observe field e2 mz1 km mz1 k0 interval nt fft kf
                         window frequency fqn fqx ;
            c   Ez field one cell below the outside radius of the beam ;
            observe field e1 mz1 k21 mz1 k21 INTERVAL NT FFT KF
                         window frequency fqn fqx ;
            c injected beam current ;
            observe field j1 i4 k3 i4 k0 interval nt   ;

            c from first gap in steps of 3 cm -  beam current ;
            define step1 .03 ;   define istep1 = step1/dz ;
            do i i8,im,istep1;
               define ig1='i';
               observe field j1 ig1 k3 ig1 k0 interval nt fft kf
```

```
                window frequency fqn fqx ;
enddo;

if ( iflux .eq. on ) then;
  flux zcav1 flx-t all indices align i6 k0 i6 k3 ;
  observe flux zcav1 current ;
  flux zslice flx-t all plane align x z7 ;
  observe flux zslice current ;
endif;
endif;

START;
STOP ;
```